ABSTRACT

Yu, Xinying. Space-Time Coding for Large Antenna Arrays. (Under the direction of Professor Brian L. Hughes.)

Multiple-input multiple-output (MIMO) systems can greatly improve the capacity and performance of wireless communications. In particular, space-time coding techniques have received much attention in recent years as an efficient approach to achieving the performance gains offered by MIMO channels. Thus far, most work on space-time coding has focused on systems with small antenna arrays or high signal-to-noise ratios (SNRs), for which it has been shown that codes should be designed according to the rank and determinant criteria. For such scenarios, coherent space-time coding and differential space-time modulation (DSTM) schemes have been designed, for systems with or without channel knowledge at the receiver, respectively. In recent years, there has been some work on coherent space-time coding for large arrays, which indicates that the code design metric should be chosen diffently from that for small arrays. In this dissertation, we study the design of space-time coding for large arrays. We focus on three aspects: performance analysis, code construction and decoding algorithms.

We first analyze the asymptotic performance of differential space-time modulation. A new upper bound on the pairwise-error probability is derived for large arrays. This bound suggests that Euclidean distance is an appropriate design criterion for DSTM with large numbers of antennas, which is similar to the design of coherent space-time coding for the large-array regime. For two transmit antennas and four or more receive antennas, we use the new design criterion to obtain several new unitary codes with large minimum Euclidean distance. The proposed codes outperform some existing codes, for example, the well-known Alamouti code, for large receive arrays.

Although the codes designed according to the new design criterion achieve good

performance, most of them require maximum-likelihood (ML) decoding, which is undesirable for high-rate codes. On the other hand, the Alamouti code, which is designed for high-SNR regime, enables simple linear ML decoding. It is of interest to design codes that perform well for large arrays, but which also allow simple decoding at the receiver. We first consider the design of unitary codes, for use with and without channel knowledge at the receiver. For two transmit antennas, we consider a structure which is a modification of the Alamouti code. We optimize the new code with respect to the Euclidean distance criterion. We then show that the new code allows us to use two suboptimal decoders that have complexity comparable to the Alamouti decoder. The analytical bit-error performance and the constellation-constrained capacity are derived for the suboptimal decoders. For coherent detection, the coding structure is extended to non-unitary constellations. We also extend the new code to more than two transmit antennas.

Conventional DSTM assumes that the channel remains constant for two adjacent transmission blocks, which is questionable for some time-varying channels. In this dissertation, we investigate the performance of the new code when fast-fading is encountered. We show that multiple-symbol decision-feedback differential detection (DFDD) can be used to reduce the performance degradation of the new code in fast-fading channels. We also consider the use of suboptimal decoders in DFDD to further reduce the decoding complexity.

Space-Time Coding for Large Antenna Arrays

by

Xinying Yu

A dissertation submitted to the Graduate Faculty of
North Carolina State University
in partial satisfaction of the
requirements for the Degree of
Doctor of Philosophy

Electrical Engineering

Raleigh

December, 2005

Approved By:

Dr. Hamid Krim	Dr. Carl Meyer
Dr. Brian L. Hughes Chair of Advisory Committee	Dr. Alexandra Duel-Hallen

To my parents, my husband and my son ...

Biography

Xinying Yu received her Bachelor of Science and Master of Science degrees in Electrical Engineering in 1996 and 1999 respectively, from Beijing University of Posts and Telecommunications, China. From 1997 to 1999, she was with CDMA Research and Development Center, Ministry of Information Industry, China, working on IS-95 CDMA base station baseband signal processing and hardware implementations. From 1999 to 2000, she worked as a wireless system engineer at Beijing Posts and Telecommunication Consulting and Design Institute, China. In August 2000, she started her work towards the PhD degree in Electrical Engineering at North Carolina State University, under the guidance of Prof. Brian L. Hughes.

Acknowledgements

First, I wish to express my deepest gratitude to my advisor, Dr. Brian L. Hughes for his guidance and continuous support throughout my Ph.D study. I have benefited tremendously from his wisdom, vision, inspiring teaching and technical insights. I sincerely appreciate his extensive effort to help me improving my research skills. I also thank him for his understanding and encouragement during hard times.

I am grateful to Dr. Alexandra Duel-Hallen, Dr. Hamid Krim and Dr. Carl Meyer for serving in my advisory committee and providing me valuable feedbacks on my research and dissertation. I also thank Dr. Huaiyu Dai, Dr. Zhilin Li and Dr. Ernie L. Stitzinger for their help in and out of class.

I am thankful to my colleagues from whom I learned a lot. My special thanks to Chris Mary James, who is always there for me when needed. Thanks are also due to Ajith Kamath, Pallav Sudarshan, Sandeep Krishnamurthy, Mahmud Jalnase, Pinak Kishore and Zhihong Hong for useful discussions on research.

There are many friends who make my time at North Carolina State University enjoyable. I want to thank Yang Wu, for all the help and constant encouragement she gave me during these years. I also thank Ming Lei, Jia Liu, Li Ma, Lei Luo and Quan Zhou for valuable discussions on many aspects of life and for their friendship.

I am forever indebted to my parents for their unconditional love and encouragement. It was their faith in me that drives me so far in life. I also thank my parents-in-law for their support. I owe a lot to my beloved husband Xuemin Yang. Without his love, patience and support, the dissertation would not have been completed. Finally, I thank my son Daniel for the joy he brought to me each and everyday.

Contents

List of Tables

List of Figures

Chapter 1

Introduction

1.1 Introduction

Wireless communications began in 1897, when Guglielmo Marconi first demonstrated the ability of electromagnetic waves to provide continuous contact with ships sailing the English Channel. Since then, wireless communications have experienced a remarkable evolution. In the last decade, wireless communication has grown tremendously, driven by high demand for cellular telephony and wireless access to the Internet. Currently, the telecommunications industries are deploying third generation (3G) cellular systems worldwide and new technologies are under development for next-generation wireless systems (4G). To meet the growing demand for high data-rate transmission, multimedia communications, seamless global roaming and quality of service management, future wireless systems will require more bandwidth-efficient communications techniques.

It is well known that wireless communication systems are constrained in both power and bandwidth. In addition, the wireless channel can be a dynamic and challenging communications medium. Due to the propagation effects such as diffraction, scattering and reflection, the transmitted signal will propagates to the receiver by a number of paths referred as multipaths, each with a distinct, time-varying amplitude, phase and angle of arrival. These multipath signals can add constructively or destructively at the receiver, which results in signal fading. Multipath fading deteriorates the link quality and can significantly increase the power required to achieve reliable communication.

Diversity has long been used as an efficient technique to combat multipath fading and improve the performance of wireless communication systems [31]. Diversity techniques provide the receiver with differently-attenuated copies of the same transmitted signal, thereby reducing the fluctuations caused by fading. Diversity can be achieved in time, frequency, space, polarization or angle. For example, channel coding with interleaving can be used to exploit temporal diversity, RAKE receivers with code-division multiple-access (CDMA) systems can be used to exploit frequency diversity and multiple receive antennas can be used to access spatial diversity. Since time or frequency diversity methods require additional transmission time or extra bandwidth, in recent years there is more interest on spatial diversity using multiple antennas.

Traditionally, most spatial diversity schemes in wireless communication systems have been based on receiver antenna arrays, which are referred to as single-input multiple-output (SIMO) systems. The capacity of a SIMO system increases loga-

rithmically with the number of antennas. Recently, it has been demonstrated that deploying multiple antennas at the transmitter as well as the receiver can result in far greater performance gains in wireless communications. In particular, Foschini and Gans [14] and Telatar [58] have demonstrated that employing multiple transmit and receive antennas can substantially improve the capacity of multipath fading channels. This result opens up a new approach to meeting the growing demand for high-data-rate cellular systems and has led to significant research efforts devoted to developing techniques that can achieve in practical communication systems.

One promising technique for multiple-antenna systems is called space-time coding. In space-time coding, the signal processing at the transmitter is done not only in the time dimension, as is typical of many single-antenna communication systems, but also in the spatial dimension. The idea of space-time coding was initially proposed by Tarokh, Seshadri and Calderbank [55]. Most early work on space-time coding assumes coherent detection, in which perfect channel-state information (CSI) is available at the receiver. Under quasi-static fading conditions with high signal-to-noise ratios (SNRs), [55] proposed the well-known *rank and determinant criteria*, which indicates that codes should be designed to have full diversity and a large product distance. In particular, Alamouti [2] proposed a simple space-time block code for two transmit antennas which achieves full diversity with simple linear decoding at the receiver.

Coherent detection requires channel estimation using training symbols, which may be costly or undesirable in some situations, such as fast-fading channels. For situations where the channel is unknown at the receiver, Hochwald and Marzetta [23]

proposed the use of unitary space-time block codes, in which the signals transmitted by different antennas are mutually orthogonal. Based on unitary space-time modulation, a transmission scheme that is better tailored for systems with no channel information at both the transmitter and the receiver is proposed by Tarokh and Jafarkhani [57], Hughes [26] and Hochwald and Sweldens [24], which is called differential unitary space-time modulation (DSTM). For high SNRs, code design for DSTM is also governed by the rank and determinant criteria.

Most work on coherent or differential space-time modulation assumes high SNRs, which is necessary in order to achieve acceptable performance for a system equipped with small number of antennas. For systems with large numbers of antennas, however, the SNR of interest often falls into low SNR regime. For such scenarios, it has been reported by Biglieri *et al.* [4], Yuan *et al.* [69] and Aktas *et al.* [1] that *Euclidean distance* between codewords is often a better indicator of code performance. In this dissertation, we will study the design of space-time coding for large antenna arrays.

In the rest of this chapter we will give an overview of multiple-antenna systems and an outline of the dissertation.

1.2 Multiple-Antenna Systems

In this section, we briefly describe the characteristics of wireless fading channels with emphasis on Rayleigh fading. The diversity techniques commonly used in wireless systems are summarized. We then introduce multiple-antenna systems and give a review of coherent and differential space-time modulation.

1.2.1 Wireless Channel Characteristics

Wireless communication suffers from inherent channel impairments which arise from the physical propagation environment and which can severely degrade system performance. As shown in Fig. 1.1, in a wireless environment, the surrounding objects, such as mountains, buildings, trees and houses, cause reflection, diffraction and scattering of the transmitted signal. Due to these effects, the transmitted electromagnetic wave travels along different paths of varying lengths and therefore have different amplitudes, phases, delays and angles of arrival. At the receiver, the destructive in-

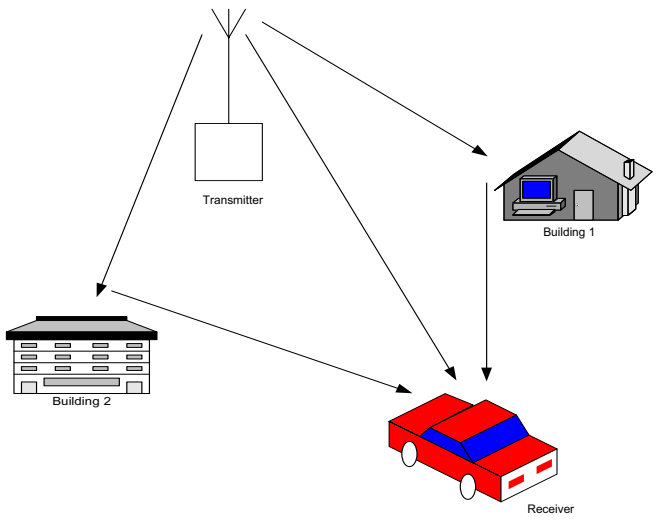

Figure 1.1: Multipath fading

teraction between these wave components causes multipath fading, and the power of

the waves decrease as the distance between the transmitter and receiver increases. Typically, propagation models are classified into two categories. Propagation models that predict the mean signal strength at a given distance from the transmitter are called *large-scale* propagation models, since they characterize signal strength over large transmitter-receiver distances (usually a few kilometers). On the other hand, *small-scale* or fading models are used to characterize the rapid fluctuations of the received signal strength over very short distances or short time durations, where the received power sometimes varies as much as 30 to 40 dB when the receiver moves only a fraction of a wavelength [43].

The statistical characteristics of fading channels are determined by many factors, such as multiple-path propagation, the relative speed of the transmitter and receiver, the speeds of surrounding objects, and the transmission bandwidth of the signal [43]. The mobile radio channel may be modeled as a linear filter with a time-varying impulse response, where the time variation is due to motion of the transmitter, receiver or scatterers. The filtering nature of the channel is caused by the summation of amplitudes and delays of the multiple arriving waves at any instant of time. A discrete model for a channel with L taps can be expressed as

$$y(n) = \sum_{l=0}^{L-1} h(n;l)x(n-l) + z(n)$$

where $x(n)$ is the transmitted signal, $y(n)$ is the received signal, $h(n;l)$ is the response at time n of the time-varying channel if an impulse is sent at time $n-l$ and $z(n)$ is the noise [41]. Two common parameters associated with fading channels are the coherence bandwidth which is the range of frequencies over which two frequency components

have a strong potential of amplitude correlation and the coherence time which refers to the time rate of change of the channel characteristics [43].

Multipath propagation delays in a fading channel can cause time dispersion. Time domain parameters for multipath fading such as root-mean-square (RMS) delay spread are derived from the power-delay profile. Coherence bandwidth is inversely proportional to the RMS delay spread, which characterizes the channel in the frequency domain. In narrowband systems, the bandwidth of the transmitted signal is smaller than the channel's coherence bandwidth and the multipath components often arrive at the receiver within a small fraction of the symbol duration. This type of fading is called *frequency-nonselective* or *flat* fading. In wideband systems, by contrast, the multipath delay spread is larger than the symbol duration, resulting in *frequency-selective* fading. In such cases, the spectrum of the channel varies over the signaling bandwidth, which leads to inter-symbol interference between transmitted signals [32].

In many situations, there is relative motion among the transmitter, receiver and scatterers. This leads to frequency spreading of the transmitted signal, called Doppler spreading, which causes signal fading to vary with time. Here spread is used to denote the fact that a pure tone of frequency f_c in Hertz spreads across a finite bandwidth $f_c \pm f_d$. The Maximum Doppler shift of the received signal is denoted by f_d and given by

$$f_d = \frac{\nu f_c}{c} \tag{1.1}$$

where ν is the velocity of the moving object and c is the speed of light. The time

autocorrelation of the flat fading channel $h(t)$ is approximated by Jakes' model [31]

$$r(\tau) = \mathcal{E}[h(t)h(t+\tau)^*] = J_0(2\pi f_d \tau) \tag{1.2}$$

where $J_0(\cdot)$ is the zeroth order modified Bessel function of the first kind. Its Fourier transform is the Doppler power spectrum. The channel coherence time is related to the RMS bandwidth f_{RMS} of the Doppler power spectrum as

$$T_c \approx \frac{1}{f_{RMS}}$$

If the coherence time is large compared to the symbol duration, the channel can be assumed to be static over several symbols, which is referred as *slow* fading. Otherwise, the channel is regarded as *fast* fading [32].

In a typical land-mobile-radio channel, it is often assumed that there is no direct line-of-sight (LOS) wave and the receiver obtains only reflected waves. Since the fading is a superposition of a large number of independent scattered components, by the central limit theorem, the components of the received signal can be assumed to be independent Gaussian processes with mean zero and variance σ^2. As a result, the envelope of the received signal at any time instant has a Rayleigh distribution and its phase is uniform between $-\pi$ and π. Therefore, in mobile radio channels, the Rayleigh distribution is commonly used to describe the statistical time-varying nature of the received envelope of a flat-fading signal, or the envelope of an individual multipath component. The Rayleigh distribution has a probability density function

(pdf) given by

$$p(r) = \begin{cases} \frac{r}{\sigma^2} \exp\left(-\frac{r^2}{2\sigma^2}\right), & 0 \leq r \leq \infty \\ 0, & r < 0 \end{cases}$$

where $2\sigma^2$ is the mean power of the multipath signal. If there is a direct (LOS) path wave, the signal envelope is no longer Rayleigh and the distribution of the signal is Ricean [43].

1.2.2 Diversity Techniques

Multipath fading impairs the wireless channel and gives rise to higher bit-error rates. Channel impairments can be reduced by introducing redundancy into the system. One widely-employed method to overcome this performance degradation in a fading channel is the use of diversity. The basic idea of diversity is that, if several independent fading copies of a signal are detected at the receiver, the probability that all of the copies fade simultaneously is very small. Thus, properly combining these independently fading copies can greatly reduce the severity of fading and improve reliability of transmission. The most common forms of diversity employed in mobile radio communications are time diversity, frequency diversity and space diversity [43]:

Time Diversity: In this case identical messages are transmitted in different time slots, ideally with separation between replicas exceeding the coherence time of the channel. Time diversity has been traditionally achieved through the use of error-control coding and interleaving, e.g., convolutional codes with interleaving. Due to the redundancy introduced in the time domain, time diversity results in a loss in

bandwidth efficiency.

Frequency Diversity: This type of diversity provides replicas of the original signal in the frequency domain. This is applicable in cases where the coherence bandwidth of the channel is small compared to the bandwidth of the signal [32]. Frequency diversity has usually been provided by spread spectrum such as direct-sequence spread-spectrum (DSSS)and frequency hopping (FH). More recently, frequency diversity can also be provided by multicarrier modulation methods, such as orthogonal frequency division multiplexing (OFDM). Similar to time diversity, frequency diversity induces a loss in bandwidth efficiency due to the redundancy introduced in the frequency domain.

Space Diversity: Space diversity is also called antenna diversity and it is an effective method for combating multipath fading. It is typically implemented using multiple antennas or antenna arrays arranged together in space for transmission and/or reception [61]. The multiple-antennas are separated by a sufficient distance to allow the signal replicas to undergo independent fading. Unlike time and frequency diversity, space diversity does not result in a loss of bandwidth efficiency, which makes it very attractive for high-data-rate wireless communications.

Depending on whether multiple antennas are used for transmission or reception, space diversity can be classified into two categories: *receive diversity* and *transmit diversity*. Receive diversity has been widely used in the uplink of cellular communication systems, with multiple antennas at the base station to pick up independent copies of the transmitted signal. Receive diversity is characterized by the number of

independent fading branches or paths. These paths are also known as the diversity order and are equal to the number of receive antennas. The replicas of the transmitted signals are properly combined to increase the overall receive SNR and mitigate fading. There are many possible combining methods, including selection combining, switching combining, maximum-ratio combining and equal-gain combining [43, 41].

Transmit diversity [47, 20], which uses multiple antennas at the transmitter, has received less attention than receive diversity. Transmit diversity often requires more signal processing at both the transmitter and the receiver. Because it is generally harder for the transmitter to obtain information about the channel, transmit diversity schemes are often more complex than receive diversity. But with the advent of space-time coding schemes, discussed in the next section, it became possible to implement transmit diversity without knowledge of the channel. In recent years, one new approach to space diversity has emerged which deploys multiple antennas at both the transmitter and the receiver, leading to the so-called multiple-input multiple-output (MIMO) systems.

It is well known that there is a trade-off between data rate and bit-error rate (BER) performance. Channel capacity is defined as the maximum possible transmission rate such that the probability of error can be made arbitrarily small by appropriate encoding and decoding. Shannon showed in his work on information theory [48] that the capacity of a single-input single-output (SISO) channel perturbed by additive white Gaussian noise (AWGN) is a function of the average received signal-to-noise ratio and the bandwidth. In 1998 and 1999, Foschini and Gans [14] and Telatar [58]

showed through information-theoretic results that MIMO systems can offer significant capacity gains compared to the traditional SISO channel. For a Rayleigh flat-fading channel with perfect channel information at the receiver, the capacity grows linearly with the minimum of the number of transmit and receive antennas. When channel state information is known at the transmitter, capacity can be increased by allocating power according to the *water filling principle*, which assigns different power to the eigenmodes of the channel. These results led to extensive research efforts to develop coding and signal processing techniques that can approach the MIMO channel capacity. Examples of these efforts include spatial multiplexing to improve throughput and space-time trellis and block codes to improve reliability.

One of the first MIMO architectures for high-speed wireless communications is the BLAST (Bell-Labs Layered Space Time) system [13, 18], which employs multiple antennas at both the transmitter and the receiver. In vertical-BLAST (V-BLAST), the transmitted data is split equally among the t transmit antennas and simultaneously sent over the channel overlapping in time and frequency, then recovered using suboptimal decoding at the receiver. The receiver has knowledge of the channel and provides receive diversity. BLAST can greatly increase the system throughput with no additional spectrum or power expenditure; however, it has two drawbacks. First, it requires the number of receive antennas be equal to or larger than the number of transmit antennas, which is not always feasible in practice. Second, the performance of the suboptimal BLAST decoding algorithms is limited by error propagation.

An effective and practical way to approach the capacity of MIMO wireless chan-

nel is to employ space-time coding, which is a joint design of error-control coding, modulation, and transmit diversity. In the following, we will briefly review the work on space-time coding.

1.2.3 Space-Time Coding

Space-time coding combines modulation, channel coding and antenna diversity. In space-time coding, the signal is coded across both spatial and time domains to introduce correlation between signals transmitted from various antennas at various time periods. By doing this, both the data rate and the performance can be significantly improved without sacrificing bandwidth. As a consequence, space-time coding has attracted much attention from academic researchers and industrial engineers alike.

The idea of space-time coding was first proposed in [55] by Tarokh, Seshadri and Calderbank. They proved that both diversity gain and coding gain can be obtained simultaneously by employing space-time coding. In order to achieve the maximum diversity advantage on quasi-static flat-fading channel, the difference matrix between any two distinct code matrices among the code constellations has to be full rank. In addition, the minimum determinant of the code difference matrices should be maximized to achieve the maximum coding advantage. The maximum diversity order is the product of the number of transmit and receive antennas. These two conditions are the well-known *rank-and-determinant design criteria*. Based on these criteria, several space time trellis-codes (STTC) have been designed by Tarokh *et al.* [55], Baro *et al.* [3], Chen *et al.* [6] and Jafarkhani *et al.* [30] to improve the performance

of wireless communication systems. While STTC provides good performance, for a fixed number of transmit antennas, the decoding of it requires a vector form of Viterbi decoder.

One of the most practically important space-time codes was proposed by Alamouti in [2], which is a space-time block code (STBC) for systems with two transmit antennas. The Alamouti code is one of the most successful space-time codes because of its good performance and simple decoding algorithm. It has been adopted in third generation cellular standards (e.g., CDMA 2000 [59] and WCDMA [63]). The Alamouti code is a special case of orthogonal space-time codes and was later generalized to any number of transmit antennas by Tarokh and Jafarkhani [56]. Full-rate complex orthogonal space-time codes only exist for two transmit antennas. Orthogonal space-time block codes with rate 3/4 for three and four transmit antennas have been proposed by Tarokh and Jafarkhani [56] and Tirkkone and Hottinen [60]. In recent years, there is some alternative approach on the design of full-rate space-time codes for more than two transmit antennas. Jafarkhani [28] proposed full-rate Quasi-orthogonal codes for four transmit antennas, for which the decoding is done for pairs of symbols. Gamal and Damen [15] proposed full-rate space-time block codes based on algebraic number theories, which can use sphere decoding algorithms.

Thus far, most work on coherent space-time coding has focused on systems with small antenna arrays or high SNRs. Recently there is some work on systems with large numbers of antennas by Biglieri *et al.* [4], Yuan *et al.* [69] and Aktas *et al.* [1], which suggests that Euclidean distance, rather than the rank and determinants,

dominates the code performance for such scenarios. Some space-time trellis codes have been proposed based on this Euclidean distance criterion by Yuan *et al.* [70].

Most of the work on space-time coding has assumed that the receiver has full knowledge of the channel, so that coherent detection can be used. Normally, channel state information (CSI) is obtained through channel estimation using training symbols which are embedded in the transmitted signal. However, channel estimation introduces additional complexity. In addition, if the channel experiences fast fading, channel estimation becomes more complex and may require too many training symbols. In such situations, channel estimation may not be desirable. For situations where the channel is unknown at the receiver, Marzetta and Hochwald [38], [22] and Zheng and Tse [71] investigated the capacity-achieving space-time coding structure. In [23], Hochwald and Marzetta proposed a coding approach for the unknown channels called unitary space-time block codes, in which the signals transmitted by different antennas are mutually orthogonal.

Based on unitary space-time modulation, differential unitary space-time modulation (DSTM) was proposed by Tarokh and Jafarkhani [57], Hughes [26] and Hochwald and Sweldens [24] independently for system with no CSI at both the transmitter and the receiver. DSTM can be regarded as an extension of differential phase-shift keying (DPSK) [41] to multiple-antenna systems. It has been shown in [26] and [24] that for high SNRs, the code design for DSTM also follows the rank-and-determinant design criteria as in the coherent detection case. However, lack of CSI at the receiver results in approximately 3 dB performance loss for differential detection.

Unitary group codes were considered in [26] and [24], for which the constellation of matrices used for transmission forms a group under matrix multiplication. The group designs simplified the analysis and makes modulation and demodulation much more transparent. There is a simple, fast decoding algorithm for diagonal group codes proposed by Clarkson *et. al* [7]. Further results on group codes have been presented by Shokrollahi *et al.* [50], Hughes [27] and Jing and Hassibi [33]. The disadvantages of group codes are that the number of groups available is rather limited, and groups do not lend themselves to very high rates with many antennas.

Tarokh and Jafarkhani proposed a differential modulation scheme for two transmit antennas based on Alamouti's code in [57] and then considered DSTM based on generalized orthogonal designs for more transmit antennas in [29]. For more than two transmit antennas, complex orthogonal codes only provide partial rate, which limits their application for high data-rate transmissions. A coding scheme aimed to provide high data-rate transmission with any number of transmit antennas has been proposed in [21], which uses Cayley transform to map data symbols onto unitary matrices and uses sphere decoding to approach ML performance.

In this section we have provided a brief overview of multiple-antenna space-time coding systems with focus on coding structures. More detailed discussion and technical reviews of MIMO and space-time coding are available in [17, 61, 39, 16, 9].

1.3 Dissertation Outline

In this dissertation, we consider the design of space-time coding for large antenna arrays. We focus on three aspects: performance analysis, code construction and decoding algorithm.

We first investigate the performance of differential space-time modulation for large numbers of antennas. We derive an upper bound on pairwise-error probability and show that the Euclidean distance between codewords is a better performance indicator for DSTM with large numbers of antennas. Therefore, instead of the rank and determinant criteria, the code design for DSTM with large numbers of antennas should follow the Euclidean distance criterion, which is similar to the coherent case. Based on the Euclidean distance criterion, we design some novel space-time codes for two transmit antennas that outperform existing codes such as the Alamouti code [2] for large numbers of antennas.

While the new codes provide superior performance, they generally use maximum-likelihood decoding, which requires an exhaustive search over the entire code constellation. For high-data-rate codes, maximum-likelihood decoding is undesirable. In this dissertation, we further propose a new family of unitary codes for two transmit antennas, based on a different parametrization of 2×2 unitary matrices, and search for good codes with respect to Euclidean distance. We show that not only do the new codes have good performance for systems with large numbers of antennas, but their structure also allows us to use low-complexity suboptimal receivers in which the individual symbols in the code can be sequentially decoded. The code is extended

to non-unitary constellations for coherent detection. We also evaluate the new codes from an information theoretic perspective and consider extensions to more than two transmit antennas.

For DSTM, the channel is usually assumed to remain constant for two adjacent blocks. However, code performance is severe degraded when fast fading is encountered. We will apply multiple-symbol decision-feedback differential detection (DF-DD) to improve the performance of DSTM on fast-fading channel. The suboptimal sequential decoders are used in DF-DD to further reduce the decoding complexity.

The rest of the dissertation is organized as follows. In chap. 2, we derive an upper bound on pairwise-error probability of DSTM with large numbers of antennas. The upper bound indicates that the Euclidean distance between distinct codewords is a good performance indicator for DSTM with large antenna arrays. Therefore codes should be designed according to the Euclidean distance criterion for large antenna arrays or low SNRs, rather than the rank and determinant criteria for high SNR regime. We present some novel unitary codes for two transmit antennas and a large number of receive antennas, which are designed with respect to the Euclidean distance criterion. The new codes outperform existing codes for large antenna arrays.

In chap. 3, we propose a new family of unitary codes for two transmit antennas, with information symbols taken from phase-shift-keying (PSK) constellations. We also derive two low-complexity suboptimal receivers based on generalized likelihood ratio test (GLRT) that allow the individual symbols in the code to be sequentially decoded. We apply the new codes to both coherent and differential space-time mod-

ulation schemes. For coherent detection, quadrature-amplitude-modulation (QAM) constellations are considered to further improve performance. We evaluate the new code by calculating the constellation-constrained capacity. The new coding structure is then extended to more than two transmit antennas.

In chap. 4, we evaluate the performance of the new code in DSTM and fast fading channels. Multiple-symbol decision-feedback differential detection combined with suboptimal GLRT decoders are derived to mitigate the error floor due to large Doppler spread. The analysis is based on the assumption that the channel remains same during a code block and varies according to Jake's model between blocks. In simulation, both block fading and symbol fading (channel varying from symbol to symbol) are investigated. Performance of perfect feedback (genie-aided) differential detection is also provided to show the effect of erroneous feedback.

Finally, in chap. 5, we summarize our conclusions and offer some possible research directions for the future.

Chapter 2

Differential Space-Time Modulation with Large Antenna Arrays

Most space-time coding schemes assume systems operating at high SNRs, which is reasonable for systems with small numbers of antennas. For such case, it has been shown that code design should follow the rank-and-determinant criteria. For systems with large antenna arrays, however, Euclidean distance has been shown to be a better performance indicator for space-time coding with perfect channel knowledge at the receiver. It is of interest to see how DSTM performs with large antenna arrays.

In this chapter, we consider the design and analysis of DSTM for large numbers of transmit and/or receive antennas. We first analyze the performance of DSTM for large arrays. Based on a novel upper bound on the pairwise-error probability, we

conclude that the Euclidean distance is a better performance indicator for DSTM with large number of antennas or low SNRs, rather than the rank and determinant for small antenna arrays or high SNRs. For two transmit antennas and many receive antennas, we design some new codes according to the Euclidean distance criterion.

2.1 Introduction

In recent years, space-time coding has gained a lot of attention because it can efficiently combat fading and significantly improve the capacity in wireless communication systems. Space-time coding is a joint design of error-control coding, modulation, and transmit diversity, in which a number of coded symbols equal to the number of transmit antennas are generated and transmitted simultaneously, one symbol from each antenna.

Most space-time coding techniques assume perfect channel state information (CSI) at the receiver, where coherent detection can be used. Only a small number of transmit and receive antennas is used in those schemes, therefore high SNRs are required to achieve good error performance. For coherent space-time coding in the high SNR regime, codes should be designed according to the rank and determinant criteria [55], that is, optimal codes should have full diversity and a large product distance (coding gain). Full diversity space-time trellis codes are designed in [55], which require a multidimensional (vector) Viterbi algorithm at the receiver for decoding. In [2], Alamouti proposed a simple space-time block code for two transmit antennas, which achieves full diversity with simple linear decoding at the receiver.

Coherent detection assumes perfect channel knowledge at the receiver. This assumption is reasonable for rich scattering environments and stationary or slow moving communicators, where relatively short and infrequent training transmissions are sufficient to track the slow variations in the channel accurately. For some situations, for example, highly mobile communications, however, the channel varies rapidly compared to the symbol rate and perfect channel estimation is questionable. Moreover, if for multiple antenna systems with larger numbers of transmit and receive antennas, longer training sequence is required which reduces the system efficiency significantly. Hence it is desirable to develop techniques that do not require accurate channel estimation at the receiver.

For such situations, Hochwald and Marzetta [23] have proposed the use of unitary space-time codes, in which the signals sent by different transmit antennas are orthogonal and have equal energy. More recently, differential space-time modulation (DSTM) schemes have been proposed that do not require channel estimates at the transmitter or receiver [26, 24, 57]. In [26, 24], it has been proposed that the error probability of differential space-time codes on quasi-static flat fading channels can be made small at high SNRs by designing codes according to the rank and determinant criteria – the same design criteria as those for coherent space-time codes.

More recently, Yuan *et al* [69], Biglieri *et al* [4] and Aktas *et al* [1] have looked at the performance of coherent space-time coding for large antenna arrays and suggested that Euclidean distance is actually a better predictor of performance when the number of transmit and/or receive antennas is large and SNR is low. It is natural to ask

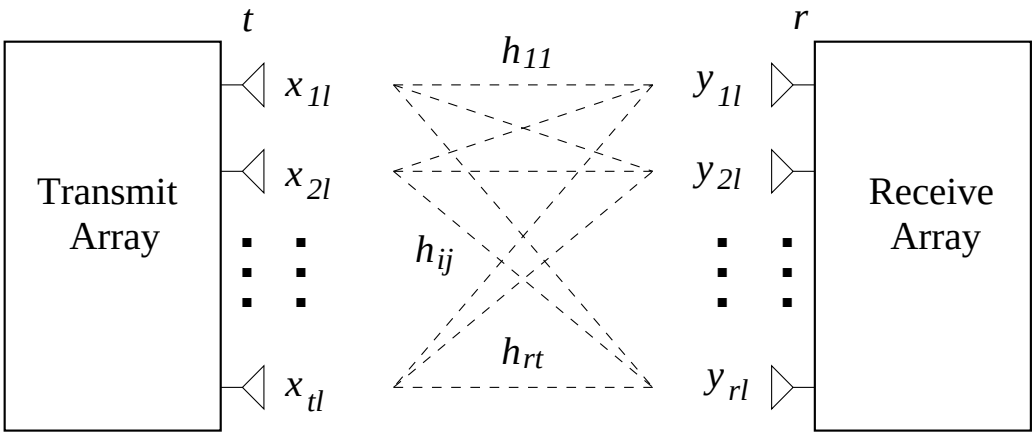

Figure 2.1: MIMO channel model

whether this observation also applies to differential space-time modulation.

In this chapter, we consider the performance analysis and code design for DSTM with large numbers of antennas. Some background on coherent and differential space-time modulation is given in Sec. 2.2. An upper bound on pairwise error probability for DSTM with large arrays is derived in Sec. 2.3. A novel code design criterion is presented and some new codes for two transmit antennas are constructed in Sec. 2.4. The performance of the new codes is examined in Sec. 2.5 and compared with that of the Alamouti code [2]. Finally, conclusions are summarized in Sec. 2.6.

2.2 Preliminary

2.2.1 System Model

Consider a single point-to-point MIMO system with t transmit and r receive antennas as shown in Fig. 2.1. We will focus on a complex baseband linear system

model described in discrete time. Let x_{jl} be the complex signal sent from transmit antenna $j = 1, \cdots, t$ at time $l = 1, \cdots, T$. Under flat-fading conditions, the received signal y_{il} at the ith receive antenna and time l is given by

$$y_{il} = \sum_{j=1}^{t} \sqrt{\rho} h_{ij} x_{jl} + n_{il}, \quad i = 1, \cdots, r, \ l = 1, \cdots, T$$

where h_{ij} is the complex fading path gain from transmit antenna j to receive antenna i and n_{il} is the additive noise. We assume the path gains h_{ij} and noise variables n_{il} are independent and identically distributed (i.i.d) complex Gaussian random variables with probability density function (pdf)

$$p(h) = \frac{1}{\pi} \exp(-|h|^2)$$

We further assume $\mathcal{E}\{\sum_{j=1}^{t} |x_{jl}|^2\} = 1$, that the transmitted signals are normalized to unit power, so that ρ represents the SNR per receive antenna.

Consider a block fading channel where the channel remains constant for a block of T symbols, then jump to independent values for another T transmissions and so on. This piecewise constant fading process mimics the approximate coherence interval of a continuously fading process. It is an accurate representation of many TDMA, frequency-hopping, and block-interleaved systems. If we collect all the transmitted symbols during the kth transmission block into a $t \times T$ matrix

$$X_k = \begin{bmatrix} x_{11} & x_{12} & \cdots & x_{1T} \\ x_{21} & x_{22} & \cdots & x_{2T} \\ \vdots & \vdots & \ddots & \vdots \\ x_{t1} & x_{t2} & \cdots & x_{tT} \end{bmatrix}$$

where columns represent different times and rows represent different antennas, we can rewrite the channel in an equivalent matrix form:

$$Y_k = \sqrt{\rho} H_k X_k + N_k, \quad k = 1, \cdots, K \tag{2.1}$$

where $Y_k = \{y_{il}\}$ is the $r \times T$ received symbols, $H_k = \{h_{ij}\}$ is the $r \times t$ fading matrix and $N_k = \{n_{il}\}$ is the $r \times T$ noise matrix for the kth block.

2.2.2 Coherent Space-Time Coding

In this work, we consider space-time block codes, for which $X_1, \cdots, X_K$ in (2.1) is taken from some $t \times T$ space-time block code constellation $\mathcal{X}$. For slowly-varying channels, CSI can be obtained by sending training symbols from the transmitter to the receiver. If CSI is available at the receiver, coherent reception can be used. For such case, the conditional pdf of the received signal is given by (the block subscript k is dropped)

$$p(Y|X, H) = \frac{1}{\pi^{tr}} \exp(- \parallel Y - \sqrt{\rho} H X \parallel^2) \tag{2.2}$$

where $\parallel A \parallel = \sqrt{\mathrm{Tr}[AA^H]}$ is the matrix Frobenius norm, A^H denotes the conjugate transpose of matrix A and $\mathrm{Tr}[\cdot]$ is the trace operator.

The optimal decoder searches over $\mathcal{X}$ to maximize (2.2), which can be expressed equivalently as

$$\hat{X} = \arg \min_{X \in \mathcal{X}} \parallel Y - \sqrt{\rho} H X \parallel \tag{2.3}$$

For coded systems, the pairwise error probability (PEP) forms the basic structure for the union bound calculation of the error probability and is used as the main criteria

for code design. For the coherent space-time decoder (2.3), the PEP between the transmitted signal X and the erroneously decoding result $\hat{X}$ is upper bounded by [55]

$$\Pr(X \to \hat{X}) \leq \frac{1}{2} \prod_{i=1}^{t} \left(1 + \frac{\rho}{4}\lambda_i\right)^{-r} \tag{2.4}$$

where λ_i denotes the ith eigenvalue of the code distance matrix $(X-\hat{X})(X-\hat{X})^H$. A code is referred as a full diversity code if each code distance matrix has a rank equal to the number of transmit antennas t, or equivalently each eigenvalue $\lambda_1, \cdots, \lambda_t$ has a positive value for all $X \neq \hat{X}$ in $\mathcal{X}$.

Most early work on coherent space-time coding assumes a system operating at high SNRs ($\rho >> 1$), where the PEP upper bound can be simplified as [55]

$$\Pr(X \to \hat{X}) \leq \frac{1}{2} \left(\frac{\rho}{4}\Lambda_p(X, \hat{X})\right)^{-rt} \tag{2.5}$$

where Λ_p is the *product distance* defined as

$$\begin{aligned} \Lambda_p(X, \hat{X}) &= |(X - \hat{X})(X - \hat{X})^H|^{1/t} && (2.6) \\ &= \left(\prod_{i=1}^{t} \lambda_i\right)^{1/t} && (2.7) \end{aligned}$$

(2.5) indicates that for better error performance, the distance matrix between any two distinct codewords among the code constellation should have full rank and a large product distance. This results in the well-known rank and determinant criteria [55]. Codes constructed according to these criteria provides both full diversity and coding gain.

For two transmit antennas, Alamouti [2] has proposed a simple space-time block

code

$$\begin{bmatrix} x_1 & x_2 \\ -x_2^* & x_1^* \end{bmatrix} \tag{2.8}$$

where x_1 and x_2 are taken from a complex constellation $\mathcal{C}$. Alamouti code achieves full diversity and its orthogonal structure ensures simple linear processing at the receiver.

The results in [55] is suitable for high SNRs, which is a reasonable assumption for systems with small numbers of antennas, for example, using only one or two receive antennas. For systems with large numbers of antennas, the bit error performance of interest normally falls in low SNR regime. In recent years, several researchers investigate the performance of coherent space-time coding for such scenarios [69, 4, 1]. For large numbers of antenna or low SNRs, the PEP can be approximated by [1] (see also [70])

$$\Pr(X \to \hat{X}) \leq \frac{1}{2}\left[1 + \frac{\rho}{4}\sum_{i=1}^{t}\lambda_i\right]^{-r} = \frac{1}{2}\left[1 + \frac{\rho}{4} \parallel X - \hat{X} \parallel^2\right]^{-r} \tag{2.9}$$

Defining the minimum *Euclidean distance* between codewords as

$$\Lambda_e \;=\; \min_{X \neq \hat{X}} \parallel X - \hat{X} \parallel \;=\; \sqrt{\mathrm{Tr}\left\{(X - \hat{X})(X - \hat{X})^H\right\}} \tag{2.10}$$

one can conclude that Λ_e is the dominant performance indicator for coherent detection with large arrays or low SNRs.

2.2.3 Differential Space-Time Modulation (DSTM)

Coherent detection requires channel estimation to obtain accurate CSI at the receiver. In some situations, for example, for fast fading channels or systems with

large numbers of transmit or receive antennas , channel estimation may be difficult or costly. Therefore, non-coherent detection becomes attractive for such scenarios.

For single antenna systems, differential phase-shift-keying (DPSK) is well known as an efficient non-coherent detection method. Several researchers [57, 26, 24] extended DPSK to differential space-time modulation (DSTM) for multiple-antenna systems. In DSTM, data are differential encoded using unitary codes. In the following, we will introduce the general structure of DSTM in [26, 24].

In DSTM, the block length is assumed to be equal to the number of transmit antennas, $T = t$. At the kth block, data is transmitted in the form of $t \times t$ information matrix U_k, which is selected from a constellation of unitary matrices $\mathcal{U}$, so that $U_k U_k^H = I_t$. The transmitted matrices are then formed by differential encoding:

$$X_k \;=\; X_{k-1} U_k,\; k = 1, \ldots, K. \tag{2.11}$$

where X_{k-1} is the previous transmitted block. Here the initial matrix X_0 is any fixed given unitary matrix.

If the fading coefficients are assumed to be approximately constant for $2t$ channel symbols, then $H_k \approx H_{k-1}$ and the received blocks are related by [24]

$$Y_k = Y_{k-1} U_k + N'_k \tag{2.12}$$

where $N'_k = N_k - U_k N_{k-1}$ is statistically independent of U_k. Notice (2.12) does not depend on channel matrix H_k or the previous transmitted matrix X_{k-1}. Hence, the information blocks can be detected without channel estimates using the simple

differential receiver [26]

$$\hat{U}_k \;=\; \arg \max_{U \in \mathcal{U}} \; \mathrm{ReTr}\{Y_k^H Y_{k-1} U\} \;, \tag{2.13}$$

where "ReTr" denotes the real part of the matrix trace.

For this detector, the pairwise error probability (PEP) is upper bounded by [26, 24]

$$\Pr(U \to \hat{U}) \leq \frac{1}{2} \prod_{i=1}^{t} \left[1 + \frac{\rho^2}{4(1+2\rho)} \lambda_i \right]^{-r} \tag{2.14}$$

where λ_i denotes the ith eigenvalue of the code distance matrix $(U - \hat{U})(U - \hat{U})^H$. Similar to the coherent modulation case, the high SNR approximation for this upper bound is

$$\Pr(U \to \hat{U}) \leq \frac{1}{2} \left(\frac{8}{\rho} \right)^{tr} \left(\prod_{i=1}^{t} \lambda_i \right)^{-r} \tag{2.15}$$

(2.15) is essentially same as the (2.5), only with 3 dB loss in the SNR term. Hence the code design of DSTM at high SNRs should also follow the rank-and-determinant criteria. The pairwise error probability of DSTM suffers a 3dB loss relative to that of coherent detection due to the lack of channel knowledge at the receiver.

There has been much work on the code design for DSTM [26, 24, 57, 21, 15]. Most work on differential space-time code design follows rank and determinant criteria, which is valid for high SNR regime. For large r and t, however, error probabilities of practical interest are often achieved by modest or low SNRs, where the rank and determinant criteria do not apply. Consequently, our aim in this work is to develop new design criteria applicable to large t and r, and low SNR. To this end, we will consider the upper bound for pairwise error probability.

2.3 Error Probability Upper Bound and Code Design Criterion

Symbol error probability (SEP) is a commonly used performance measures for diversity schemes. Unfortunately, the SEP is not always analytically tractable for the purpose of design of diversity techniques. Instead, the pairwise error probability (PEP), which is commonly used to upper bound the SEP [41], is more convenient to analyze. An advantage of PEP based criteria is that they are independent of the symbol constellation.

In this section, we will analyze the PEP for the differential decoder (2.13) with large antenna arrays. To this end, we begin by deriving a bound on the pairwise error probability, conditioned on the current channel fading matrix H.

For the differential decoder (2.13), the transmitted matrix U is erroneously decoded as $\hat{U}$ only if

$$\Delta \;=\; \mathrm{ReTr}\{(\hat{U}-U)Y_k^H Y_{k-1}\} \geq 0 \;.$$

Therefore the pairwise error probability, conditioned on H, can be written as

$$\Pr(U \to \hat{U}|H) = \Pr(2\Delta \geq 0|U,H) \;. \tag{2.16}$$

An upper bound on this conditional pairwise error probability can be obtained using methods similar to [25]. We start by obtaining an approximation for the equivalent received signal

$$Y_{k-1}^H Y_k \;=\; (\sqrt{\rho}HX_{k-1}+N_{k-1})^H(\sqrt{\rho}HX_k+N_k)$$

$$
\begin{aligned}
&= \rho X_{k-1}^H H^H H X_k + \sqrt{\rho} X_{k-1}^H H^H N_k + \sqrt{\rho} N_{k-1}^H H X_k + N_{k-1}^H N_k \\
&\approx \rho X_{k-1}^H H^H H X_k + \sqrt{\rho} X_{k-1}^H H^H N_k + \sqrt{\rho} N_{k-1}^H H X_k
\end{aligned}
$$

where the second-order noise term is ignored. Therefore the difference metric is approximated by

$$
\begin{aligned}
\Delta &= -\rho \mathrm{ReTr}\left\{X_{k-1}^H H^H H X_k (U-\hat{U})^H\right\} - \sqrt{\rho}\mathrm{ReTr}\left\{X_{k-1}^H H^H N_k (U-\hat{U})^H\right\} \\
&\quad -\sqrt{\rho}\mathrm{ReTr}\left\{N_{k-1}^H H X_k (U-\hat{U})^H\right\}
\end{aligned}
$$

Applying the Chernoff bound, we obtain for all $s \geq 0$

$$
\begin{aligned}
&\Pr(U \to \hat{U}|U,H) = \Pr(2\Delta \geq 0|U,H) \\
&\leq \exp\left[-(2s\rho)\mathrm{ReTr}\left\{X_{k-1}^H H^H H X_k (U-\hat{U})^H\right\}\right] \\
&\quad \times \mathcal{E}_{N_k}\left(\exp\left[-2s\sqrt{\rho}\mathrm{ReTr}\left\{X_{k-1}^H H^H N_k (U-\hat{U})^H\right\}\right]\right) \\
&\quad \times \mathcal{E}_{N_{k-1}}\left(\exp\left[-2s\sqrt{\rho/t}\mathrm{ReTr}\left\{N_{k-1}^H H X_k (U-\hat{U})^H\right\}\right]\right) \\
&= \exp\left[-s\rho(1-2s)\mathrm{Tr}\left\{H(U-\hat{U})(U-\hat{U})^H H^H\right\}\right] . \qquad (2.17)
\end{aligned}
$$

For fixed H, this bound is minimized by $s = 1/4$, which yields

$$
\begin{aligned}
\Pr(U \to \hat{U}|U,H) &\leq \exp\left[-\frac{\rho}{8}\mathrm{Tr}\left\{H(U-\hat{U})(U-\hat{U})^H H^H\right\}\right] \\
&= \exp\left[-\frac{\rho}{8} \parallel H(U-\hat{U}) \parallel^2\right] \qquad (2.18)
\end{aligned}
$$

For fixed t, it is shown in [4] that

$$
\frac{1}{r}\mathrm{Tr}\left\{H(U-\hat{U})(U-\hat{U})^H H^H\right\}
$$

converges almost surely as $r \to \infty$ to $\parallel U-\hat{U} \parallel^2$. The same is shown for $r, t \to \infty$ with $r/t \to c > 0$. In [70], the authors assert without proof that the exponent above converges to a Gaussian random variable as $r \cdot \nu \to \infty$, where ν is the rank of $(U-\hat{U})$.

For fixed t and $r \to \infty$, this is clearly true; however, for fixed r and $\nu \to \infty$, it is not difficult to contrive counterexamples. It therefore appears that additional conditions on $U - \hat{U}$ are needed. We now show that if U and $\hat{U}$ are *unitary*, and the distance per dimension is bounded away from zero

$$\frac{1}{\nu} \parallel U - \hat{U} \parallel^2 \geq \ d \ > \ 0 \ , \tag{2.19}$$

then convergence of the (suitably normalized) exponent to a Gaussian distribution is assured as $\nu \to \infty$.

To this end, define the $t \times t$ codeword distance matrix

$$A(U, \hat{U}) = (U - \hat{U})(U - \hat{U})^H \ . \tag{2.20}$$

Since $A(U, \hat{U})$ is a nonnegative-definite Hermitian matrix, there exists a unitary matrix V and a real diagonal matrix Λ such that $VA(U, \hat{U})V^H = \Lambda$. Let $\mathbf{v}_1, \mathbf{v}_2, \cdots, \mathbf{v}_t$ and $\mathbf{h}_i, \ldots, \mathbf{h}_r$ denote the rows of V and H, respectively, and define $U_{ij} = |\mathbf{h_i v_j}^H|^2$. The bound (2.18) can then be rewritten as

$$\Pr(U \to \hat{U}|U, H) \ \leq \ \exp\left(-\frac{\rho}{8} \sum_{i=1}^{r} \sum_{j=1}^{\nu} \lambda_j U_{ij}\right) \ . \tag{2.21}$$

where $\lambda_j > 0, j = 1, 2, \ldots, \nu$ are the non-zero eigenvalues of $A(U, \hat{U})$. Since the rows of V are orthonormal, $\mathbf{h_i v_j}^H$ are i.i.d $\mathcal{C}N(0, 1)$ random variables. It follows that the U_{ij} are i.i.d. exponential random variables with pdf $p(t) = e^{-t}u(t)$, and mean and variance 1.

Now consider the normalized sum

$$S_{r\nu} = \sum_{i=1}^{r} \sum_{j=1}^{\nu} Z_{ij} \ \text{ where } \ Z_{ij} = \frac{\lambda_j (U_{ij} - 1)}{\sqrt{r \sum_{j=1}^{\nu} \lambda_j^2}} \ . \tag{2.22}$$

Observe that Z_{ij} has mean zero and variance

$$\sigma_{ij}^2 = \frac{\lambda_j^2}{r\sum_{j=1}^{\nu}\lambda_j^2} \quad \text{where} \quad \sum_{i=1}^{r}\sum_{j=1}^{\nu}\sigma_{ij}^2 = 1 \ .$$

Let $\xrightarrow{d}$ denote convergence in distribution. By the Lindeberg-Feller version of the Central Limit Theorem [49, pp. 326], a sufficient condition for $S_{r\nu} \xrightarrow{d} \mathcal{N}(0,1)$ as $r\nu \to \infty$ is the *Lindeberg condition*: For all $\epsilon > 0$, we have

$$\lim_{rv\to\infty}\sum_{i=1}^{r}\sum_{j=1}^{\nu}\mathcal{E}\left[Z_{ij}^2 I_{[\epsilon,\infty)}\left(|Z_{ij}|\right)\right] \ = \ 0$$

where $I_{[\epsilon,\infty)}(x)$ is the indicator function. Substituting Z_{ij} into the sum above, we obtain

$$\begin{aligned}
&\sum_{i=1}^{r}\sum_{j=1}^{\nu}\sigma_{ij}^2\int_{|\sigma_{ij}(t-1)|>\epsilon}(t-1)^2e^{-t}u(t)dt \\
&\quad\leq \ e\sum_{i=1}^{r}\sum_{j=1}^{\nu}\sigma_{ij}^2\int_{|\sigma_{ij}(t-1)|>\epsilon}(t-1)^2e^{-|t-1|}u(t)dt \\
&\quad\leq \ 2e\sum_{i=1}^{r}\sum_{j=1}^{\nu}\sigma_{ij}^2\int_{\epsilon/\sigma_{ij}}^{\infty}y^2e^{-y}dy \ , \qquad (2.23)
\end{aligned}$$

where the first step follows from $t \geq |t-1|-1$ for $t \geq 0$, and the second from $u(t) \leq 1$ and the change of variable $y = t-1$. Observing that $g(y) = y^4e^{-y}$ takes on its maximum value for $y \geq 0$ at $y = 4$ and $2eg(4) < 26$, we can bound the right side above by

$$\begin{aligned}
2e\sum_{i=1}^{r}\sum_{j=1}^{\nu}\sigma_{ij}^2\int_{\epsilon/\sigma_{ij}}^{\infty}\frac{g(y)}{y^2}dy \ &\leq \ \sum_{i=1}^{r}\sum_{j=1}^{\nu}\sigma_{ij}^2\int_{\epsilon/\sigma_{ij}}^{\infty}\frac{26}{y^2}dy \ = \ \frac{26}{\epsilon}\sum_{i=1}^{r}\sum_{j=1}^{\nu}\sigma_{ij}^3 \\
&= \ \frac{26\sum_{j=1}^{\nu}\lambda_j^3}{\epsilon\sqrt{r}(\sum_{j=1}^{t}\lambda_j^2)^{\frac{3}{2}}} \ . \qquad (2.24)
\end{aligned}$$

From this it is clear (as noted in [69]) that $S_{r\nu}$ always satisfies the Lindeberg condition for fixed t and $r \to \infty$. We now show that $S_{r\nu}$ also satisfies the Lindeberg condition

for fixed r and $\nu \to \infty$, provided that (2.19) is satisfied.To prove this, let $\bar{\lambda}(A)$ denote the spectral norm of A. Since U and $\hat{U}$ are unitary, we have $\bar{\lambda}(U) = \bar{\lambda}(\hat{U}) = 1$. We therefore have

$$\bar{\lambda}(A(U,\hat{U})) = \bar{\lambda}(U-\hat{U})^2 \leq \left(\bar{\lambda}(U) + \bar{\lambda}(\hat{U})\right)^2 = 4$$

and thus each λ_j is bounded between 0 and 4. By convexity of $f(x) = x^2$, we have

$$\frac{1}{\nu}\sum_{j=1}^{\nu}\lambda_j^2 \;\geq\; \left(\frac{1}{\nu}\sum_{j=1}^{\nu}\lambda_j\right)^2 \geq d^2 \;.$$

Combining these facts, we obtain

$$\frac{26\sum_{j=1}^{\nu}\lambda_j^3}{\epsilon\sqrt{r}(\sum_{j=1}^{\nu}\lambda_j^2)^{\frac{3}{2}}} \;\leq\; \frac{26\cdot 4}{\epsilon\sqrt{r}(\sum_{j=1}^{\nu}\lambda_j^2)^{\frac{1}{2}}} \;\leq\; \frac{104}{\epsilon\sqrt{r}(\sum_{j=1}^{\nu}\lambda_j^2)^{\frac{1}{2}}} \leq \frac{104}{\epsilon d\sqrt{r\nu}} \;,$$

from which we conclude that $S_{r\nu}$ satisfies the Lindeberg condition for $\nu \to \infty$. Therefore, $S_{r\nu} \xrightarrow{d} \mathcal{N}(0,1)$ as $r\nu \to \infty$. It follows that the quantity $(1/r)\sum_{i=1}^{r}\sum_{j=1}^{\nu}\lambda_j U_{ij}$ approaches a Gaussian random variable D with $\mathcal{N}(\mu_D, \sigma_D^2)$ where

$$\mu_D = \sum_{j=1}^{\nu}\lambda_j \quad \text{and} \quad \sigma_D^2 = \sum_{j=1}^{\nu}\lambda_j^2/r$$

The differential pairwise error probability is then bounded by

$$\begin{aligned}
\Pr(U \to \hat{U}) &\leq \int_{-\infty}^{+\infty}\exp(-\frac{\rho r}{8}D)p(D)dD \\
&= \exp(-\frac{\rho r}{8}\mu_D + \frac{\rho^2 r^2}{128}\sigma_D^2) \\
&\approx \exp\left(-\frac{\rho r}{8}\Lambda_e^2(U,\hat{U})\right) \qquad (2.25)
\end{aligned}$$

where $\Lambda_e = ||U - \hat{U}||$ as the Euclidean distance of U and $\hat{U}$ and the last approximation is valid for small $\rho \ll 1$. Thus we conclude that, for large arrays and low

SNRs, Euclidean distance is an appropriate design criterion for differential space-time modulation.

Recall that for small arrays or high SNR, the pairwise error probability of DSTM is bounded by (2.15), which depends on the rank and product distance of the code distance matrices. Therefore the code design is constrained to full diversity codes. For large arrays or low SNR, however, (2.25) indicates that optimal codes may not have full diversity.

Therefore, the differential pairwise error probability upper bounds (2.25) and (2.15) suggest that the design criteria for DSTM over quasi-static Raleigh fading channel depend on the array size, which leads to the following code design criteria: For small arrays, (2.15) shows that the rank and product distance are the dominant parameters in code performance. In order to minimize the error probability for small arrays, codes should have full diversity. In addition, the minimum product distance (2.7) over all pairs of distinct matrices in $\mathcal{U}$ should be maximized.

For large arrays, (2.25) suggests that the pairwise error probability is dominated by Euclidean distance. In order to minimize the error probability for large arrays, we need to maximize the minimum Euclidean distance over all pairs of distinct matrices in $\mathcal{U}$. As (2.25) doesn't depend on the rank ν, codes that achieve good performance for large arrays may not have full diversity.

Note that this design criterion is essentially the same as the one given in [69] for perfect channel state information at the receiver. Therefore, if a unitary space-time code is designed to be optimal when perfect channel estimates are available at the

receiver, then the differentially-encoded version of this code will also be optimal in absence of CSI.

2.4 Code Construction for Large Arrays

We have shown that for system with large numbers of antennas, Euclidean distance is a better indicator of the performance. This result widens the scope for space-time block code design. Previously, most of the space-time block codes are restricted to have full diversity. Removing this constraint might result in codes that perform better than existing codes for large arrays.

We now use the Euclidean distance criterion to construct new differential unitary space-time codes appropriate for two transmit antennas and many receive antennas. For two transmit antennas, several codes with good performance for small arrays have already been presented in the literature, such as the differential scheme based on Alamouti's code in [57] and the group codes in [26, 24]. In this section, we begin with reconsidering the performance of these codes using the Euclidean distance criterion. Then we will proposing some new codes that perform well for a large number of receive antennas .

Group Codes

Group codes, in which the code constellation forms a group under multiplication, have been investigated in [26] and [23]. It has been shown by Hughes [26] that for

$M = 2^p > 1$, all full diversity unitary group codes with constellation size $|\mathcal{U}| = M$ and $t = 2$ are either cyclic or dicyclic codes. For small arrays, optimal group codes that have full rank and maximum of the minimum product distance over the code constellation have been designed for $2 \leq M \leq 32$. The optimal group codes for large arrays, however, may not have full diversity. In the following, we will give the following generalized form for cyclic and dicyclic group codes:

The (M, k, n) cyclic group code is given by

$$\mathcal{U} = \left\langle \begin{bmatrix} \eta_M^n & 0 \\ 0 & \eta_M^k \end{bmatrix} \right\rangle \tag{2.26}$$

where $\eta_M = \exp(2\pi j/M)$, and $1 \leq n \leq k \leq \frac{M}{2} - 1$. The cyclic code takes values in the M-PSK constellation and has $|\mathcal{U}| = M$ code matrices. The minimum Euclidean distance over $\mathcal{U}$ is

$$\Lambda_e = \min_{U \neq \hat{U}} \Lambda_e(U, \hat{U}) = \min_{1 \leq l \leq M-1} 2\sqrt{\left[\sin^2(\pi ln/M) + \sin^2(\pi lk/M)\right]}$$

For all $M \geq 8$, the (M, k, n) dicyclic group code is given by

$$\mathcal{U} = \left\langle \begin{bmatrix} \eta_{M/2}^n & 0 \\ 0 & \eta_{M/2}^k \end{bmatrix}, \begin{bmatrix} 0 & -1 \\ 1 & 0 \end{bmatrix} \right\rangle \tag{2.27}$$

with $1 \leq n \leq k \leq M/4 - 1$. Its minimum Euclidean distance is given by $\Lambda_e = \min \langle \Lambda_e(M/2), 2 \rangle$, where $\Lambda_e(M/2)$ is the Euclidean distance of the $(M/2, k, n)$ cyclic code.

The optimal group codes for large arrays are given in Table 2.1 for $2 \leq M \leq 64$. For each code, we list the Euclidean distance and product distance. We also list the optimal group codes in terms of rank and determinant criteria for small arrays as in

Table 2.1: Optimal unitary group codes for large and small receive arrays

	Large Arrays			Small Arrays		
R	$\mathcal{U}$	Λ_e	Λ_p	$\mathcal{U}$	Λ_e	Λ_p
0.5	(2,1,1) cyclic	2.8284	4	(2,1,1) cyclic	2.8284	4
1.0	(4,1,1) cyclic	2	2	(4,1,1) cyclic	2	2
1.5	(8,3,1) dicyclic	2	2	(8,3,1) dicyclic	2	2
2	(16,3,1) dicyclic	2	0	(16,7,1) dicyclic	1.0824	0.5858
2.5	(32,4,1) dicyclic	1.4142	0	(32,9,1) cyclic	1.0824	0.2487
3	(64,5,3) dicyclic	1.0824	0	(64,19,1) cyclic	0.7349	0.1576

Table I of [26]. It is clear that the optimal group codes for small arrays may not be optimal for large arrays.

Alamouti Code

As already shown in (2.8), The Alamouti code [2] transmits two information symbols per block. It is an special case of space-time orthogonal codes [56] applied to two transmit antennas. The Alamouti code has full diversity and it achieves capacity for one receive antenna. The application of this codes to differential transmission was proposed in [57]

$$U \;=\; \frac{1}{\sqrt{2}} \begin{bmatrix} x_1 & x_2 \\ -x_2^* & x_1^* \end{bmatrix} , \tag{2.28}$$

where x_1 and x_2 are taken from M-ary phase shift key (PSK) constellation and $\frac{1}{\sqrt{2}}$ is the normalization factor.

The Euclidean distance of the Alamouti code can be expressed as

$$\Lambda_e \;=\; \min_{U \neq \hat{U}} ||U - \hat{U}|| \;=\; 2\sin(\pi/M) \tag{2.29}$$

For example, for rate $R = 3$ bps/Hz, the elements of the Alamouti code matrix lie in the 8PSK constellation and hence we have $\Lambda_e = 0.7654$.

Steiner code

Next, we will consider the construction of unitary codes based on the Gram-Schmidt procedure. For a matrix

$$U = \frac{1}{\sqrt{2}} \begin{bmatrix} x_1 & x_2 \\ x_4 & x_3 \end{bmatrix}$$

to be unitary, we must have $|x_1|^2 + |x_2|^2 = 2$, $|x_3|^2 + |x_4|^2 = 2$ and $x_4 x_1^* = -x_3 x_2^*$. For simplicity, if we impose the constraint that x_1, x_2, x_3 and x_4 are taken from the M-PSK constellation, we obtain

$$U = \frac{1}{\sqrt{2}} \begin{bmatrix} x_1 & x_2 \\ -x_3 x_2^* x_1 & x_3 \end{bmatrix}, \tag{2.30}$$

Notice that an equivalent form of this code has been presented by Steiner *et al* in [51], therefore we will denote this code as Steiner code. The authors in [51] indicate this code can be used for large antenna array by observing that one extra information symbol is used compared to the Alamouti code. We will now consider the performance of this code by looking at its Euclidean distance

$$\Lambda_e = \min_{U \neq \hat{U}} ||U - \hat{U}|| = 2\sin(\pi/M) \tag{2.31}$$

Notice that the Euclidean distance expression of the Steiner code takes the same form as (2.29) for the Alamouti code. That's, for a given M-PSK constellation, the Alamouti code and the Steiner codes have the same minimum Euclidean distance.

The Steiner code, however, achieves a rate that is 1.5 times larger. Alternatively, for the same rate, the Steiner code can use a smaller scalar constellation and thereby achieve a larger Euclidean distance. Take the rate 3 bps/Hz code for example. The Alamouti code with 8 PSK has $\Lambda_e = 0.7654$. By contrast, the elements of the rate 3 Steiner code matrix lie in the QPSK ($M = 4$) constellation, which yields a larger Euclidean distance $\Lambda_e = 1.4142$.

Note that the Steiner code do not have full rank, therefore it is not a full diversity code. Hence, this code is of interest primarily for large receiver arrays.

Modified-Alamouti (MA) Code

We next consider a family of codes which are closely related to the Alamouti code, given by

$$U = \frac{1}{\sqrt{2}} \begin{bmatrix} x_1 & x_2 \\ -x_2^* \triangle_{\mathbf{x}} & x_1^* \triangle_{\mathbf{x}} \end{bmatrix} \tag{2.32}$$

where x_1, x_2 and $\triangle_{\mathbf{x}}$ are unit-magnitude numbers, and $\triangle_{\mathbf{x}}$ is a function of x_1 and x_2. We call this code the Modified-Alamouti (MA) code. For simplicity, we let $\triangle_{\mathbf{x}} = x_1^m x_2^n$ with m and n taken from $[0 : 0.5 : M/2]$ and choose m and n to maximize the resulting Euclidean distance Λ_e. Generally, we can get optimal MA codes that have better Euclidean distance than Alamouti code. For example, for $R = 3$ bps/Hz, the choice $m = 4$ and $n = 2.5$ yields a code with the largest Euclidean distance, $\Lambda_e = 1.2593$. This code also achieves full diversity, although the product distance is smaller than that of the corresponding Alamouti code.

Modified Steiner (MS) code

We now consider a class of unitary codes given by

$$G = \frac{1}{\sqrt{2}} \begin{bmatrix} x & x^p \\ x^q & -x^{p+q-1} \end{bmatrix} \tag{2.33}$$

where x is taken from M-PSK constellation. Notice that this coding structure has some similarity to the Steiner code in the sense that the fourth symbol is the multiplication (conjugate) of three other symbols. Hence we refer this code as Modified Steiner (MS) code. Here, instead of taking three symbols independently from PSK constellation as in Steiner code, all the symbols are function of one parameter x. Consequently, in order to achieve the same rate, x must be taken from a larger constellation than those for x_1, x_2 and x_3 in (2.30). For example, x need to be taken from 64 PSK to construct a rate 3 bps/Hz code.

The minimum Euclidean distance of the MS code can be expressed as

$$\Lambda_e = \min_{n \in \{1,\cdots,M-1\}} \sqrt{f_e(n)} \tag{2.34}$$

where

$$\begin{aligned} f_e(n) &= 2\sin^2(\pi n/M) + 2\sin^2(\pi p n/M) \\ &\quad +2\sin^2(\pi q n/M) + 2\sin^2(\pi(p+q-1)n/M) \end{aligned}$$

For simplicity, here we let p and q take integer values and choose them to maximize the resulting minimum Euclidean distance Λ_e. We can get codes that have better Euclidean distance than the Alamouti code. For example, for rate $R = 3$ bps/Hz, the full diversity MS code with $p = 44$, $q = 34$ has $\Lambda_e = 1.3725$, which is larger than

that of the Alamouti code $\Lambda_e = 0.7654$. At this rate, the Steiner code without full diversity has $\Lambda_e = 1.4142$, which has slight gain relative to the MS code.

Table 2.2 summarizes the Euclidean distance performance of the codes discussed above. Also shown for comparison are the product distances of these codes. Cyclic and dicyclic denote the cyclic and dicyclic group codes respectively. The parameters for MS and MA codes are (p, q) and (m, n), respectively. From the table, we can conclude that codes that have large Λ_e may not necessarily have large Λ_p, which confirms the results in Sec. 2.3.

Table 2.2: Code comparison for large receive arrays

R	$\mathcal{U}$	Λ_e	Λ_p
1	Alamouti	2	2
	MS(0,0)	2	2
	MA(0,0)	2	2
	cyclic(4,1,1)	2	2
2	Alamouti	1.4142	1
	Steiner(9,3)	2	1.4142
	MA(2,2)	2	1
	dicyclic(16,3,1)	2	0
3	Alamouti	0.7654	0.2929
	dicyclic(64,5,3)	1.0824	0
	MA(4,2.5)	1.2593	0.0297
	MS(44,34)	1.3725	0.0341
	Steiner	1.4142	0
4	Alamouti	0.3902	0.0761
	dicyclic(256, 53,4)	0.5683	0
	MA(8,6.5)	0.7654	0.0297
	Steiner	0.7654	0
	MS(221,42)	0.9719	0.0315

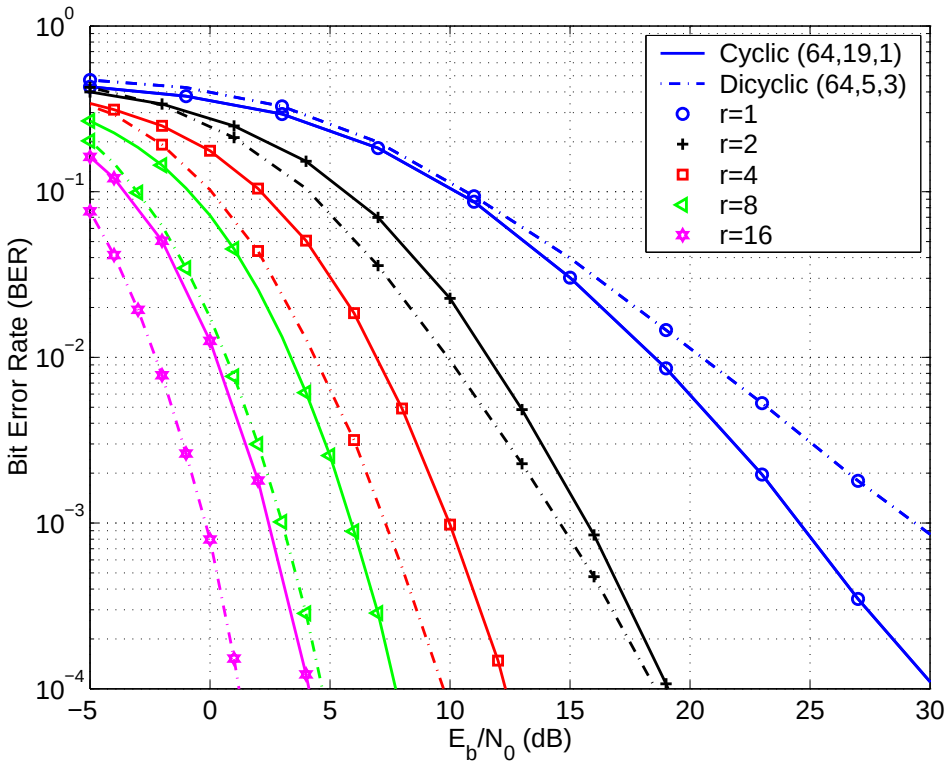

Figure 2.2: BER performance of cyclic vs dicyclic group codes for $R = 3$ bps/Hz and $r = 1, 2, 4, 8, 16$

2.5 Numerical Results

In this section, we will investigate the performance of the codes discuss in Sec. 2.4 for differential space-time modulation. For each code, we consider the rate of $R = 3$ bps/Hz and the number of receive antennas varies from 1, 2, 4, 8 to 16. The codes are taken from Table. 2.2. Here Rayleigh flat fading channel is assumed where the channel coefficients remains constant for two adjunct blocks.

We will first compare the performance of the (64, 19, 1) cyclic group code and (64, 5, 3) dicyclic group code, designed for small and large arrays respectively for $R = 3$ bps/Hz. The simulated bit-error rate (BER) performance is shown in Fig. 2.2.

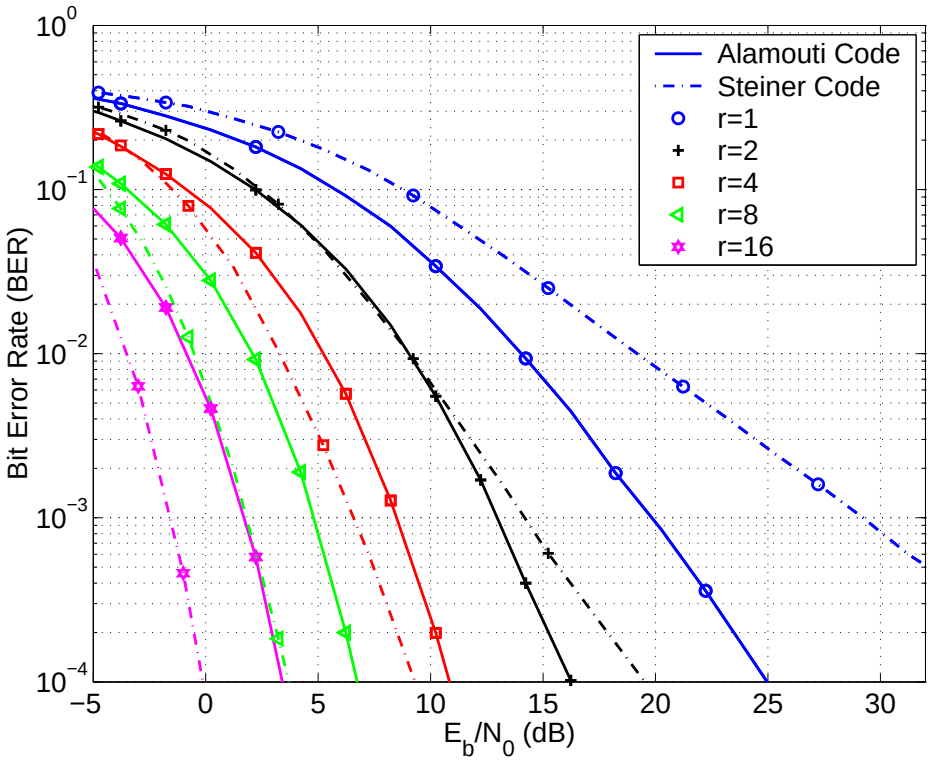

Figure 2.3: BER performance of Alamouti vs Steiner codes for $R = 3$ bps/Hz and $r = 1, 2, 4, 8, 16$

On the far right of the figure, the cyclic group code outperforms the dicyclic group code by several dB for $r = 1$, which can be explained by the fact that the cyclic group code has full diversity while the dicyclic group code is rank deficient. However, beginning from $r = 2$, the dicyclic group outperforms the cyclic group. In particular, at a BER of 10^{-4}, the dicyclic code outperforms the cyclic code by approximately 2 dB for $r = 4$, and by 3 dB for $r = 16$. The simulated results confirm the analytical results in Table.2.1 that the code design for small and large antenna arrays follows different criteria.

We now show the performance of the Steiner code, the Modified Steiner code and

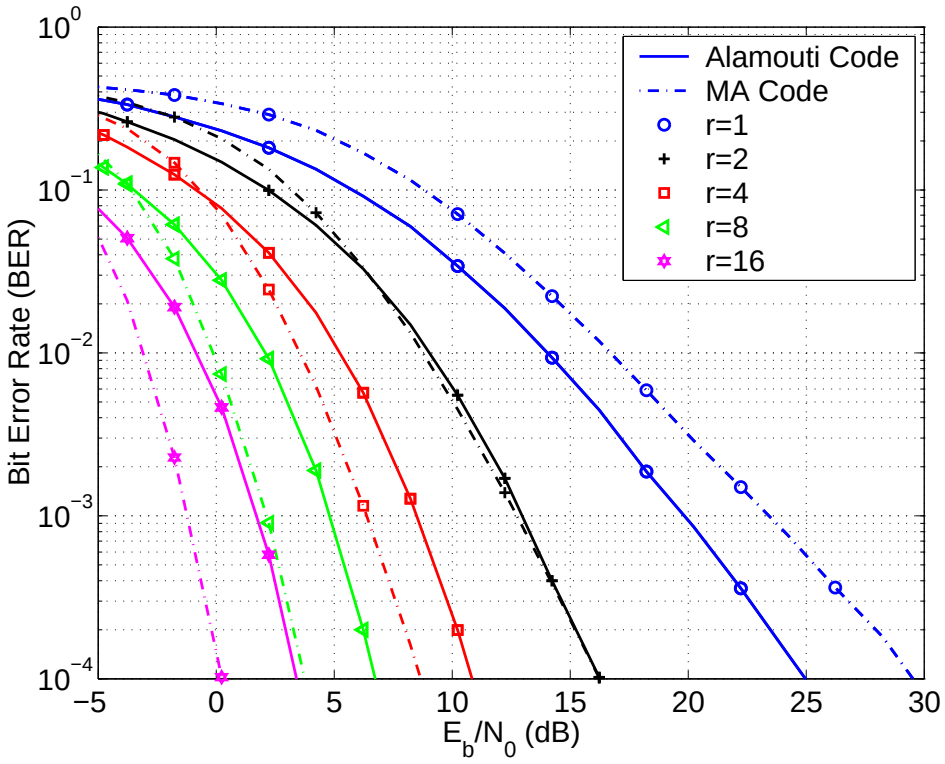

Figure 2.4: BER performance of Alamouti vs Modified Alamouti codes for $R = 3$ bps/Hz and $r = 1, 2, 4, 8, 16$

the Modified Alamouti code. We will use the Alamouti code as a reference because it is the optimal code for one receive antenna. Fig. 2.3 compares the performance of the Steiner code and the Alamouti code for rate $R = 3$ bps/Hz. We can see the Alamouti code significantly outperforms the Steiner code for $r = 1$, because the Alamouti code has the largest product distance among the evaluated codes. For $r = 2$, the performance gap between the Steiner code and the Alamouti code is much smaller than for $r = 1$. For $r > 2$ the Steiner code outperforms the Alamouti code. For example, at a BER of 10^{-4} and for $r = 16$, the Steiner code outperforms the Alamouti code by more than 3.5 dB. Fig. 2.4 and Fig. 2.5 compare the performance

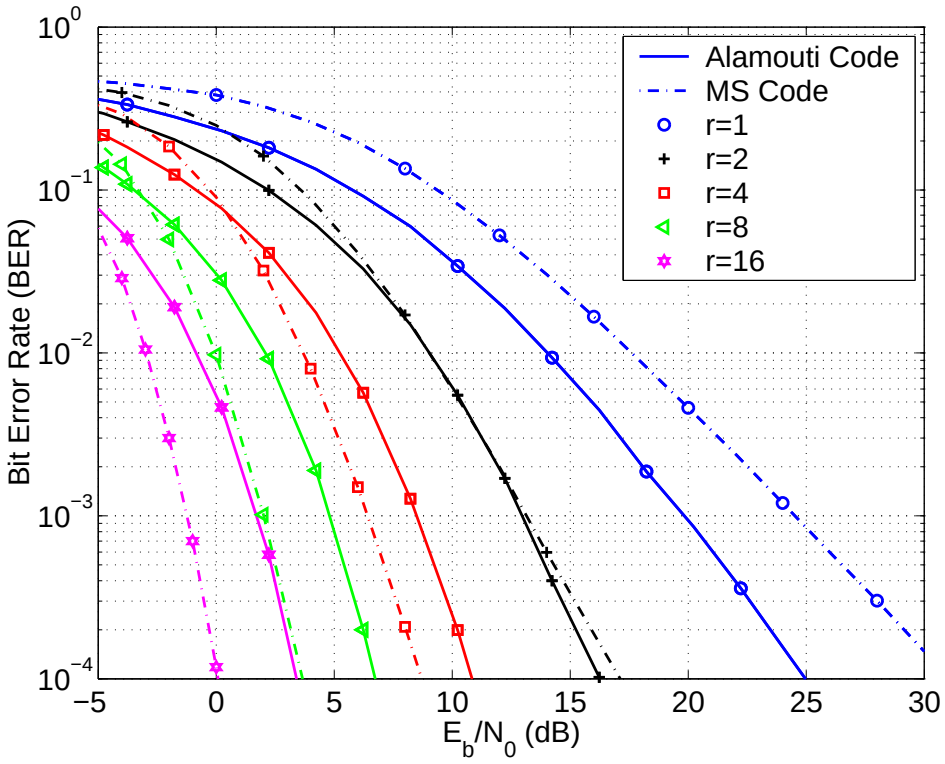

Figure 2.5: BER performance of Alamouti vs Modified Steiner codes for $R = 3$ bps/Hz and $r = 1, 2, 4, 8, 16$

of the Alamouti code with the Modified Alamouti code and the Modified Steiner code respectively. Again we observe the performance advantage of these two codes relative to the Alamouti code for large array size. Compare to Fig. 2.3, the Modified Alamouti code and the Modified Steiner code perform slightly worse than the Steiner code, which can be explained by the difference in their Euclidean distance. These two codes, however, have full diversity, hence they perform closer to the Alamouti code than the Steiner code for small arrays.

These simulated results provide additional evidence that Euclidean distance is an appropriate design criterion for large arrays, and that the new codes can improve the

performance of DSTM in this regime. We further observe from the figures that Λ_e appears to be a good indicator of performance even for relatively small arrays, such as $t = 2, r = 4$.

We should note that although these new codes improve the performance of DSTM for large arrays, most of them require maximum likelihood decoding, which involves an exhaustive search over the entire code constellation. The Alamouti code, by contrast, allows simple decoupled linear decoder for each information symbol to provide maximum-likelihood performance. Therefore, we will investigate codes with simple decoding structures for large arrays in the next chapter.

2.6 Conclusion

In this chapter, we considered the design and analysis of DSTM when the number of transmit and/or receive antennas is large. We evaluated the error performance of differential space-time modulation and derived a new upper bound on the pairwise-error probability for large arrays. This bound suggests that Euclidean distance is a good design criterion in the large-array regime, rather than the well-known rank and determinant criteria for small array regime or high SNRs. For two transmit antennas and many receive antennas, we investigated the performance of some existing code structure in terms of the Euclidean distance. To improve the performance for large arrays, we use the new design criterion to construct several new differential codes with large minimum Euclidean distance. Simulations of bit-error-rate performance confirm that the new codes outperform existing codes for DSTM with four or more receive

antennas, hence they are better candidates for systems with a large number of receive antennas. Generally, maximum-likelihood decoding are required in the decoding of these new codes.

Chapter 3

Improved Space-Time Coding with Low Complexity Decoders

In this chapter, we will present a new family of space-time unitary block codes for two transmit antennas and large numbers of receive antennas. The code is based on a modification of the Alamouti code by adding a third symbol. We optimize the new code in terms of Euclidean distance. We show that not only the new code provides good performance for systems with a large number of antennas, but it can utilize simple suboptimal sequential decoders with close-to-optimal performance. The code and the suboptimal decoders can be used in coherent or differential space-time coding/modulation, for systems with or without channel state information at the receiver, respectively. We also consider the extension of the new code to non-unitary constellations and more than two transmit antennas. Moreover, we evaluate this new coding structure in the mutual information point of view.

3.1 Introduction

Space-time coding can greatly improve the performance of wireless communication by employing multiple antennas at both sides of the channel. Most space-time coding schemes assume systems equipped with small antenna arrays. To further improve the system performance, more antennas can be put at one or both end of the channel. The availability of more diversity provided by more antennas enables the system to operating at moderate or low SNRs. For such scenarios and when the channel state information is known at the receiver, it has been reported [4, 69, 1] that Euclidean distance between codewords is often a better indicator of code performance. Some space-time trellis codes have been proposed based on this Euclidean distance criterion [70].

For differential space-time modulation (DSTM), in [64, 65] we have derived an upper bound on the pairwise error probability for large antenna arrays using Gaussian approximation and illustrated that Euclidean distance is the dominant parameter in the code performance for large arrays . Some existing structures such as group codes have been reconsidered and some new unitary space-time block codes have been designed according to the Euclidean distance criterion for two transmit antennas and many receive antennas [64, 65], which achieve good performance. Wang *et al.* [62] also suggested Euclidean distance criterion using a different approached and designed some cyclic group codes for two to four transmit antennas and many receive antennas. Liang and Xia [34] considered the code design for low SNR scenarios, which also follows the Euclidean criterion. While group codes considered in [64, 65, 62] can

utilize a fast decoding algorithm [7], the group structure limits their performance in terms of Euclidean distance. On the other hand, most codes investigated in [64, 65] require maximum likelihood decoding. Recently, Taherzadeh *et al.* [54] proposed some high rate differential space-time codes by embedding more information symbols in the unitary codes. For two transmit antennas, a simplified decoding method employing several parallel Alamouti decoder has been proposed to perform maximum-likelihood decoding. On the other hand, Steiner *et al.* [52] considered serial concatenation which uses the code proposed in [51] (referred as Steiner code here) as inner code and turbo code as outer code. A suboptimal decoding method for the inner code has been proposed to reduce the number of candidates in calculating the extrinsic information between the inner and outer decoders. This SVD decomposition based suboptimal decoder assumes the code being a general unitary code by discarding any constellation constraints associated with the information matrix, thus only provide a gross estimation for the signals. Furthermore, SVD decomposition is not very efficient in computation. In [53], Steiner *et al.* used decision-feedback demodulation to improve the performance of [52], but with extra complexity.

In this chapter, we propose a new family of codes for two transmit antennas, based on a different parametrization of two by two unitary matrices, and search for good codes with respect to Euclidean distance. To reduce the decoding complexity to a level comparable to the Alamouti decoder, we propose two low-complexity suboptimal receivers that allow the individual symbols in the code to be sequentially decoded. The idea behind these suboptimal receivers is the Generalized Likelihood

Ratio Test (GLRT). We apply the new coding structure to both coherent and differential space-time modulation schemes. It is shown through simulation that the new code outperforms some existing codes for large numbers of receive antennas. Furthermore, the performance of the suboptimal receivers approach that of optimal maximum-likelihood decoding as the number of receive antennas increases. We also evaluate the mutual information aspect of the new code and consider the generalization of the new code to the non-unitary constellations. The extension to more than two transmit antennas is also investigated.

The rest of this chapter is organized as follows. In Sec. 3.2, a new unitary code structure for two transmit antennas is introduced and its Euclidean distance is investigated. Extension to non-unitary constellations is addressed. In Sec. 3.3, we propose two low-complexity receivers for the new code, followed by error performance analysis, computational complexity and numerical results. We evaluate the new code structure in the information theory point of view in Sec. 3.4 and investigate the extension to four transmit antennas in Sec. 3.5. The concluding remarks are given in Sec. 3.6.

3.2 A New Family of Space-Time Block Code

From previous discussion, we can conclude that for both coherent and differential space-time modulation systems with large antenna arrays, codes should be designed to maximize the minimum Euclidean distance over the code constellation. Coding and receiver design for system with large numbers of antennas has been considered, in [64, 65, 62, 52, 54] and reference therein. Generally, these schemes require much

higher decoding complexity than that of the Alamouti linear decoder. The propose of this paper is to design codes that perform well with large receiver arrays, but also allow us to use simply decoding methods that are comparable to the Alamouti decoder. Our main focus is systems with two transmit antennas. We will start with unitary codes, which can be utilized with or without CSI at the receiver.

3.2.1 Unitary Space-Time Block Code

Existing unitary code designs for two transmit antennas exploit different parametrization of 2×2 unitary codes. These codes have been designed either to achieve full diversity and large product distance [2, 26, 24], or to achieve high rate or large Euclidean distance [51, 65, 54]. Here we will consider another parametrization which is a modified version of the Alamouti code and optimize it in terms of Euclidean distance.

Recall the Alamouti code which transmits two symbols via the normalized matrix

$$Q(\mathbf{x}) = \frac{1}{\sqrt{2}} \begin{bmatrix} x_1 & x_2 \\ -x_2^* & x_1^* \end{bmatrix} \tag{3.1}$$

where $\mathbf{x} = \{x_1, x_2\}$ and x_1, x_2 has unit average power. For $|x_1| = |x_2| = 1$, the matrices generated by (3.1) are unitary. The application of this code to differential transmission was proposed in [57]. The Alamouti code has full rank and large product distance and it performs well at high SNRs. In addition, its orthogonal structure allows the receiver to use a very simple linear decoder with low complexity. However, as shown in [64, 65], the Alamouti code is not a good candidate for transmission

systems with a large number of receive antennas.

In this work, we show that a third symbol ϕ can be added to the Alamouti code

$$U(\mathbf{x},\phi) = e^{j\phi}Q(\mathbf{x}) = \frac{1}{\sqrt{2}}e^{j\phi}\begin{bmatrix} x_1 & x_2 \\ -x_2^* & x_1^* \end{bmatrix} \tag{3.2}$$

thereby yielding a unitary code of larger rate. Furthermore, low-complexity decoders exist that allow ϕ, x_1 and x_2 to be decoded sequentially. Note that the addition of ϕ generally results in a code that is not of full rank; hence, these codes are of interest primarily when large receiver arrays are available.

For simplicity, assume $-\pi/2 < \phi \leq \pi/2$ and that $e^{j2\phi}$, x_1 and x_2 are taken from unit-magnitude PSK constellations with size $M_{2\phi}$, M_{x_1} and M_{x_2} respectively. Since $-\pi/2 < \phi \leq \pi/2$, $e^{j\phi}$ takes value on the right semi-circle of the $2M_{2\phi}$ PSK constellations. For example, if $e^{j2\phi}$ lies in the QPSK constellation, then $\phi \in \{-\frac{\pi}{4}, 0, \frac{\pi}{4}, \frac{\pi}{2}\}$. This leads to a unitary code with rate $R = \log_2(M_{2\phi}M_{x_1}M_{x_2})/2$.

The trace of the code distance matrix between codeword U and

$$\hat{U} = e^{j\hat{\phi}}\frac{1}{\sqrt{2}}\begin{bmatrix} \hat{x}_1 & \hat{x}_2 \\ -\hat{x}_2^* & \hat{x}_1^* \end{bmatrix}$$

can be written as

$$\begin{aligned}
\Lambda &= \mathrm{Tr}\{(U-\hat{U})(U-\hat{U})^\dagger\} \\
&= (|e^{j\phi}x_1 - e^{j\hat{\phi}}\hat{x}_1|^2 + |e^{j\phi}x_2 - e^{j\hat{\phi}}\hat{x}_2|^2 + |e^{j\hat{\phi}}\hat{x}_2^* - e^{j\phi}x_2^*|^2 + |e^{j\phi}x_1^* - e^{j\hat{\phi}}\hat{x}_1^*|^2)/2 \\
&= (|x_1|^2 + |\hat{x}_1|^2 + |x_2|^2 + |\hat{x}_2|^2) - \mathrm{Re}\{e^{j(\phi-\hat{\phi})}(x_1\hat{x}_1^* + \hat{x}_1x_1^* + x_2\hat{x}_2^* + \hat{x}_2x_2^*)\} \\
&= (|x_1|^2 + |\hat{x}_1|^2 + |x_2|^2 + |\hat{x}_2|^2) - 2\mathrm{Re}\{e^{j(\phi-\hat{\phi})}\}\mathrm{Re}\{x_1\hat{x}_1^* + x_2\hat{x}_2^*\} \\
&= 4 - 2\mathrm{Re}\{e^{j(\phi-\hat{\phi})}\}\mathrm{Re}\{x_1\hat{x}_1^* + x_2\hat{x}_2^*\}
\end{aligned}$$

where the last equation follows that all the symbols are taken from unitary constellations. Notice that for unitary constellations, Λ only depends on the phase difference of each information symbol. Letting $M_x = \max\{M_{x_1}, M_{x_2}\}$, we can show that the minimum Euclidean distance in (2.10) is given by

$$\Lambda_e = \begin{cases} 2\sqrt{2}\sin\left(\frac{\pi}{2M_{2\phi}}\right), & 2M_{2\phi} > M_x \\ 2\sin\left(\frac{\pi}{M_x}\right), & \text{otherwise} \end{cases} \tag{3.3}$$

We can therefore easily search for the best codes in terms of Euclidean distance.

Table 3.1 compares the Euclidean distance and the number of nearest neighbors N_n of the new code with those of the Alamouti code and the Steiner code (2.30) for $R = 3$ and 4 bps/Hz. Note the new code also has good Euclidean distance as well as a small number of neighbors.

Table 3.1: Comparison of Euclidean distance of unitary codes

R	$\mathcal{U}$	Λ_e	$(M_{x_1}, M_{x_2}, M_{2\phi}(M_{x_3}))$	N_n
3	Alamouti	0.7654	(8,8,–)	4
	Steiner	1.414	(4,4,4)	12
	New code	1.0824	(4,4,4)	2
4	Alamouti	0.3902	(16,16,–)	4
	Steiner	0.7654	(8,8,4)	6
	New code	0.7654	(8,8,4)	4

3.2.2 Non-Unitary Space-Time Block Codes

Up to now, we restrict our code constellations in (3.2) to be unitary, in which $e^{j2\phi}, x_1$ and x_2 are taken from PSK constellations. Taking information symbols from unit circle simplifies both the transmitter and receiver design. In addition, unitary

codes can be used for both coherent and differential detection. For large constellation sizes, however, PSK constellations suffer from performance loss compared to quadrature-amplitude-modulation (QAM) constellations, which transmit information in both phase and amplitude. Assuming the receiver has perfect channel knowledge, now we will extend the new code structure by considering x_1 and x_2 taken from QAM constellations with normalized power of one. The average power of the code remains to be unit; however, the instantaneous power varies each block.

We can show that the minimum Euclidean distance for the generalized code structure is given by

$$\Lambda_e = \min\left\{2\sqrt{E_{\min_1}+E_{\min_2}}\sin\left(\frac{\pi}{2M_{2\phi}}\right), d_{\min_1}, d_{\min_2}\right\} \tag{3.4}$$

where $E_{\min}$ and $d_{\min}$ denote the minimum power and minimum distance of the QAM constellation respectively. Note that if x_1 and x_2 are taken from PSK constellations, the above expression becomes (3.3).

Table. 3.2 compares the Euclidean distance of the new code with the Alamouti code, for different rates and constellations. We can see that the new code with generalized constellations has larger Euclidean distance than the Alamouti code. For a same rate, the new code lies on smaller constellations. For example, for rate 5 bps/Hz, the new code lies on 16-QAM constellations while the Alamouti code lies on 32-QAM.

Table 3.2: Comparison of Euclidean distance for generalized constellations

R	$\mathcal{U}$	Λ_e	$(x_1, x_2, e^{2\phi})$
4	New code(PSK)	0.7654	(8PSK,8PSK,QPSK)
	Alamouti (PSK)	0.3902	(16PSK,16PSK,–)
	Alamouti (QAM)	0.6325	(16QAM,16QAM,–)
5	New code(PSK)	0.3902	(16PSK,8PSK,8PSK)
	New Code(QAM)	0.4841	(16QAM,16QAM,QPSK)
	Alamouti(PSK)	0.1960	(32PSK,32PSK,–)
	Alamouti(QAM)	0.4472	(32QAM,32QAM,–)
6	New Code(QAM)	0.3423	(32QAM,32QAM,QPSK)
	New code(PSK)	0.2772	(16PSK,16PSK,16PSK)
	Alamouti(PSK)	0.098	(64PSK,64PSK,–)
	Alamouti(QAM)	0.3086	(64QAM,64QAM,–)

3.3 Suboptimal Decoders with Low Complexity

Unlike the Alamouti code, maximum-likelihood (ML) decoding of the code in (3.2) will generally require a search of all 2^{2R} possible code matrices. For high-rate codes, this may be undesirable. We now show ϕ, x_1 and x_2 can be decoded sequentially by two simple suboptimal algorithms. The suboptimal decoding algorithms are inspired by the generalized likelihood ratio test (GLRT). In the following, we will first give a brief introduction of GLRT, and then derive two suboptimal sequential receivers for the new code. We will also evaluate the error performance and the decoding complexity of the suboptimal receivers. Our arguments are first made by assuming coherent space-time coding and then extended to DSTM.

3.3.1 Generalized Likelihood Ratio Test (GLRT)

In detection and estimation problems, very often the parameters characterizing a hypothesis may not be known. In such cases, the hypothesis is called a composite hypothesis. The GLRT technique is a common method for detecting signals for such scenarios. It replaces the unknown parameters by their maximum-likelihood estimates (MLE) under each hypothesis.

Let H_0 and H_1 be the hypothesis and θ be the unknown parameter. We use the required data $\mathbf{y}$ to estimate θ, as though hypothesis H_0 is true. We also estimate θ as though hypothesis H_1 is true. Then, we use these estimates in the likelihood ratio test as if they are the correct values. If the estimates used are the maximum-likelihood estimates, the generalized likelihood ratio is given by

$$\Lambda(\mathbf{y}) = \frac{\max_{\theta_1} \mathbf{f_{Y|\Theta_1}}(\mathbf{y}|\theta_1)}{\max_{\theta_0} \mathbf{f_{Y|\Theta_0}}(\mathbf{y}|\theta_0)} \underset{\mathbf{H_0}}{\overset{\mathbf{H_1}}{\gtrless}} \eta$$

where $f_{\mathbf{Y}|\mathbf{\Theta}}(\mathbf{y}|\theta)$ is the conditional pdf of given θ, η is the detection threshold and θ_1 and θ_0 are the unknown parameters to be estimated under hypothesis H_1 and H_0, respectively.

3.3.2 Sequential GLRT decoders for Coherent Detection

For a unitary code matrix U as in (3.2), the maximum likelihood receiver in (2.3) leads to a log-likelihood decision metric of the form

$$\begin{aligned} \Lambda(Y|H, \mathbf{x}, \phi) &= \mathrm{ReTr}\left[e^{j\phi} Y^{\dagger} H Q(\mathbf{x})\right] \\ &= \mathrm{ReTr}\left[A Q(\mathbf{x})\right] \end{aligned}$$

$$
\begin{aligned}
&= \frac{1}{\sqrt{2}}\mathrm{Re}\left\{[(a_{11}x_1 - a_{12}x_2^* + a_{21}x_2 + a_{22}x_1^*)]\right\} \\
&= \frac{1}{\sqrt{2}}\mathrm{Re}\left[(a_{11} + a_{22}^*)x_1 + (a_{21} - a_{12}^*)x_2\right] \qquad (3.5)
\end{aligned}
$$

where $A = e^{j\phi}Y^H H$. Optimal ML decoding is a joint decoding of ϕ, x_1 and x_2. To decouple detection of ϕ from x_1 and x_2, we can apply GLRT and get a decision metric on ϕ as

$$
\begin{aligned}
\Lambda(Y|H,\phi) &= \max_{\mathbf{x}:|\mathbf{x}|^2/2=1} \mathrm{ReTr}\left[\sqrt{2}e^{j\phi}Y^H H Q(\mathbf{x})\right] \\
&= \max_{\mathbf{x}:|\mathbf{x}|^2/2=1} \mathrm{Re}\left\{[(a_{11} + a_{22}^*)x_1 + (a_{21} - a_{12}^*)x_2]\right\} \\
&\overset{(a)}{=} \sqrt{|a_{11} + a_{22}^*|^2 + |a_{21} - a_{12}^*|^2} \\
&= \sqrt{\| A \|^2 + 2\mathrm{Re}[\det(A)]}
\end{aligned}
$$

where step (a) follows by observing that the maximum is attained by $\mathbf{x} = \sqrt{2}\mathbf{a}^*/|\mathbf{a}|$ with $\mathbf{a} = (a_{11} + a_{22}^*, a_{21} - a_{12}^*)$. Defining $B = Y^H H$ and substituting $A = e^{j\phi}B$ into the above equation,, we obtain

$$
\begin{aligned}
\hat{\phi}_{GLRT1} &= \arg\max_{\phi} \sqrt{\| Y^H H \|^2 + 2\mathrm{Re}[\det(e^{j\phi}Y^H H)]} \\
&= \arg\max_{\phi} \ \mathrm{Re}[\det(Y^H H)e^{j2\phi}] \\
&= \arg\max_{\phi} \ \mathrm{Re}[\det(B)e^{j2\phi}] \qquad (3.6)
\end{aligned}
$$

Thus ϕ can be estimated directly from the determinant of the 2×2 matrix $Y^H H$.

Note that we have restricted x_1 and x_2 to lie in a PSK constellation, so that $|x_1| = |x_2| = 1$. Thus, a better detector might be obtained by considering that constraint:

$$
\Lambda = \max_{|x_1|=|x_2|=1} \mathrm{Re}\left[(a_{11} + a_{22}^*)x_1 + (a_{21} - a_{12}^*)x_2\right]
$$

$$= \quad |a_{11} + a_{22}^*| + |a_{21} - a_{12}^*| \ .$$

Substituting $A = e^{j\phi} Y^H H = e^{j\phi} B$ above, we get another detector

$$\begin{aligned} \hat{\phi}_{GLRT2} &= \arg\max_{\phi} |e^{j2\phi} b_{11} + b_{22}^*| + |e^{j2\phi} b_{21} - b_{12}^*| \\ &= \| \ e^{j2\phi} \mathbf{b_1} - \mathbf{b_2}^* \ \|_1 \end{aligned} \tag{3.7}$$

where $\mathbf{b_1} = [b_{11}, b_{21}]$, $\mathbf{b_2} = [-b_{22}, b_{12}]$ and $\| \cdot \|_1$ denote the vector 1-norm. This receiver is also based on the 2×2 matrix $Y^H H$, but followed by a vector norm operation.

Once ϕ has been detected, the receiver can then substitute the detected value of $e^{j\hat{\phi}}$ into the decision metric (3.5) and use the conventional Alamouti linear decoder [2] to conduct parallel decoding of x_1 and x_2. Thus, the two sequential receivers proposed in this section provide a simple way to decouple the decoding of individual information symbols in this nonlinear code. Here, we denote these two receivers as GLRT receivers because the first step in decoding is based on GLRT.

Unlike (3.5), for coherent space-time codes with non-unitary constellations, the log-likelihood decision metric depends also on the instantaneous power of the transmitted matrix

$$\Lambda(Y|H, \mathbf{x}, \phi) = \mathrm{ReTr}\left[2e^{j\phi} Y^H H Q(\mathbf{x})\right] - ||H||^2 (|x_1|^2 + |x_2|^2)/2 \tag{3.8}$$

Generally, instantaneous values of $|x_1|^2$, $|x_2|^2$ or $(|x_1|^2 + |x_2|^2)/2$ are not unit, therefore conditions for the two GLRT receivers for ϕ do not hold. For the first GLRT receiver, however, the decoder for ϕ takes the same form as (3.6). The decoder for x_1 and x_2, however, requires more computation to take different amplitude level into account.

3.3.3 Error Performance Analysis

In this part we will derive bit error rate probabilities for the sequential GLRT receivers based on equivalent channel models. We will consider unitary space-time codes. However, the extension to non-unitary codes is trivial. For simplicity, the analysis is based on the first GLRT receiver (GLRT1).

The first GLRT decoder for ϕ in eq. (3.6) can be rewritten as

$$\hat{\phi} = \arg \max_{\phi} \mathrm{Re}\{\det(H^H Y) e^{-j2\phi}\}.$$

Consider a transformation of the received signal

$$\begin{aligned} H^H Y &= \sqrt{\rho} e^{j\phi} H^H H Q + H^H N \\ &= S + \tilde{N} \end{aligned}$$

where $S = \sqrt{\rho} e^{j\phi} H^H H Q$ and $\tilde{N} = H^H N$. Expand $\det(H^H Y)$ to first order in the noise as

$$\begin{aligned} \det(H^H Y) &= \det(S) + \tilde{n}_{11} s_{22} - \tilde{n}_{12} s_{21} - \tilde{n}_{21} s_{12} + \tilde{n}_{22} s_{11} + \text{h.o.t} \\ &\approx \det(S) + \mathrm{Tr}\left(\begin{bmatrix} s_{22} & -s_{12} \\ -s_{21} & s_{11} \end{bmatrix} H^H N \right) \\ &= \det(S) + \mathrm{Tr}\left(\det(S) S^{-1} H^H N \right) \\ &= \rho \det(H^H H) e^{j2\phi} + \alpha \tilde{n} \end{aligned}$$

where $\tilde{n}$ is a complex Gaussian random variable with $\mathcal{C}N(0,1)$ and α is a scalar with

$$\begin{aligned} \alpha^2 &= \| \det(S) S^{-1} H^H \|^2 \\ &= \rho \det(H^H H) \mathrm{Tr}(H^H H) \end{aligned}$$

Denote $\det(H^H Y)$ as $\tilde{y}_\phi$ and then we come up with an equivalent channel for ϕ as

$$\tilde{y}_\phi \approx \rho \det(H^H H) e^{j2\phi} + \sqrt{\rho \det(H^H H) \mathrm{Tr}(H^H H)} \tilde{n} \tag{3.9}$$

If $e^{j2\phi}$ takes values in an $M_{2\phi}$-ary PSK distribution, and if the symbol error rate (SER) of $M_{2\phi}$ PSK for the additive white Gaussian noise channel $y = \sqrt{\gamma} e^{j2\phi} + n$ is $P_{M_{2\phi}}(\gamma)$, then the SER of decoding ϕ is

$$P_{s_\phi} \quad = \quad E\left[P_{M_{2\phi}} \left(\rho \frac{\det(H^H H)}{\mathrm{Tr}(H^H H)} \right) \right] \tag{3.10}$$

It is well known [12, pg. 39] that if H is $r \times t$ with $r \geq t$, then H^H can is unitarily similar to an $t \times r$ matrix

$$\begin{bmatrix} x_{2r} & & & & 0 & \cdots & 0 \\ y_{2(t-1)} & x_{2(r-1)} & & & \cdot & & \cdot \\ & \ddots & \ddots & & \vdots & & \vdots \\ & & y_2 & x_{2(r-(t-1))} & 0 & \cdots & 0 \end{bmatrix}$$

and hence $\det(H^H H)$ has the same distribution as $\chi^2_{2r}\chi^2_{2(r-1)} \cdots \chi^2_{2(r-t+1)}$, where χ^2_k denotes a chi-square distribution with k degree of freedom and parameter $1/2$. By the same argument, it appears that

$$\mathrm{Tr}[H^H H] \sim \chi^2_{2r} + \chi^2_{2(r-1)} + \cdots \chi^2_{2(r-t+1)} + \tilde{\chi}^2_{2(t-1)} + \cdots \tilde{\chi}^2_2$$

where all of the variables are independent.

For $t = 2$, we have $\det(H^H H) \sim \chi^2_{2r}\chi^2_{2(r-1)}$ and $\mathrm{Tr}[H^H H] \sim \chi^2_{2r} + \chi^2_{2(r-1)} + \tilde{\chi}^2_2$. Thus

$$\frac{\det(H^H H)}{\mathrm{Tr}(H^H H)} \sim \frac{\chi^2_{2r}\chi^2_{2(r-1)}}{\chi^2_{2r} + \chi^2_{2(r-1)} + \tilde{\chi}^2_2} \, .$$

If ϕ is correctly detected, the sequential decoder for $Q(x)$ acts as the conventional Alamouti decoder. The equivalent channel model for $x_i (i = 1, 2)$ can be expressed as

$$\tilde{y}_i = \sqrt{\rho/2} \parallel H \parallel^2 x_i + \tilde{n}_i \tag{3.11}$$

where $\tilde{y}_i$ is a linear combination of Y and $\tilde{n}_i \sim \mathcal{CN}(0, ||H||^2)$. Therefore the conditional SER for x_i given $\hat{\phi} = \phi$ can be expressed as

$$\{P_{s_{x_i}} | \hat{\phi} = \phi\} = E\left[P_{M_{x_i}}\left(\frac{\rho}{2} \parallel H \parallel^2\right)\right] \tag{3.12}$$

If ϕ is erroneously decoded, we approximate the SER of x_i by $1/2$. So the SER for x_i can be expressed as

$$P_{s_{x_i}} = \{P_{s_{x_i}} | \hat{\phi} = \phi\}(1 - P_{s_\phi}) + \frac{1}{2} P_{s_\phi} \tag{3.13}$$

For a M-PSK symbol with gray mapping, the bit error rate (BER) can be approximated using SER by

$$P_b \approx \frac{1}{\log_2 M} P_s$$

Therefore we can approximate the BER of the GLRT receiver by

$$\begin{aligned} P_b &= \frac{\left(\log_2 M_{x_1} P_{b_{x_1}} + \log_2 M_{x_2} P_{b_{x_2}} + \log_2 M_{2\phi} P_{b_\phi}\right)}{2R} \\ &= \frac{\left(P_{s_{x_1}} + P_{s_{x_2}} + P_{s_\phi}\right)}{2R} \end{aligned} \tag{3.14}$$

3.3.4 Computation Complexity

We now compare the complexity of the GLRT receivers with those of optimal ML decoding and the Alamouti linear receiver at the same rate. The ML receiver in (3.5),

the GLRT receivers in (3.6, 3.7) and the Alamouti decoder with equivalent metric (3.5) all begin with calculating $Y^H H$. For constellation size $|\mathcal{U}| = M_{x_1} M_{x_2} M_{2\phi}$, ML decoder then multiplies each matrix in $\mathcal{U}$ by $Y^H H$. In contrast, GLRT decoders and the Alamouti decoder optimize the decision metric for each information symbol separately. In particular, the Alamouti decoder conducts parallel decoding of x_1 and x_2. The GLRT decoders first detect ϕ, then detect x_1 and x_2 in parallel. It is obvious that the complexity of the GLRT receivers and the Alamouti decoder increases as a function of individual element constellation, while the joint ML decoding complexity is a function of the whole constellation size.

Table. 3.3 gives an example of the number of operations used by different decoding methods, for systems using eight receive antennas at different rates. We list the number of floating point operations in terms of real multiplications (RM) and real additions (RA) for each decoding methods. We can see that the GLRT receivers proposed in this paper provide significant complexity advantages over the ML receiver, especially for high rate codes. Furthermore, for the same rate, the suboptimal GLRT decoders have computational operations similar to that of the Alamouti decoder for PSK constellations. If QAM constellation are used, the suboptimal decoders compare favorably to the Alamouti decoder. Therefore, the new code with GLRT receivers provides efficient decoding and better performance compared to the Alamouti code.

Table 3.3: Decoding complexity for $r = 8$ and different rates

Decoder	$R = 3$		$R = 4$		$R = 5$	
	RM	RA	RM	RA	RM	RA
ML(PSK)	2176	2240	8320	8576	32896	33920
ML(QAM)	-	-	-	-	34048	35072
Alamouti(PSK)	192	164	256	196	384	260
Alamouti(QAM)	336	308	416	356	576	452
GLRT1(PSK)	200	170	232	186	280	210
GLRT1(QAM)	-	-	-	-	456	378
GLRT2(PSK)	224	192	256	208	344	268
GLRT2(QAM)	-	-	-	-	480	404

3.3.5 Sequential Decoders for DSTM

For differential space-time modulation with the unitary code (3.2), the maximum-likelihood receiver in (2.3) leads to a log-likelihood decision metric of the form

$$\Lambda(Y_k, Y_{k-1}|, \mathbf{x}, \phi) = \mathrm{ReTr}\left[e^{j\phi} Y_k^H Y_{k-1} Q(\mathbf{x})\right] \tag{3.15}$$

This metric has the same form as the decision metric for coherent detection (3.5), only by replacing H by Y_{k-1}. it is easy to show that we can use the same method to get the GLRT receivers for ϕ in DSTM, by replacing H with Y_{k-1}. The resulting receivers for ϕ can also be expressed as (3.6) and (3.7), with B defined as $B = Y_k^H Y_{k-1}$, and followed by the differential receiver for the Alamouti code. The suboptimal receivers for DSTM have the same computation complexity as those for coherent detections with PSK constellations. The error performance analysis in Sec. (3.3.3) can be easily extended to DSTM. Therefore the new code and the low-complexity sequential GLRT receivers can be used with or without channel knowledge at the receiver.

As we will see from the simulated performance results, these two receivers achieve

good performance for large receive arrays.

3.3.6 Numerical Results

In this section, we will evaluate the bit-error-rate (BER) performance of the proposed code with the optimal ML decoder and the two GLRT decoders, respectively. Furthermore, we will compare the performance of the new code with that of the Alamouti code (3.1) and Steiner code (2.30), both with ML decoding. We also compare the simulated BER performance of GLRT1 with its analytical approximation. In all the simulations, we assume $t = 2$ transmit antennas and the number of receive antennas varies from $r = 4, 8$ to 16. We will first consider coherent detection.

Fig. 3.1 compares the BER performance of the new code with $R = 3$ bps/Hz and coherent detection for three different decoders: ML decoding, the first GLRT decoder (GLRT1) in (3.6), and the second GLRT decoder (GLRT2) in (3.7). For $r = 4$, note that there is a gap of more than 2.5 dB between the GLRT2 and optimal ML decoding, and the GLRT1 decoder suffers an additional loss of nearly 2 dB compared to the GLRT2. As the number of receive antennas increases, however, the performance loss of the GLRT receivers compared to ML decoding decreases, as does the gap between the two GLRT receivers. In particular, for $r = 16$, the performance of the two GLRT receivers is nearly the same, and both are within about 0.7 dB of ML decoding.

Fig. 3.2 compares the performance of the new $R = 3$ bps/Hz code using the GLRT2 receiver with the Alamouti and Steiner codes, both using ML decoding. For $r = 16$, the proposed code with suboptimal receiver outperform the Alamouti code

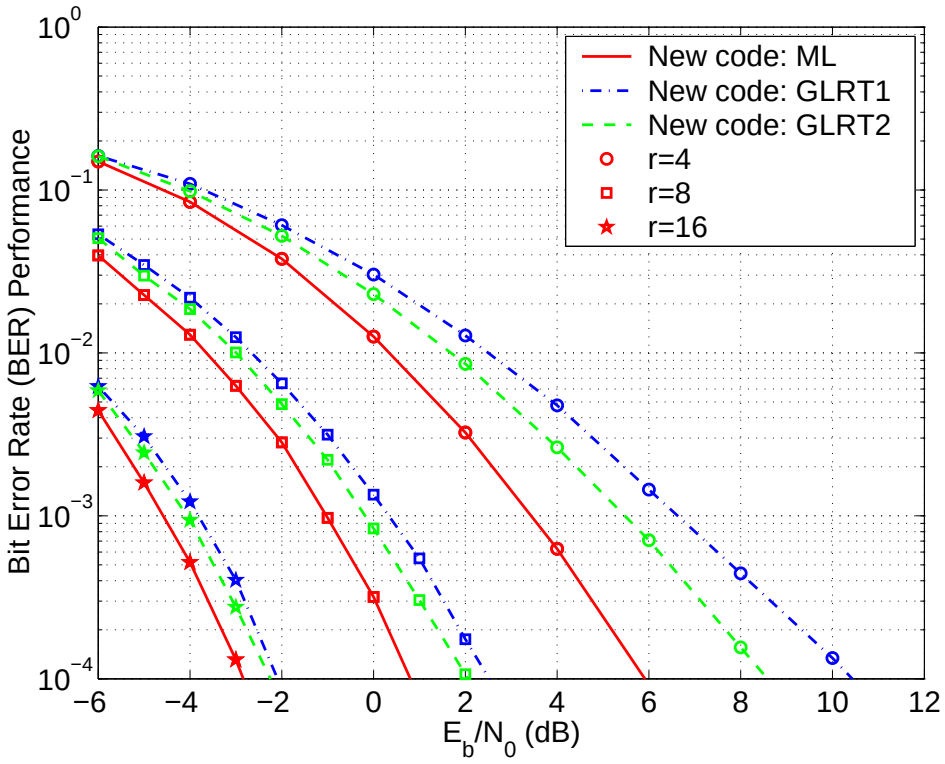

Figure 3.1: BER performance of the new code with ML, GLRT1 and GLRT2 decoding at $R = 3$ bps/Hz for $t = 2$ and $r = 4, 8, 16$ with coherent detection.

by about 2.3 dB, but are about 1.3 dB inferior to the Steiner code. From Fig. 3.1, it is clear that approximately 0.6 dB of this gap is due to the suboptimal decoder; the remaining 0.7 dB can be explained by the larger Euclidean distance of the Steiner code. As shown in the complexity analysis, however, the GLRT decoders are far less complex than the ML decoding used with the Steiner code.

The performance of the new code with coherent detection for $R = 4$ bps/Hz is shown in Fig. 3.3. Note that the performance gap between the ML and GLRT receivers is smaller than in the $R = 3$ bps/Hz case. Specifically, from $r = 8$, the performance of the GLRT receivers is nearly the same as ML decoding.

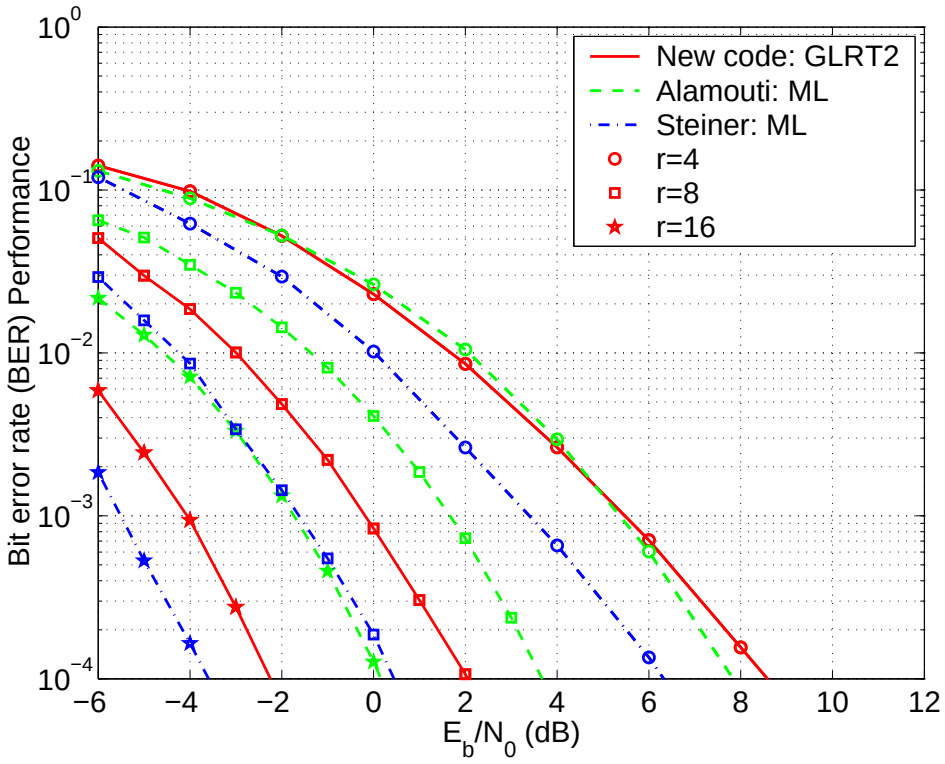

Figure 3.2: BER comparison of the new code using GLRT2 decoding with the Alamouti and Steiner codes using ML decoding at $R = 3$ bps/Hz for $t = 2$ and $r = 4, 8, 16$ with coherent detection.

Fig. 3.4 compares the performance of the proposed code at 4 bps/Hz using the GLRT2 receiver and the Alamouti with 16PSK and 16QAM constellations respectively for coherent detection. Notice that the proposed code outperforms the Alamouti code with both QAM and PSK constellations from $r = 4$ and the performance gain increases as the number of receive antennas increases. In particular, for $r = 8$, the new code with the suboptimal decoder outperforms Alamouti code with QAM and PSK constellations for nearly 2 dB and 5.7 dB respectively.

For $R = 5$ bps/Hz, Fig. 3.5 compares the performance of the proposed code with 16QAM, 16QAM and QPSK symbol constellations and GLRT1 decoder with the

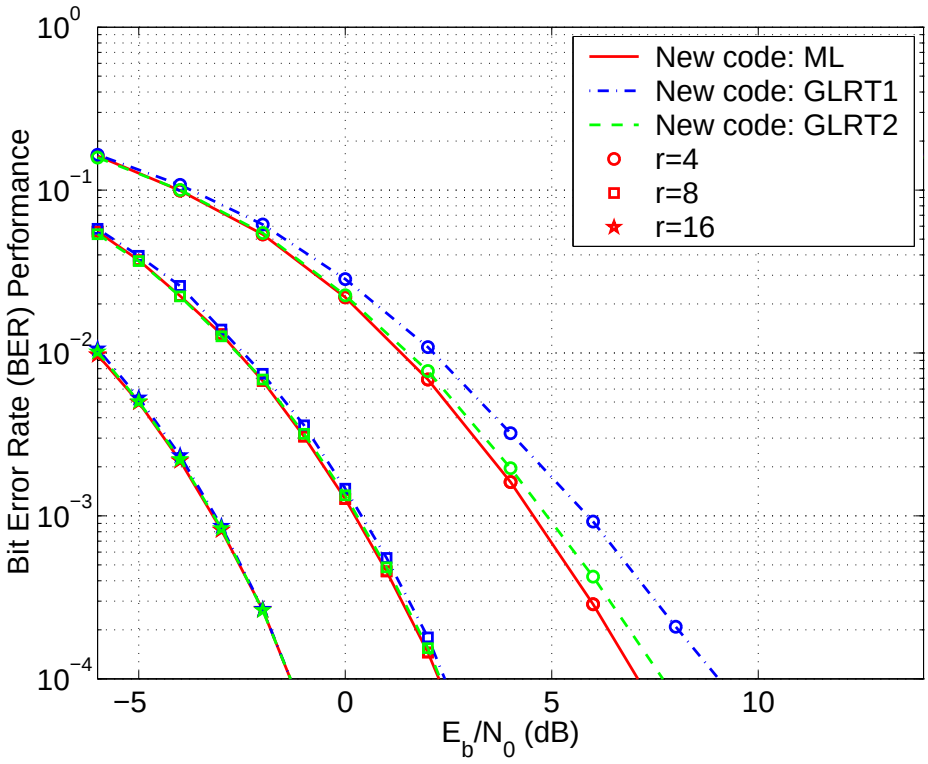

Figure 3.3: BER of new code with ML, GLRT1 and GLRT2 decoding at $R = 4$ bps/Hz for $t = 2$ and $r = 4, 8, 16$ with coherent detection.

Alamouti code with 32QAM symbol constellations. For $r = 4$, the new code with suboptimal decoder outperforms the Alamouti code for BER larger than 10^{-4} level. After that point, Alamouti code performs better. For $r = 8$, the new code has about 2 dB performance gain relative to the Alamouti code even with suboptimal GLRT1 decoder.

Fig. 3.6 compares the simulated BER performance for the GLRT1 receiver with coherent detection and the theoretical approximation for rate 4. We can conclude that the approximation gives a good indicator for the actual bit error performance.

For differential space-time modulation, Fig. 3.7 shows the proposed code with the

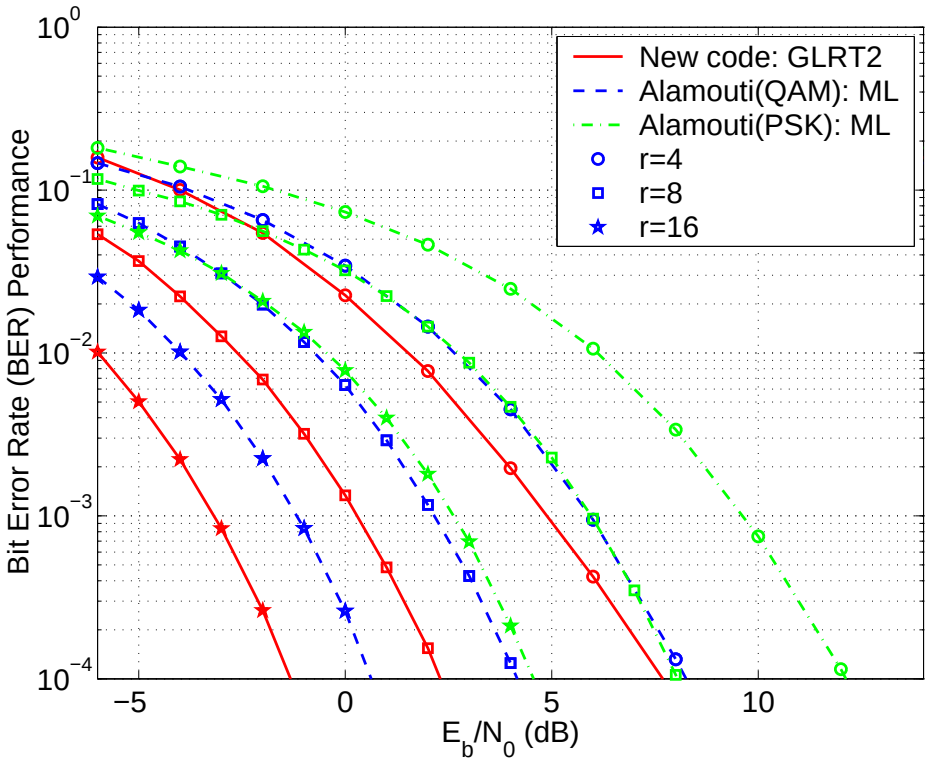

Figure 3.4: BER comparison of the new code using GLRT2 decoding with the Alamouti code with QAM and PSK respectively at $R = 4$ bps/Hz for $t = 2$ and $r = 4, 8, 16$.

GLRT2 receiver outperforms the Alamouti and Steiner codes with ML decoding for $r = 4, 8$ and 16. In particular, for $r = 16$, the performance gains relative to the Steiner and Alamouti codes are 0.9 dB and 5.5 dB, respectively. The new codes provide good performance with a simple decoding algorithm, even for a relatively modest number of receive antennas. Here, all these codes take on PSK constellations.

From the above simulation, we conclude that the new code has good performance compared to existing codes, for both coherent and differential space-time modulation, and at various rates. The performance of suboptimal decoders approaches that of the ML decoder for large receive arrays ($r \geq 4$), with greatly reduced decoding complexity.

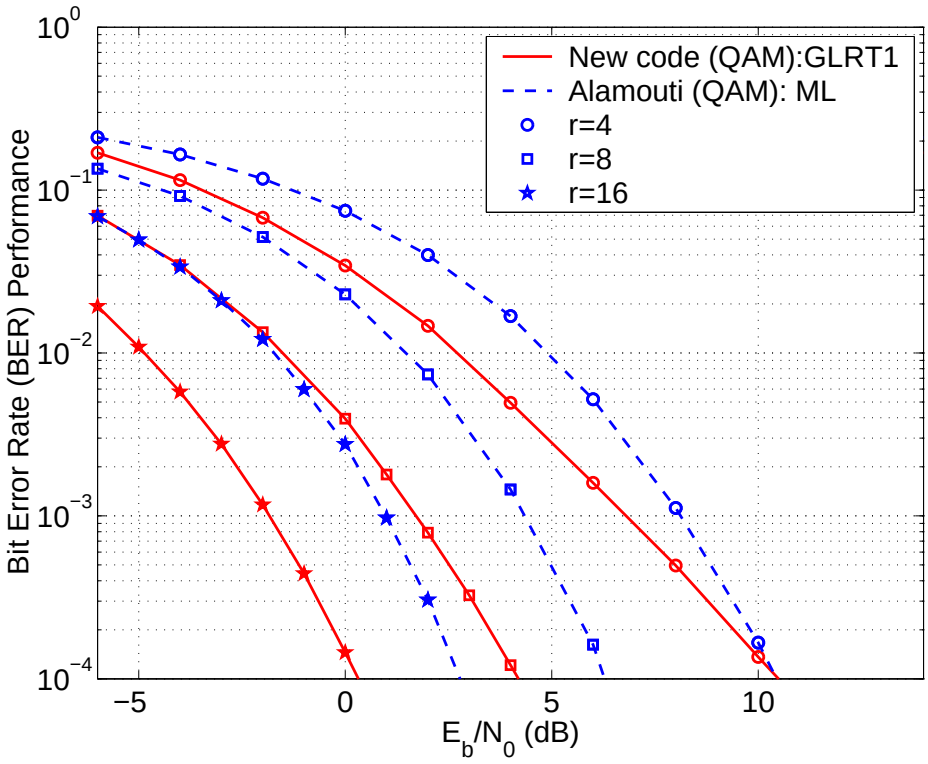

Figure 3.5: BER comparison of new code with GLRT1 decoding and Alamouti code at $R = 5$ bps/Hz for $t = 2$, $r = 4, 8, 16$ with coherent detection.

3.4 Mutual Information

In this section, we will compute the constellation-constrained capacity when the proposed code is used as input. We then compare the capacity of the new code with existing codes. Here we assume coherent detection is used. We will start with a brief introduction on channel capacity.

3.4.1 Channel Capacity

As mentioned in chapter one, channel capacity is the maximum possible transmission rate such that the probability of error is arbitrarily small. For wireless fading

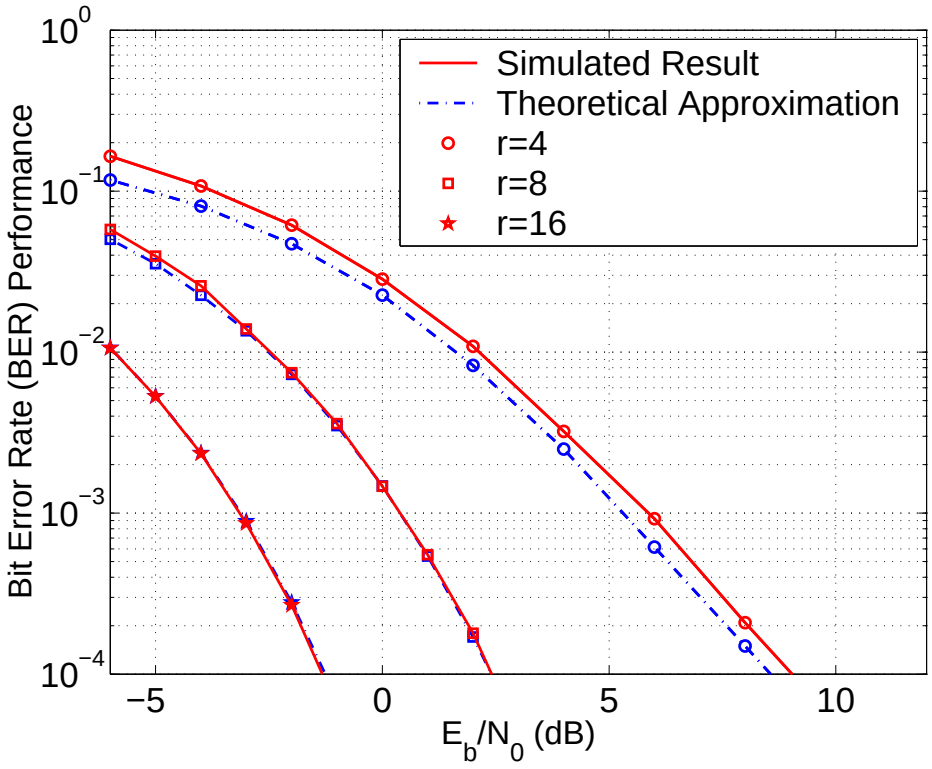

Figure 3.6: Comparison of simulated BER performance and theoretical approximation for GLRT1 decoder at $R = 4$ bps/Hz for $t = 2$ and $4, 8, 16$

channels, since the fading gain is a random parameter, the maximum throughput will also be a random variable. One commonly used statistic in analyzing capacity for such channels is called ergodic capacity. Ergodic capacity is the ensemble average of information rate over the distribution of the elements of the channel matrix H [39]. It is the appropriate measurement of capacity when the channel varies fast so that for each channel use, the channel is drawn from an independent realization.

Using multiple antennas at both ends of a wireless channel can greatly increase the channel capacity. If the channel between each transmitter and receiver fades independently, i.e, elements of H are modeled as i.i.d complex Gaussian variables, the

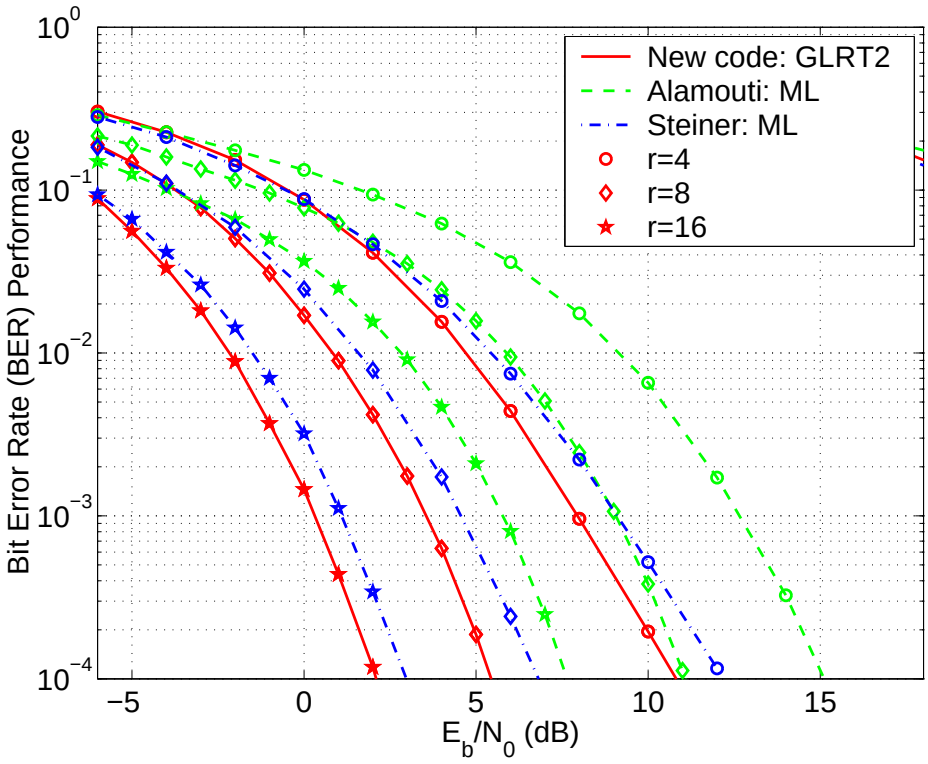

Figure 3.7: BER comparison of the new code using GLRT2 decoding with the Alamouti and Steiner codes at $R = 4$ bps/Hz for $t = 2$ and $r = 4, 8, 16$ in DSTM

capacity increases linearly with minimum number of transmit and receive antennas [14, 58]. For the MIMO channel model (2.1) with CSI at the receiver but not at the transmitter, the ergodic channel capacity can be expressed as

$$C = \sup_{p_x} \mathcal{E}_H\{I(X;Y|H)\} \tag{3.16}$$

$$= \mathcal{E}_H\left\{\log_2 |I_r + \frac{\rho}{t} HH^H|\right\} \tag{3.17}$$

where $\mathcal{E}_H$ is the expectation with respect to H, the supreme is over all input probability distributions p_x subject to the power constraint $\mathcal{E}\{\mathrm{Tr}(\mathrm{XX^H})\} = \mathrm{t}$, and $I(X;Y|H)$ is the conditional mutual information between the variables X and Y conditioned on the channel realizations H.

To achieve any point on the capacity curve, generally a symbol constellation with a Gaussian distribution is needed. In practice, however, the input is often restricted to a fixed code constellation. The constellation-constrained capacity is obtained by averaging the mutual information over a given distribution of transmitted signals.

3.4.2 Capacity of the New Code

For the unitary matrix U in (3.2), the average mutual information between the transmitted code U and the received signal Y can be computed from

$$I(U,Y|H) = H(U) - H(U|Y,H) \tag{3.18}$$

where $H(\cdot) = -\mathcal{E}\log p(\cdot)$ is the entropy function.

For the proposed code, if $e^{2\phi}, x_1$ and x_2 are taken independently from PSK constellations, the resulting code constellation has $|\mathcal{U}|$ equally likely distributed codes. Therefore, the input entropy is given by

$$H(U) = -\mathcal{E}\{\log_2 \mathrm{p(U)}\} = \log_2 |\mathcal{U}| \tag{3.19}$$

Using Bayes' rule, the conditional entropy can be computed according to

$$\begin{aligned} H(U|Y,H) &= -\mathcal{E}\{\log_2 \mathrm{p(U|Y,H)}\} \\ &= -\mathcal{E}\left\{\log_2 \frac{\mathrm{p(Y|U,H)p(U)}}{\mathrm{p(Y)}}\right\} \\ &= -\mathcal{E}\left\{\log_2 \frac{\mathrm{p(Y|U,H)}\frac{1}{|\mathcal{U}|}}{\frac{1}{|\mathcal{U}|}\sum_U \mathrm{p(Y|U,H)}}\right\} \\ &= -\mathcal{E}\left\{\log_2 \frac{\mathrm{p(Y|U,H)}}{\sum_U \mathrm{p(Y|U,H)}}\right\} \end{aligned} \tag{3.20}$$

where p(Y|U, H) is given in (2.2). Substituting (3.19) and (3.20) into (3.18), the mutual information can be expressed as

$$I(U,Y|H) = \log_2 |\mathcal{U}| - \mathcal{E}\left\{\log_2 \frac{\sum_U \mathrm{p}(Y|U,H)}{\mathrm{p}(Y|U,H)}\right\} \tag{3.21}$$

If suboptimal decoding methods are used, we can get an approximate expression on the mutual information using the equivalent channel model for each symbol. For ϕ, from the equivalent channel (3.9), we obtain

$$I(\phi,Y|H) = \log_2(M_{2\phi}) - \mathcal{E}\left\{\log_2 \frac{\sum_\phi \mathrm{p}(\tilde{\mathrm{y}}_\phi|\phi,\mathrm{H})}{\mathrm{p}(\tilde{\mathrm{y}}_\phi|\phi,\mathrm{H})}\right\}$$

Assume for worst cases, if ϕ is erroneously decoded, the received signal attains no information about x_1 and x_2. Then the mutual information between x_i $(i = 1, 2)$ and Y is lower bounded by the value if ϕ is correctly decoded. From (3.11), we have

$$I(x_i,Y|H) = \log_2(M_{x_i}) - \mathcal{E}\left\{\log_2 \frac{\sum_{x_i} \mathrm{p}(\tilde{\mathrm{y}}_\mathrm{i}|\mathrm{x}_\mathrm{i},\mathrm{H})}{\mathrm{p}(\tilde{\mathrm{y}}_\mathrm{i}|\mathrm{x}_\mathrm{i},\mathrm{H})}\right\}$$

The total mutual information is expressed as

$$I(U,Y|H) \approx I(\phi,Y|H) + I(x_1,Y|H) + I(x_2,Y|H) \tag{3.22}$$

Note that the mutual information expression for the suboptimal receivers assumes no information of x_i is used when decoding ϕ.

3.4.3 Capacity of Isotropically Random Unitary Codes

In above section, we calculate the constellation-constrained capacity of the proposed unitary code. It is of interest to see how much of the capacity is constrained by

the unitary structure and how much is limited by specific parametrization. To this end, we will investigate the constellation-constrained capacity of the isotropically random (IR) unitary codes.

A $t \times T$ isotropically distributed unitary code Φ satisfies $\Phi\Phi^H = I_t$ and has a density that is unchanged when it is right-multiplied by any $T \times T$ unitary matrix. Here t and T denote the number of transmit antennas and code duration length respectively. It has been shown by Marzetta and Hassibi [38] that if $T >> t$, the capacity of multi-antenna Raleigh fading channel is approached by unitary codes constructed by multiplying Φ with a real independent nonnegative diagonal matrix. Hassibi and Marzetta [22] obtained a closed form of the probability density of the received signal when transmitting IR unitary matrix when H is unknown at the receiver.

Here, we are interested in the constellation constrained capacity of the two by two IR unitary matrix, given that the receive has channel knowledge H. It will serve as an upper bound for the capacity of unitary codes. Generally for a channel with t transmit antennas and r receive antennas, the $r \times t$ noise matrix N has a density

$$p(N) = \frac{1}{\pi^{tr}} \exp(-\mathrm{Tr}[NN^H])$$

Thus if $Y = \sqrt{\rho}H\Phi + N$, the conditional mutual information between Φ and Y can be expressed as

$$I(\Phi; Y|H) = H(Y|H) - H(Y|\Phi, H) = H(Y|H) - tr\log(\pi e) \tag{3.23}$$

where $h(Y|H)$ is the differential entropy with respect to

$$\begin{aligned} p(Y|H) &= \int d\Phi\ p(Y|H,\Phi)p(\Phi) \\ &= \frac{1}{\pi^{tr}} \int d\Phi \exp(-\mathrm{Tr}[(Y-\sqrt{\rho}H\Phi)(Y-\sqrt{\rho}H\Phi)^H])p(\Phi) \\ &= \frac{1}{\pi^{tr}} \exp(-\mathrm{Tr}[YY^H+\rho HH^H]) \int d\Phi \exp(\sqrt{\rho}\mathrm{Tr}[H^HY\Phi^H+\Phi Y^HH])p(\Phi) \end{aligned}$$

In order to evaluate the last integral, define $B = \sqrt{\rho}H^HY$ and let $B = V_l^H D V_r$ be the singular value decomposition (SVD) of B, where $D = \mathrm{diag}(d_1, \ldots, d_t)$ and V_l, V_r be the left and right $t \times t$ unitary matrix respectively. Observing that multiplying Φ by any random unitary matrix does not change the distribution of Φ, the integral can be expressed as

$$\int d\Phi \exp(\mathrm{Tr}[B\Phi^H + \Phi B^H])p(\Phi) = \int d\Phi \exp(\mathrm{Tr}[D\Phi^H + \Phi D^H])p(\Phi)$$

For $t = 2$ and $D = \mathrm{diag}\{d_1, d_2\}$ where d_i are the (real) singular values of B, the above integral can be rewritten as

$$\begin{aligned} &\int d\Phi \exp(\mathrm{Tr}[D\Phi^H + \Phi D^H])p(\Phi) \\ &= \mathcal{E}\left[\exp(\mathrm{Tr}[D\Phi^H + \Phi D^H])\right] \\ &= \mathcal{E}\left\{\exp\left(d_1(\phi_{11}+\phi_{11}^*) + d_2(\phi_{22}+\phi_{22}^*)\right)\right\} \\ &= \mathcal{E}\left\{\exp\left(2d_1|\phi_{11}|\cos(\theta_1) + 2d_2|\phi_{22}|\cos(\theta_2)\right)\right\} \\ &= \mathcal{E}\left\{I_0(2d_1|\phi_{11}|)I_0(2d_2|\phi_{22}|)\right\} \end{aligned}$$

where I_0 and I_1 are modified Bessel function of first kind. The second step above follows by observing that multiplying Φ by any the random unitary matrix $\mathrm{diag}\{e^{j\theta_1}, e^{j\theta_2}\}$ where θ_i are independent and uniform does not change the distribution of Φ. Note

that for any 2×2 unitary matrix Φ, it is easy to see that $|\phi_{11}| = |\phi_{22}|$. Further note that $|\phi_{11}|^2$ will have the same distribution as

$$\frac{\xi_1^2 + \xi_2^2}{\xi_1^2 + \xi_2^2 + \xi_3^2 + \xi_4^2}$$

where all the variables are $N(0, \frac{1}{2})$. It can also be expressed as $Z = P/(P+Q)$ where P and Q are independent exponentially distributed random variables. Thus for $0 < z < 1$

$$\Pr\{Z \leq z\} = \Pr\{(1-z)P \leq zQ\} = \int_0^\infty e^{-(1-z)x/z} e^{-p} dp = z$$

so Z is uniform. thus

$$\int d\Phi \exp(\mathrm{Tr}[D\Phi^H + \Phi D^H]) p(\Phi) \quad = \quad \int_0^1 I_0(2d_1\sqrt{z}) I_0(2d_2\sqrt{z}) dz$$

Using the Bessel integral equation [19]

$$\int I_\nu(a\sqrt{z}) I_\nu(b\sqrt{z}) dz == \frac{2\sqrt{z}}{a^2 - b^2} (a I_\nu(b\sqrt{z}) I_{\nu+1}(a\sqrt{z}) - b I_{\nu+1}(b\sqrt{z}) I_\nu(a\sqrt{z}))$$

and assuming $d_1 \geq d_2$, the above integral becomes

$$\begin{aligned}
&\int d\Phi \exp(\mathrm{Tr}[D\Phi^H + \Phi D^H]) p(\Phi) \\
&= \frac{\sqrt{r}}{(d_1^2 - d_2^2)} (d_1 I_0(2d_2\sqrt{r}) I_1(2d_1\sqrt{r}) - d_2 I_1(2d_2\sqrt{r}) I_0(2d_1\sqrt{r}))|_0^1 \\
&= \frac{1}{d_1^2 - d_2^2} (d_1 I_0(2d_2) I_1(2d_1) - d_2 I_1(2d_2) I_0(2d_1))
\end{aligned}$$

Therefore the conditional pdf of Y given H is

$$\begin{aligned}
p(Y|H) \quad = \quad & \frac{1}{\pi^{TN}(d_1^2 - d_2^2)} \exp(-\mathrm{Tr}[YY^H + \rho H H^H]) \\
& \cdot (d_1 I_0(2d_2) I_1(2d_1) - d_2 I_1(2d_2) I_0(2d_1))
\end{aligned}$$

Since the calculation of its differential entropy requires integration over a log function of the above equation, which is hard to get a simple close form. We will evaluate the differential entropy through Monte-Carlo simulations. The calculation of $p(X|H)$ depends on the singular values of $\sqrt{\rho}H^H Y$. We now show that averaging the singular value only requires us to average over H and N, without requiring averaging over the IR unitary matrix.

$$H^H Y = \sqrt{\rho}H^H H\Phi + H^H N$$

Multiplying unitary matrix Φ^H on its right side doesn't change the singular values d_i of $\sqrt{\rho}H^H Y$, i.e

$$\begin{aligned} d(H^H Y) &= d(H^H Y\Phi^H) \\ &= d(\sqrt{\rho}H^H H + H^H N\Phi^H) = d(\sqrt{\rho}H^H + H^H\tilde{N}) \end{aligned}$$

Similarly averaging over $\mathrm{Tr}(\mathrm{YY^H})$ is equivalent to averaging over $Tr(Y\Phi^H\Phi^H Y^H)$. Therefore, we can use an equivalent receiver

$$\tilde{Y} = Y\Phi^H = \sqrt{\rho}H + \tilde{N}$$

in the Monte-Carlo simulations of the differential entropy.

3.4.4 Numerical Results

We compute the constellation-constrained ergodic capacities achieved by the new code with optimal and suboptimal decoding, and compare with those of the Alamouti code and the Steiner code for different rates and receive array size.

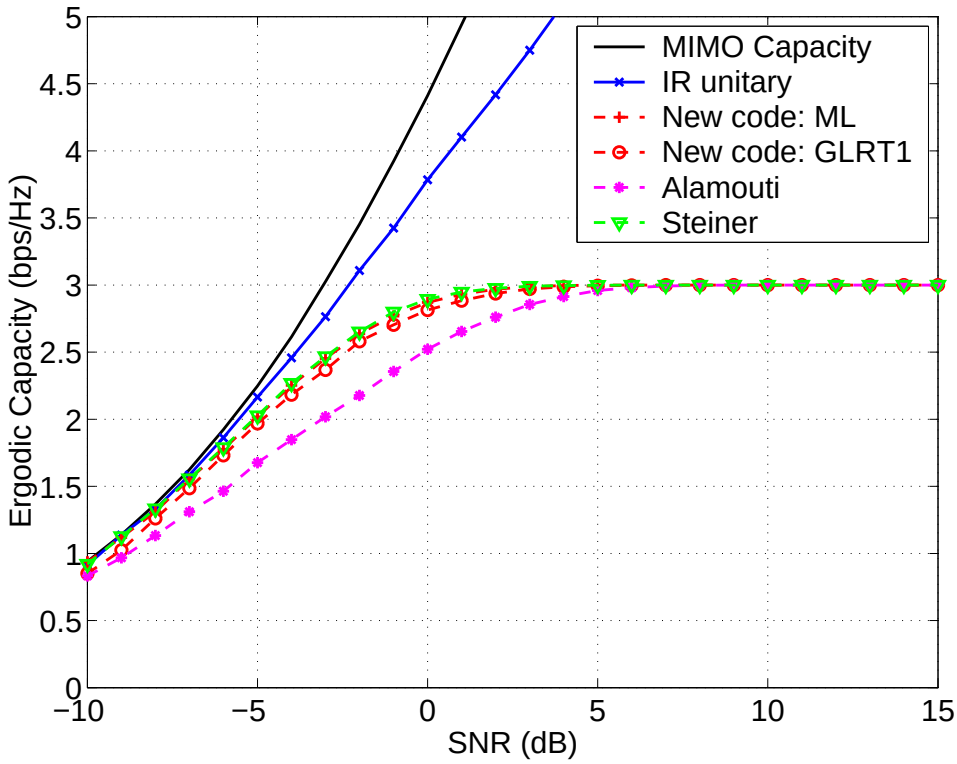

Figure 3.8: Ergodic capacity of the new code with ML and GLRT1 decoding, Alamouti code and Steiner code at $R = 3$ bps/Hz for $t = 2$, $r = 8$.

Fig. 3.8 shows the results for $R = 3$ bps/Hz and $r = 8$. We also include the channel capacity as in (3.17) and the capacity achieved by the isotropically random unitary code (3.23) as upper bounds for arbitrary inputs and unitary codes respectively. We observe that the Steiner code has slightly larger capacity than the new code with ML decoding. The capacity of the new code with the suboptimal GLRT1 decoder is within 0.4 dB of the ML capacity. On the other band, Alamouti code suffers much capacity loss compares to the Steiner code and the new code. For capacity of 2 bps/Hz, the new code with ML decoding is about 0.5dB from the capacity of IR unitary code and 0.7dB from the MIMO capacity.

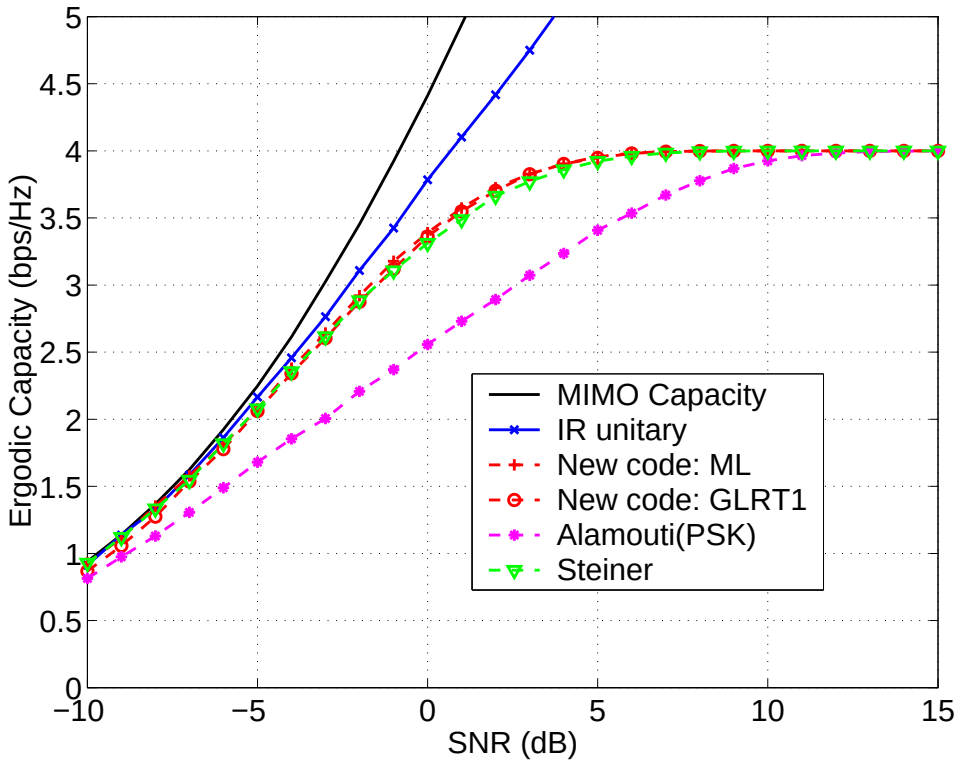

Figure 3.9: Ergodic capacity of the new code with ML and GLRT1 decoding, Alamouti code and Steiner code at $R = 4$ bps/Hz for $t = 2$, $r = 8$.

For rate 4 bps/Hz and $r = 8$, as shown in Fig. 3.9 the capacities of the new code with both decoding structures and the Steiner code are very close, all within 1.4 dB of the MIMO capacity at 3 bps/Hz. Nearly half of the gap is due to the unitary constraint. The capacity loss of the Alamouti code compared to the new code is larger than that for the rate 3 case.

In Fig. 3.10, we compare the capacity of the rate 4 new code with those of the Alamouti code with 16QAM and 16PSK for one and eight receive antennas respectively. It is clear that for one receive antenna, the Alamouti code with 16QAM has the largest capacity, which is not surprising because the Alamouti code with Gaussian

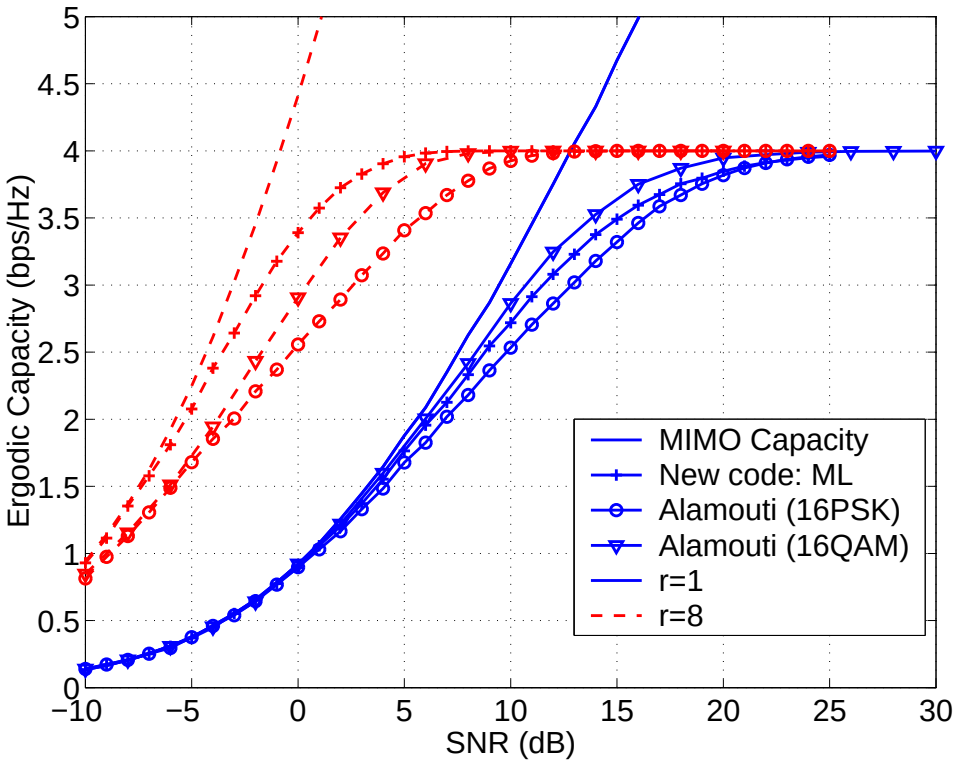

Figure 3.10: Comparison of ergodic capacity of the new code and Alamouti code at $R = 4$ bps/Hz for $t = 2$, $r = 1$ and $r = 8$ respectively.

input is the capacity achieving code. However, for 8 receive antennas, the new code has larger capacity than the Alamouti code with both 16QAM and 16PSK.

The capacity results shows that the new code is a good candidate for large antenna arrays, which verifies the BER performance results from information theory point of view.

3.5 Extension to More Than Two Transmit Antennas

3.5.1 Introduction

Up to now, we have considered space-time coding for two transmit antennas. It is of interest to consider the design of space-time codes for more than two transmit antennas. This is especially important for downlink transmission for cellular networks. Due to the size and cost limitation, it is usually difficult for the mobile handset to employ large number of antennas. A more practical solution for high date rate downlink transmission is to equip the base station with more transmit antennas.

Space-time block codes based on orthogonal design have gained much interest because the orthogonal structure enables a simple maximum likelihood decoding. It has been shown by Tarokh *et al.* [56], however, that full rate and full diversity complex orthogonal design only exists for two transmit antennas, which is the Alamouti code. Only some sparse codes of rate more than a half exist for more than two transmit antennas. For example, for 4 transmit antennas, a rate 3/4 code with a simple form is given by Tirkkone and Hottinen [60] as

$$U = \frac{1}{\sqrt{3}} \begin{bmatrix} x_1 & x_2 & x_3 & 0 \\ -x_2^* & x_1^* & 0 & -x_3 \\ -x_3 & 0 & x_1^* & x_2^* \\ 0 & x_3^* & -x_2^* & x_1 \end{bmatrix}. \tag{3.24}$$

The orthogonal structure ensures that each information symbol has a separate de-

coding metric, therefore the decoding is decoupled.

Since it is impossible to have full rate full diversity complex design for more than two transmit antennas, non-orthogonal codes are designed to achieve full rate transmission for $t > 2$. One approach is the quasi-orthogonal codes proposed by Jafarkhani [28] which is closely related to the Alamouti code. Let U_{12} and U_{34} be the alamouti code with information symbols x_1, x_2 and x_3, x_4 respectively, then a full rate quasi-orthogonal code for four transmit antennas can be obtained by

$$U_q = \frac{1}{\sqrt{2}} \begin{bmatrix} U_{12} & U_{34} \\ -U_{34}^* & U_{12}^* \end{bmatrix} = \frac{1}{2} \begin{bmatrix} x_1 & x_2 & x_3 & x_4 \\ -x_2^* & x_1^* & -x_4^* & x_3^* \\ -x_3^* & -x_4^* & x_1^* & x_2^* \\ x_4 & -x_3 & -x_2 & x_1 \end{bmatrix} \tag{3.25}$$

Denote $\mathcal{V}_i, i = 1, 2, 3, 4$ as the ith column of U_q, it is easy to see that the subspace created by $\mathcal{V}_1$ and $\mathcal{V}_4$ is orthogonal to the subspace created by $\mathcal{V}_2$ and $\mathcal{V}_3$. Using this orthogonality, the maximum-likelihood decision metric can be expressed as the sum of two terms $f_{14}(x_1, x_4) + f_{23}(x_2, x_3)$, where f_{14} is independent of x_2 and x_3 and f_{23} is independent of x_1 and x_4. Therefore, the ML decoding works with pairs of transmitted symbols instead of the individual symbols for the orthogonal designs. However, it achieves a higher rate compared to the orthogonal structure.

The minimum Euclidean distances for the orthogonal code and the quasi-orthogonal code are

$$\Lambda_e = \frac{4}{\sqrt{3}} \sin(\frac{\pi}{M_x}) \tag{3.26}$$

and

$$\Lambda_e = 2\sin(\frac{\pi}{M_x}) \tag{3.27}$$

respectively. For a same rate, the quasi-orthogonal code has larger Euclidean distance compared to the orthogonal code.

Quasi-orthogonal codes are not unitary codes, i.e, not all the columns are orthogonal to each other. Therefore, it is primarily interested for coherent detection. On the other hand, the orthogonal design can be used for differential detection as well.

We will show that both orthogonal codes and quasi-orthogonal codes can be improved by adding one extra information symbol. In addition, the suboptimal decoders can be utilized to reduce the decoding complexity.

3.5.2 Code Construction and Decoding Structure

We can get a new code with improved rate by adding a fourth parameter $e^{j\phi}$ to the 4×4 orthogonal code (3.24), where $-\frac{\pi}{2} < \phi \leq \frac{\pi}{2}$

$$U = \frac{1}{\sqrt{3}} e^{j\phi} \begin{bmatrix} x_1 & x_2 & x_3 & 0 \\ -x_2^* & x_1^* & 0 & -x_3 \\ -x_3 & 0 & x_1^* & x_2^* \\ 0 & x_3^* & -x_2^* & x_1 \end{bmatrix} \tag{3.28}$$

The Euclidean distance of the new code can be expressed as

$$\begin{aligned} \mathrm{Tr}\{(U-\hat{U})(U-\hat{U})^H\} &= \frac{4}{3}(|x_1|^2 + |\hat{x}_1|^2 + |x_2|^2 + |\hat{x}_2|^2 + |x_3|^2 + |\hat{x}_3|^2) \\ &\quad -\frac{4}{3}\mathrm{Re}\{e^{j(\phi-\hat{\phi})}(x_1\hat{x}_1^* + \hat{x}_1 x_1^* + x_2\hat{x}_2^* + \hat{x}_2 x_2^* + x_3\hat{x}_3^* + \hat{x}_3 x_3^*)\} \end{aligned}$$

$$= \quad 8 - \frac{8}{3}\mathrm{Re}\{e^{j(\phi-\hat{\phi})}\}\mathrm{Re}\{x_1\hat{x}_1^* + x_2\hat{x}_2^* + x_3\hat{x}_3^*\}$$

From which we can observe that the minimum Euclidean distance of the new code can be expressed as

$$\Lambda_e = \min\left\{\frac{4}{\sqrt{3}}\sin(\frac{\pi}{M_x}),\ 4\sin(\frac{\pi}{2M_{2\phi}})\right\} \tag{3.29}$$

where M_x is the maximum constellation size for x_1, x_2, x_3. Let $B_{4\times 4}$ defined by $B = Y^H H$ and $B = Y_{k-1}^H Y_{k-1}$ for coherent and differential detection, respectively. The ML decoding metric for this code can be expressed as

$$\begin{aligned}\Lambda(Y|x_1,x_2,x_3,\phi) \quad &= \quad [(b_{11}+b_{44})e^{j\phi} + ((b_{22}+b_{33})e^{j\phi})^*]x_1 \\ &\quad +[(b_{21}+b_{43})e^{j\phi} - ((b_{12}+b_{34})e^{j\phi})^*]x_2 \\ &\quad +[(b_{31}+b_{42})e^{j\phi} + ((b_{24}+b_{13})e^{j\phi})^*]x_3\end{aligned}$$

Comparing this with (3.5), we can conclude that similar to the code for two transmit antennas, here we can also use suboptimal GLRT receivers to decode ϕ first and then use conventional parallel decoders for x_i $(i = 1, 2, 3)$.

For coherent detection, consider the quasi-orthogonal code (3.25). We can also add a fifth parameter $e^{j\phi}$, where $-\frac{\pi}{2} < \phi \leq \frac{\pi}{2}$ to this code

$$U = \frac{1}{2}e^{j\phi}\begin{bmatrix} x_1 & x_2 & x_3 & x_4 \\ -x_2^* & x_1^* & -x_4^* & x_3^* \\ -x_3^* & -x_4^* & x_1^* & x_2^* \\ x_4 & -x_3 & -x_2 & x_1 \end{bmatrix} \tag{3.30}$$

The Euclidean distance for the new code can be expressed as

$$\mathrm{Tr}\{(U-\hat{U})(U-\hat{U})^H\} = \sum_{i=1}^{4}|x_i|^2 + |\hat{x}_i|^2 - 2\mathrm{Re}\{e^{j(\phi-\hat{\phi})}\}\mathrm{Re}\{\sum_{i=1}^{4} x_i\hat{x}_i^*\}$$

For symbols taken from PSK constellations, the minimum Euclidean distance can be written as

$$\Lambda_e = \min\left\{2\sin(\frac{\pi}{M_x}),\ 4\sin(\frac{\pi}{2M_{2\phi}})\right\} \tag{3.31}$$

Comparing this with (3.3), we can conclude that here ϕ is better protected.

The ML decoding metric is to maximize the two functions

$$f_{14}(x_1,x_4,\phi) = f_1(x_1,\phi) + f_4(x_4,\phi) - \mathrm{Re}\{\mathrm{x_1x_4^*}\}\mathrm{Re}\{\mathbf{h_4^H h_1 - h_3^H h_2}\} \tag{3.32}$$

and

$$f_{23}(x_2,x_3,\phi) \;=\; f_2(x_2,\phi) + f_3(x_3,\phi) + \mathrm{Re}\{\mathrm{x_2x_3^*}\}\mathrm{Re}\{\mathbf{h_4^H h_1 - h_3^H h_2}\} \tag{3.33}$$

where $\mathbf{h_i}$ denote the i th column of H. We can apply the GLRT decoders for ϕ based on the metric

$$\begin{aligned}
\Lambda_\phi &= f_1(x_1,\phi) + f_4(x_4,\phi) + f_2(x_2,\phi) + f_3(x_3,\phi) \\
&= \mathrm{Re}\{[(\mathrm{b_{11}+b_{44}})\mathrm{e}^{\mathrm{j}\phi} + (\mathrm{b_{22}^*+b33^*})\mathrm{e}^{-\mathrm{j}\phi}]\mathrm{x_1} \\
&\quad +[(b_{14}+b_{41})e^{j\phi} - (b_{23}^*+b_{32}^*)e^{-j\phi}]x_4\} \\
&\quad +\mathrm{Re}\{[(\mathrm{b_{21}-b_{34}})\mathrm{e}^{\mathrm{j}\phi} + (\mathrm{b_{43}^*-b_{12}^*})\mathrm{e}^{-\mathrm{j}\phi}]\mathrm{x_2} \\
&\quad +[(b_{31}-b_{24})e^{j\phi} + (b_{42}^*-b_{13}^*)e^{-j\phi}]x_3\}
\end{aligned}$$

using a similar approach for two transmit antennas. Then substitute the detected value $e^{j\phi}$ into (3.32) and (3.33) to do pair decoding of x_1, x_4 and x_2, x_3 respectively.

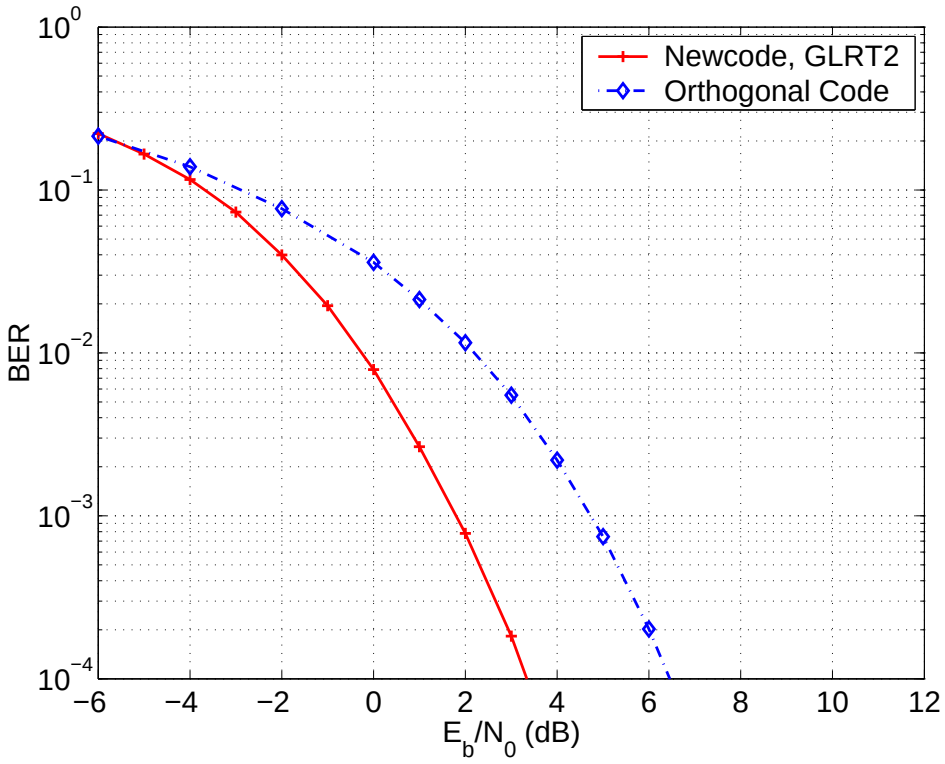

Figure 3.11: BER of new code at $R = 2$ with GLRT2 receiver and Orthogonal code at $R = 2.25$ for $t = 4$, $r = 8$ receive antennas and DSTM structure.

3.5.3 Numerical Results

We now presents the simulated BER performance of the new codes constructed from 4×4 orthogonal and Quasi-orthogonal codes respectively. We also plot the performance of the orthogonal and Quasi-orthogonal codes for comparison. Eight receive antennas are assumed.

Fig. 3.11 compares the new code at rate 2 bps/Hz with 4 parameters $(x_1, x_2, x_3, e^{j2\phi})$ all taken from QPSK constellations and the orthogonal code at rate 2.25 bps/Hz with 3 parameters (x_1, x_2, x_3) all taken from 8PSK constellations. We assume differential space-time modulation is used. We can see that the new code has more than 2 dB

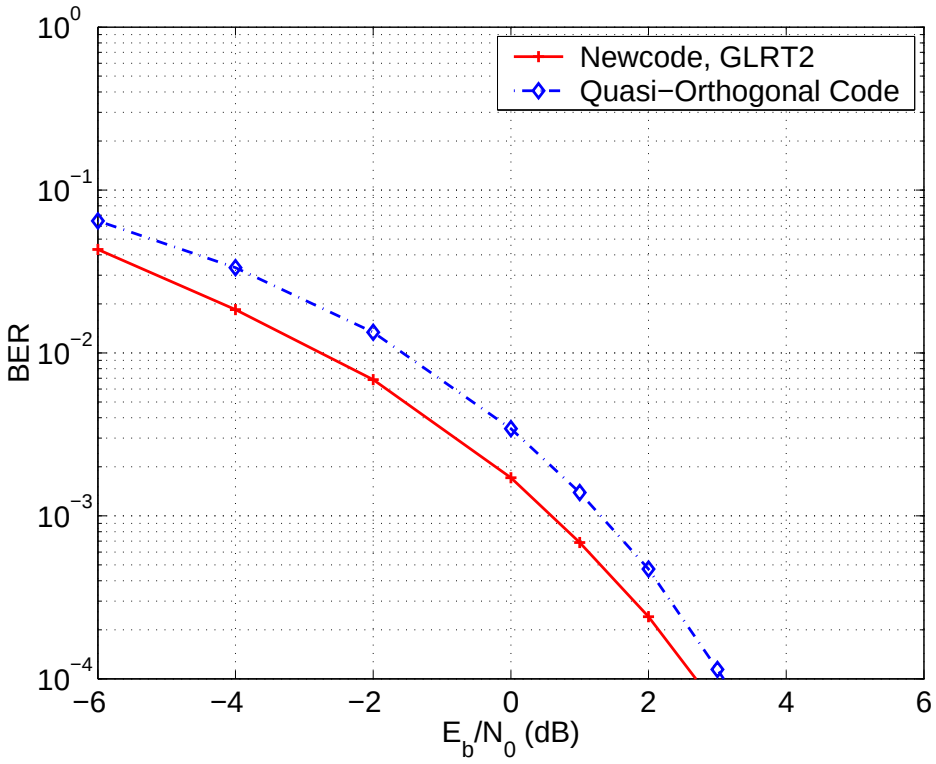

Figure 3.12: BER of new code with GLRT2 receiver and Quasi-orthogonal code for rate $R = 3$ bps/Hz, $t = 4$, $r = 8$ receive antennas and coherent detection.

advantage although the rate for orthogonal code is a little bit higher.

Fig. 3.12 compares the new code with 5 parameters $(x_1, x_2, x_3, x_4, e^{j2\phi})$ taken from (8PSK, 8PSK, QPSK,QPSK, QPSK) and the quasi-orthogonal code with 4 parameters (x_1, x_2, x_3, x_4) all taken from 8PSK constellations. Both codes result in rate 3 bps/Hz. Coherent detection is assumed. The new code outperforms the quasi-orthogonal code by about 0.5 dB. The new code also has advantage in decoding complexity by reducing the constellation size in pair decoding.

3.6 Conclusion

In this chapter, we have proposed a new family of unitary space-time block codes, that is useful for two transmit antennas and a large number of receive antennas. We optimized the new code with respect to the Euclidean distance criterion. We then derived two suboptimal low-complexity sequential receivers based on GLRT, which allow the individual symbols in the code to be sequentially decoded. The decoding complexity of these suboptimal decoders is comparable to the Alamouti linear decoder. The proposed unitary codes can be used for both coherent and differential space-time modulations. When coherent detection is used, we also extend the code from PSK constellations to QAM constellations to further improve performance. Through simulation results, we can conclude that the new code achieves better performance than some existing codes for large numbers of receive antennas. Furthermore, the suboptimal receivers perform close to optimal ML decoding as the number of receive antennas increases. We analyzed the bit-error rate performance of the suboptimal decoders through the decoupled equivalent channels for each information symbol. The analytical result provides a good approximation to the simulated BER performance.

We also evaluated the new code from an information theoretic perspective through the calculation of constellation-constrained capacity. The capacity results also provide evidence that the proposed code is a good candidate for systems with large receive arrays. We then extended the proposed coding structure to four transmit antennas, based on modification of orthogonal codes and quasi-orthogonal codes. The newly designed codes improve performance with both coherent and differential detection.

Chapter 4

Multiple-Symbol Decision-Feedback DSTM in Fast Fading Channels

In previous chapters, the discussion on differential space-time modulation is based on the assumption that the channel remains approximately the same for two adjacent blocks. In this chapter, we will evaluate the performance of DSTM with the proposed code and suboptimal decoders, in the presents of fast fading channels. We show that the code performance suffers from degradation when fast fading is encountered. We will apply multiple-symbol decision-feedback differential detection (DFDD) to improve the performance of DSTM in fast-fading channel. The suboptimal decoders [67] are utilized in DFDD to further reduce the decoding complexity.

4.1 Introduction

For differential space-time modulation, usually a slow fading channel is assumed, where the channel coefficients remain approximately constant for two adjacent transmission blocks. Under such assumption, conventional differential detection detects the information signal matrix using only the received signals for current and previous blocks. The lack of channel state information results in about 3 dB performance loss compared to the corresponding coherent receiver.

For DSTM with two transmit antennas and large numbers of receive antennas, we proposed a new family of space-time codes [66, 67, 68]. The new code can achieve good performance and can use low-complexity suboptimal sequential receivers based on GLRT with near-optimal performance for large antenna arrays.

If this slow-fading condition is not fulfilled, the conventional differential detection (DD) will suffer from severe performance degradations. The autocorrelation function for time-varying channel is usually predicted by the Jake's model [31]. Peel and Swindlehurst [40] analyzed the performance of DSTM under continuous changing channel through the derivation of effective SNR. They adopted a first-order autoregressive (AR) model for the time-variations of the channel coefficients by matching the autocorrelation of the AR process to Jakes' model. It is shown that for a continuous fading channels with a large Doppler shift, there will be a error floor.

For systems with single transmit antenna, it is well known that multiple-symbol differential detection (MSDD) can mitigate the flooring effect [10, 11]. The computational complexity of MSDD is exponential in the observation length. A simple

and efficient decoding method is to use multiple symbol decision-feedback differential detection (DFDD) [45]. This techniques is extended to systems employing multiple antenna systems and space-time differential coding in [46] by Schober and Lampe and in [36] by Liu and Wang. [46] focuses on diagonal group codes. The DFDD receiver is utilized for decoding diagonal group codes in continuous fading channels where the channel coefficients vary symbol by symbol. The fast decoding algorithm [7] is used for the diagonal group codes. [36] focuses on the Alamouti code structure. To simplify the analysis, the channel is assumed to have block fading, for which the channel remains constant inside a block, but varies between blocks according to Jakes' model. The performance of DFDD in both block fading and symbol fading channels was evaluated through simulation. DFDD for channels with symbol fading was considered later in [35] by Ling *et al.*, but with more decoding complexity.

In this work, we will evaluate the performance of our proposed unitary space-time codes in continuously fading channels. To reduce the performance degradation caused by the time-selective fading, we employ a multiple symbol DFDD receiver for the new codes. The suboptimal decoders based on GLRT will be applied in the DFDD scheme to further reduce the receiver complexity. For simplicity, we assume a block fading channel.

4.2 Channel Model

Consider a flat fading, spatially uncorrelated and time varying channel. For a system with t transmit antennas and r receive antennas, the received signal for the

ith receive antenna at time l can be expressed as

$$y_{il} = \sum_{j=1}^{t} \sqrt{\rho} h_{ij}(l) x_{jl} + n_{il}, \quad i = 1, \cdots, r, \ l = 1, \cdots, T$$

where $h_{ij}(l)$ is the channel coefficient from the jth transmit antenna to the ith receive antenna at time l. As mentioned in chapter two, the time-correlated fading channel is usually modeled using Jakes' model. If the channel varies from symbol to symbol, each spatially independent fading path will have a normalized autocorrelation function of

$$r_{hh}(n) = \mathcal{E}[h(\tau)h^*(\tau + nT_s)] = J_0(2\pi f_d n T_s) \tag{4.1}$$

where $J_0(\cdot)$ is the zero-th order modified Bessel function of the first kind, f_d is the maximum Doppler shift, which is proportional to the vehicle speed and carrier frequency as in (1.1), τ is the time index and T_s is the symbol duration. $f_d T_s$ is the normalized Doppler shift. For non-diagonal DSTM, the symbol fading assumption results in a rather complex receiver structure. To simplify the analysis, here we assume that the channel remains constant over one transmission block, under which the for the kth block the channel can be written as

$$Y_k = \sqrt{\rho} H_k X_k + N_k$$

(2.1). Here, instead of $H_k = H_{k-1}$ assumed in conventional DSTM, the correlation between block i and j can be expressed as

$$r_{hh}(2) = J_0(4\pi f_d T_s) \tag{4.2}$$

4.3 Decision Feedback Differential Detection

In this section, we will derive the DFDD for the new code with suboptimal receivers. The analysis is similar to the approach in [36] for the Alamouti code.

Consider multiple symbol differential detection (MSDD) with observation length K. Stacking the variables involved in MSDD and denote

$$\begin{aligned}
\bar{U}_k &= [U_k, U_{k-1}, \cdots, U_{k-K+2}] \\
\bar{X}_k &= \text{diag}[X_k, X_{k-1}, \cdots, X_{k-K+1}] \\
\bar{H}_k &= [H_k, H_{k-1}, \cdots, H_{k-K+1}] \\
\bar{Y}_k &= [Y_k, Y_{k-1}, \cdots, Y_{k-K+1}] \\
\bar{N}_k &= [N_k, N_{k-1}, \cdots, N_{k-K+1}]
\end{aligned}$$

We thus have an equivalent channel model

$$\bar{Y}_k = \bar{H}_k \bar{X}_k + \bar{N}_k \tag{4.3}$$

The conditional probability density functions of $\bar{Y}_k$ given $\bar{U}_k$ or equivalently $\bar{X}_k$ is expressed as

$$p(\bar{Y}_k|\bar{U}_k) = \frac{\exp(-\text{Tr}(\bar{Y}_k R_{\bar{U}_k}^{-1} \bar{Y}_k^H))}{(\pi^{tK} \det(R_{\bar{U}_k}))^r} \tag{4.4}$$

where $R_{\bar{U}_k}$ is the auto correlation matrix of $\bar{Y}_k$ for single receive antenna system when $\bar{U}_k$ is transmitted. Let $\bar{\mathbf{y}}_\mathbf{k}$ and $\bar{\mathbf{h}}_\mathbf{k}$ denote the first row of $\bar{Y}_k$ and $\bar{H}_k$ respectively, then $R_{\bar{U}_k}$ is given by

$$R_{\bar{U}_k} = \mathcal{E}[\bar{\mathbf{y}}_\mathbf{k}^\mathbf{H} \bar{\mathbf{y}}_\mathbf{k}]$$

$$
\begin{aligned}
&= \bar{X}_k^H \mathcal{E}[\bar{\mathbf{h}}_\mathbf{k}^\mathbf{H} \bar{\mathbf{h}}_\mathbf{k}] \bar{\mathbf{X}}_\mathbf{k} + \frac{\mathbf{1}}{\rho} \mathbf{I_{2K}} \\
&= \bar{X}_k^H \left[\left(R_{\bar{H}} + \frac{1}{\rho} I_K \right) \otimes I_2 \right] \bar{X}_k
\end{aligned}
$$

where $R_{\bar{H}}$ denotes the normalized $K \times K$ autocorrelation matrix with elements

$$
R_{\bar{H}}(m,n) = J_0(4\pi f_d T_s(m-n)), \quad m = 0, \cdots, K-1, \quad n = 0, \cdots, K-1.
$$

according to (4.2). Here $\otimes$ denotes the Kronecker matrix product.

Note that the matrix identity $\det(I+AB) = \det(I+BA)$ and the unitary property $\bar{X}_k \bar{X}_k^H = \bar{X}_k^H \bar{X}_k = I_{2K}$ imply that $\det(R_{\bar{U}_k})$ does not depend on $\bar{U}_k$. Denote $T = (R_{\bar{H}} + \frac{1}{\rho} I_K)^{-1}$, further note that

$$
\left[\left(R_{\bar{H}} + \frac{1}{\rho} I_K \right) \otimes I_2 \right]^{-1} = T \otimes I_2. \tag{4.5}
$$

Given these results, the multiple symbol differential detection rule can be expressed as

$$
\bar{U}_k = \arg \max_{\bar{U}_k} \Lambda(\bar{U}_k) = \mathrm{Tr} \left[-\bar{Y}_k \bar{X}_k^H (T \otimes I_2) \bar{X}_k \bar{Y}_k^H \right] \tag{4.6}
$$

Notice that T is symmetric and use the unitary property, the above decision metric can be expressed as

$$
\begin{aligned}
\Lambda &= \mathrm{Tr} \left\{ - \sum_{i=0}^{K-1} \sum_{j=0}^{K-1} t_{ij} Y_{k-j} X_{k-j}^H X_{k-i} Y_{k-i}^H \right\} \\
&= - \sum_{i=0}^{K-1} t_{ii} Y_{k-i} X_{k-i}^H X_{k-i} Y_{k-i}^H - \sum_{i=0}^{K-1} \sum_{j=0, j \neq i}^{K-1} t_{ij} Y_{k-j} X_{k-j}^H X_{k-i} Y_{k-i}^H \\
&= - \sum_{i=0}^{K-1} t_{ii} ||Y_{k-i}||^2 - 2\mathrm{ReTr} \left\{ \sum_{i=0}^{K-1} \sum_{j=i+1}^{K-1} t_{ij} Y_{k-i}^H Y_{k-j} \left(\prod_{\nu=i}^{j-1} U_{k-\nu} \right) \right\}
\end{aligned}
$$

where

$$\prod_{\nu=i}^{j-1} U_{k-\nu} = U_{k-(j-1)} \cdots U_{k-i}.$$

Omit the terms that don't depend on $\bar{U}_k$, the above decision metric can be simplified as

$$\bar{U}_k = \arg\max_{\bar{U}_k} \mathrm{ReTr}\left\{ -\sum_{i=0}^{K-1} \sum_{j=i+1}^{K-1} t_{i,j} Y_{k-i}^H Y_{k-j} \left(\prod_{\nu=i}^{j-1} U_{k-\nu} \right) \right\} \tag{4.7}$$

The multiple symbol differential detection of $\bar{U}_k$ in eq. (4.7) involves a computational complexity growing exponentially with observation length K. The requiring complexity makes MSDD not very practical even for relatively small observation length and data rates. For example, a rate 4 bps/Hz code with $K = 4$ will require 2^{24} exhaustive searches on unitary matrices. To simplify the receiver design, in deciding U_k, the previous transmitted information matrix $U_{k-1}, \cdots, U_{k-K+2}$ is replaced by the decision-feedback matrices $\hat{U}_{k-1}, \cdots, \hat{U}_{k-K+2}$ to achieve a simple block by block decision. By taking only the terms depending on U_k, the decision matric becomes

$$\hat{U}_k = \arg\max_{U_k} \mathrm{ReTr}\left\{ -U_k Y_k^H \sum_{j=1}^{K-1} t_{0,j} Y_{k-j} \left(\prod_{\nu=1}^{j-1} \hat{U}_{k-\nu} \right) \right\} \tag{4.8}$$

Notice in the above the decision-feedback differential detection rule, if $K = 2$, it results in the conventional differential detection of structure

$$\hat{U}_k = \arg\max_{U_k} \mathrm{ReTr}\{U_k Y_k^H Y_{k-1}\}$$

Therefore for continuous fading channels, we can still use the same decoding structure as in slow fading channels, only by replacing the reference signal Y_{ref} from Y_{k-1} to

$$Y_{\mathrm{ref}} = \sum_{v=1}^{K-1} t_{0,j} Y_{k-v} \left(\prod_{\nu=i}^{v-1} \hat{U}_{k-\nu} \right)$$

It follows that for DFDD, we can also use the two suboptimal sequential GLRT receivers to further reduce decoding complexity. The GLRT DFDD receivers have the same form as (3.6), (3.7), where B is defined as $B = Y_k^H Y_{\text{ref}}$ here.

4.4 Numerical Results

We now consider the performance of the DFDD for time-varying channel with different Doppler shift values. Here we consider the rate 4 bps/Hz unitary code with 8 receive antennas. Let fdt denote the normalized Doppler shift, so that $fdt = f_d T_s$. We will compare the performance of conventional DD with observation size $K = 2$ and the DFDD with observation length $K = 4$ for $fdt = 0.01$, 0.03 and 0.05 in Fig. 4.1 - 4.3 respectively. In the simulation, we assume two channel conditions: the channel varies from block to block or from symbol to symbol. The second GLRT suboptimal receiver is used in all the cases. For $fdt = 0.01$, the DFDD with $K = 4$ outperforms the conventional DD by about 0.7dB at BER of 10^{-4}. This performance difference increases as the Doppler shift increases. For $fdt = 0.05$, the conventional DD suffers from error floor while the DFDD mitigates the floor effect. Moreover, although our analysis is based on the assumption that the channel varies per block of two symbols, the DFDD performs well when the channels actually vary from symbol to symbol. For small Doppler shift, DFDD with symbol fading performs close to the block fading case. For $fdt = 0.05$, the violation of the assumption results in 3 dB performance loss when channel varies per symbol, but DFDD still suppresses much of the error floor for such case.

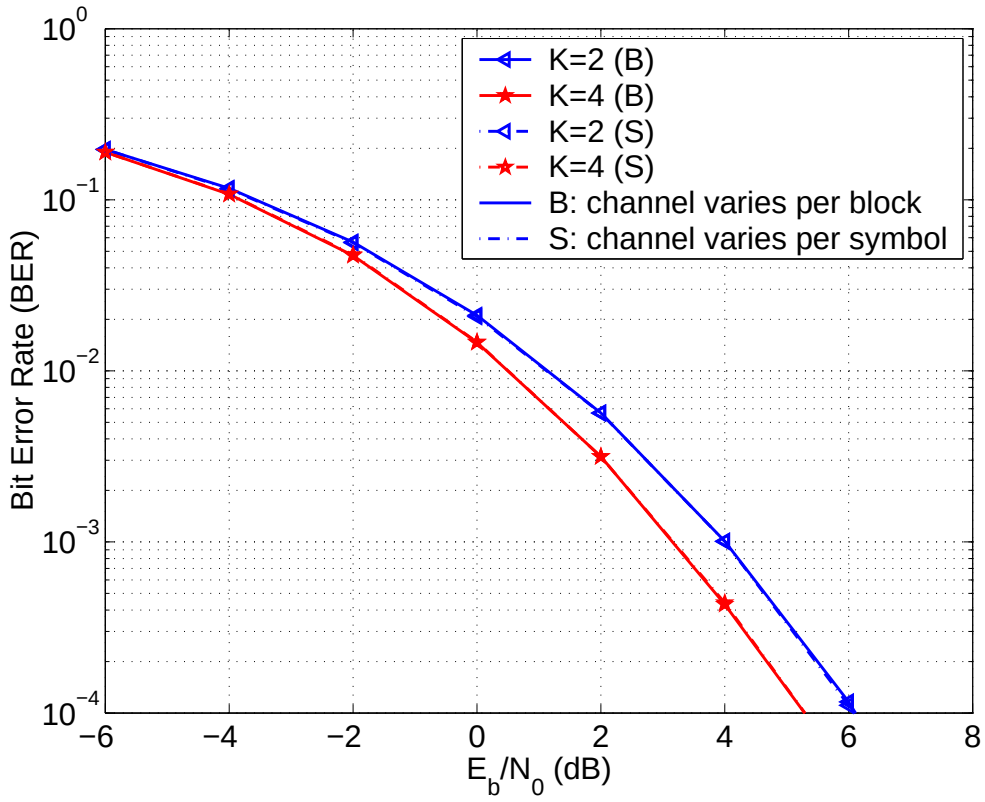

Figure 4.1: Comparison of performance of GLRT2 receiver for conventional DD (K=2) and DFDD (K=4), with $R = 4$ bps/Hz, $t = 2$ transmit antennas, $r = 8$ receive antennas and fdt=0.01.

It is not easy to compare DFDD with MS-DD because MS-DD simulation is not very practical even for a small observation length. Here in order to see the effect of erroneous feedback, we consider the performance of *genie-aided* DFDD in which all feedback signals are assumed to be perfect. In Fig. 4.4 and Fig. 4.5, we compare the performance of genie-aided DFDD with practical DFDD for channels varying per block or per symbol, respectively. It is shown that in both cases, DFDD with imperfect feedback performs close to the genie-aid DFDD as SNR increases, especially for large Doppler shift.

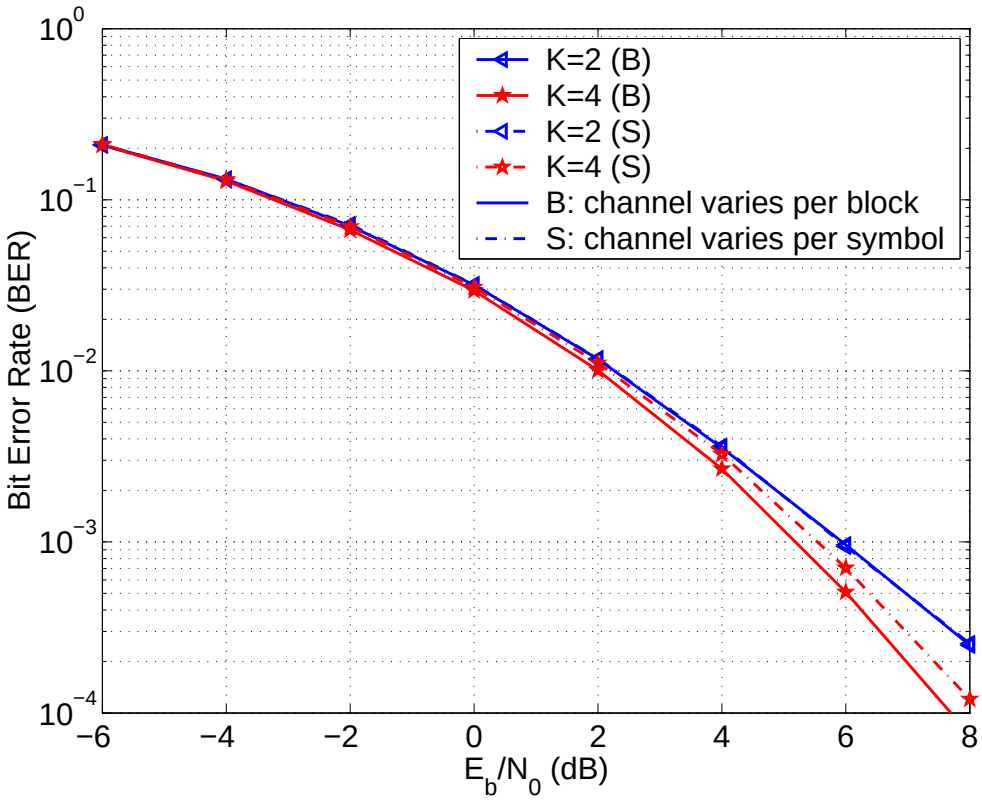

Figure 4.2: Comparison of performance of GLRT2 receiver for conventional DD (K=2) and DFDD (K=4), with $R = 4$ bps/Hz, $t = 2$ transmit antennas, $r = 8$ receive antennas and fdt=0.03.

4.5 Conclusion

In this chapter, we consider the performance of DSTM with the new unitary code and suboptimal decoders in time-selective fading channels. It is shown that the conventional differential detection method for slow fading channels will suffer from significant performance degradation. To improve the performance of DSTM in fast fading, multiple symbol differential detection is considered and decision-feedback is applied to reduce the computing complexity. For the new code, we showed that the suboptimal GLRT receivers designed for slow-fading channels can be extended to

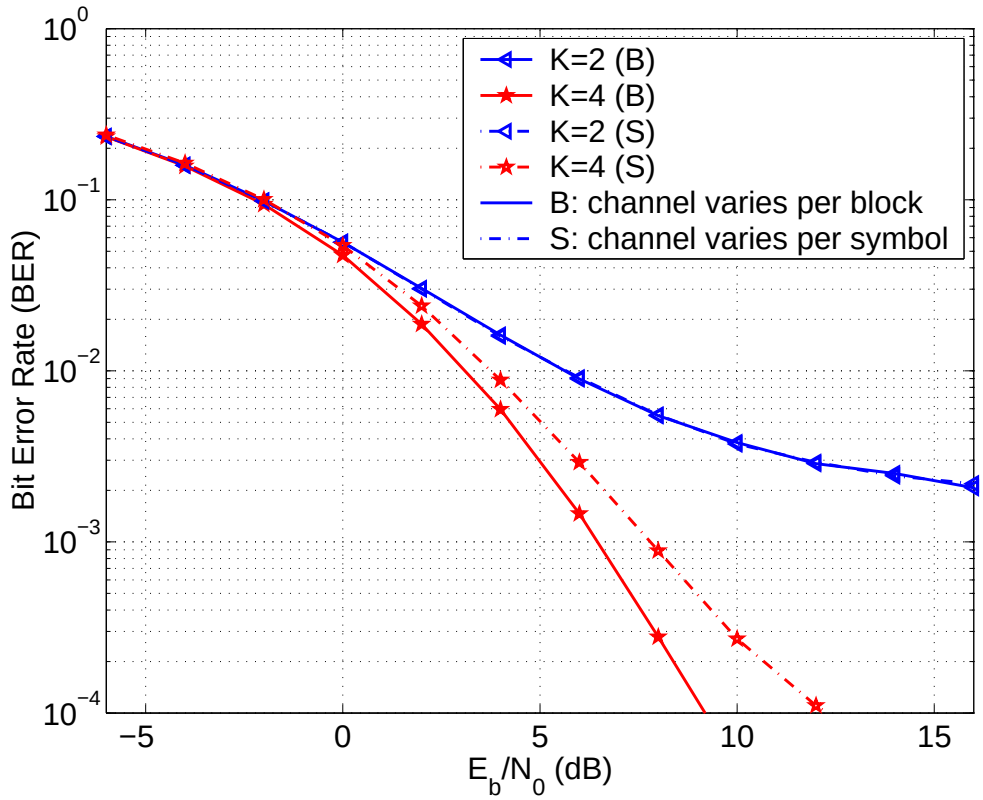

Figure 4.3: Comparison of performance of GLRT2 receiver for conventional DD (K=2) and DFDD (K=4), with $R = 4$ bps/Hz, $t = 2$ transmit antennas, $r = 8$ receive antennas and fdt=0.05.

fast fading channels to further reduce the decoding complexity. The GLRT decision-feedback differential detector only uses the second order statistic of the fading channel and has low-complexity. Through simulation results, we can see that it can reduce the performance degradation suffered by the conventional differential detection for large Doppler spread. The analysis of the decoding algorithm is based on the assumption that the channel changes from block to block according to the Jakes' model, however, it also provide good performance for channels that actually vary symbol by symbol.

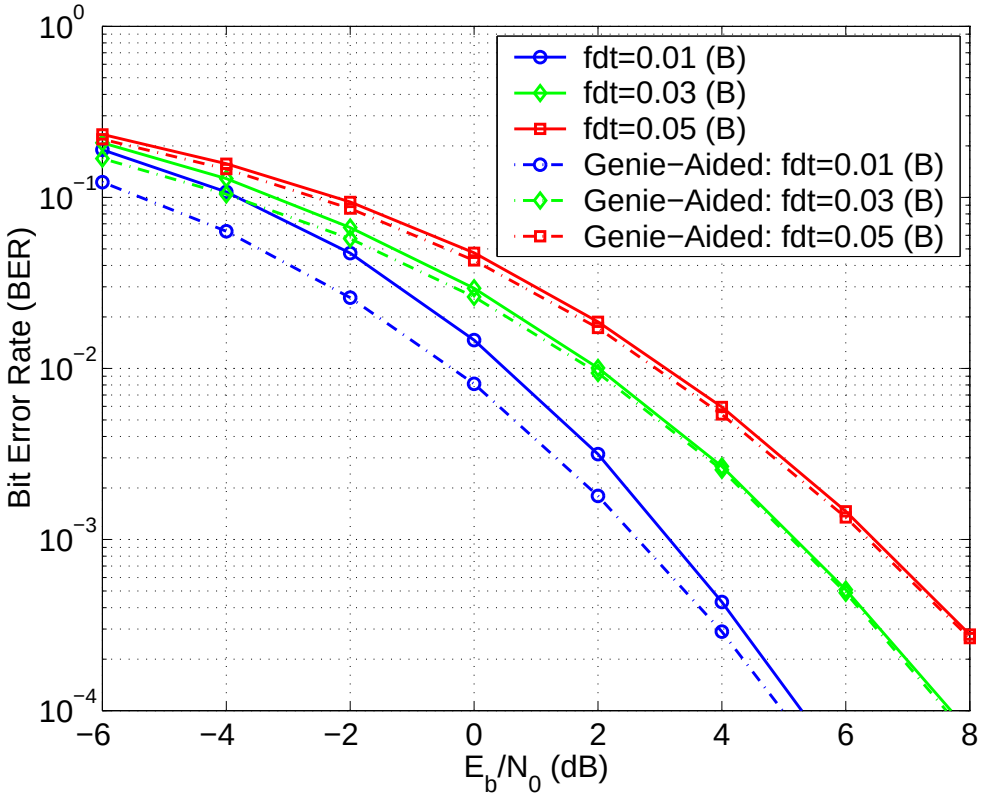

Figure 4.4: Comparison of performance of GLRT2 receiver with DFDD or Genie-Aided DFDD ($R = 4$ bps/Hz, $t = 2$ transmit antennas and $r = 8$ receive antennas and $fdt = 0.01, 0.03, 0.05$ respectively. Channel varies block by block.

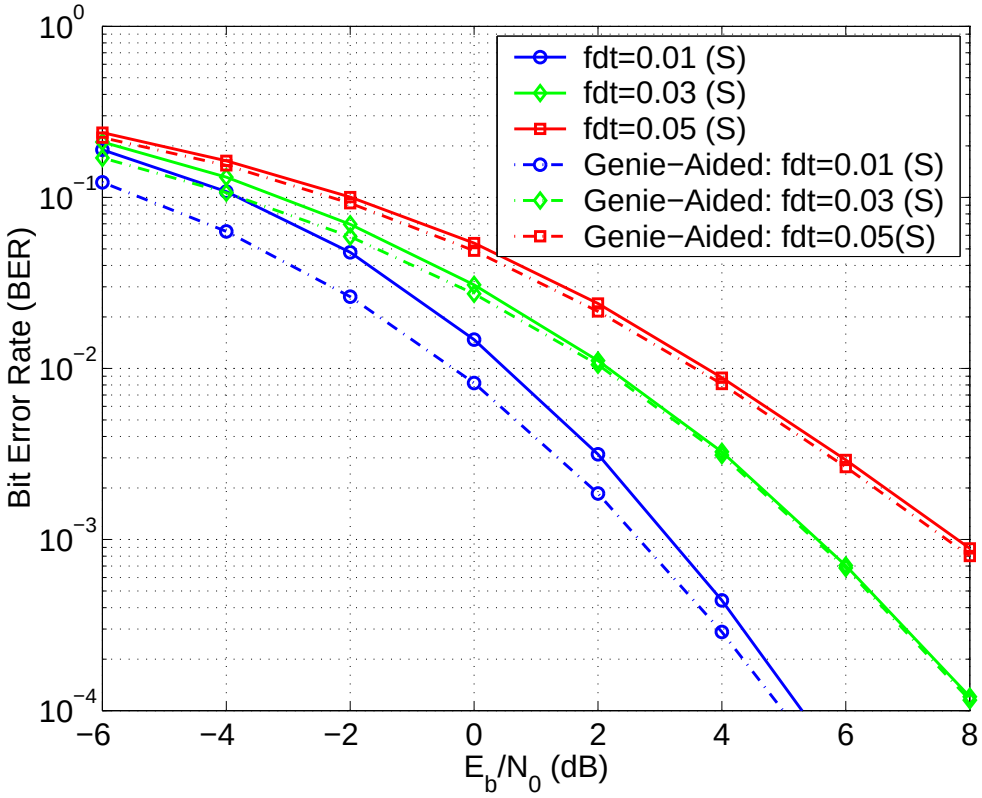

Figure 4.5: Comparison of performance of GLRT2 receiver with DFDD or Genie-Aided DFDD ($R = 4$ bps/Hz, $t = 2$ transmit antennas and $r = 8$ receive antennas and $fdt = 0.01, 0.03, 0.05$ respectively. Channel varies symbol by symbol.

Chapter 5

Conclusions

In this dissertation, we considered the design of space-time coding for large numbers of antennas. For systems with large numbers of transmit and/or receive antennas, error probabilities of practical interest are often achieved by modest or low SNRs, so the conventional design criterion for high SNRs does not apply. We focused on the error probability performance, code construction and decoding structure for large antenna arrays.

We first considered the design and analysis of DSTM when the number of antennas is large. We evaluated the error performance of DSTM and derived a new upper bound on the pairwise-error probability for large arrays. This bound suggests that Euclidean distance criterion is the appropriate design criterion for the large-array regime, rather than the well-known rank and determinant criteria for small arrays or high SNRs. For two transmit antennas and many receive antennas, we used the new design criterion to construct several new differential codes with large Euclidean

distance. Simulations of BER performance confirmed that the new codes outperform existing differential codes, e.g., the Alamouti code, for four or more receive antennas. We can conclude that the new codes are better candidates for systems with a large number of receive antennas. Generally maximum-likelihood decoding is required in the decoding of these new codes, the complexity of which is much higher than the Alamouti linear decoder for high-rate codes.

To reduce the decoding complexity, we then proposed a new family of space-time unitary block codes, that is useful for two transmit antennas and a large number of receive antennas. The new code is optimized with respect to the Euclidean distance criterion. We showed that the new code can utilize two suboptimal low-complexity sequential receivers based on GLRT, which allow the individual symbols in the code to be sequentially decoded. The decoding complexity of these suboptimal decoders is comparable to the Alamouti decoder. We apply the proposed unitary code in both coherent and differential space-time modulations. When coherent detection is used, the new code is extended to non-unitary constellations to further improve performance. We analyzed the bit-error rate performance and mutual information of the new code with the suboptimal decoders, based on the decoupled equivalent channels for each information symbol. Both analytical and simulation results indicate that the new code achieves better performance than some existing codes for large antenna arrays. Furthermore, the suboptimal receivers perform close to optimal ML decoding as the number of receive antennas increases. We also extended the proposed coding structure to four transmit antennas, based on modifications of orthogonal

codes and quasi-orthogonal codes. The new codes improve performance for both coherent and differential space-time modulation systems.

Finally, we investigate the performance of DSTM with the new unitary code in time-selective fading channels. It is shown that the conventional differential detection method designed for slow fading channels will suffer from significant performance degradation. To improve the performance of DSTM in fast fading, DFDD is applied to reduce the computing complexity. We showed that the suboptimal GLRT receivers designed for slow-fading channels can be extended to fast fading channels to further simplify the decoding process. We showed that DFDD can mitigate the error floor suffered by the conventional differential detection for large Doppler spread, for channels varying block by block or symbol by symbol.

Several related issues could be further exploited. In this dissertation, we focused on space-time block codes. In the future, we might consider the concatenation of the proposed space-time block codes with Turbo coding to further improve the system performance. In addition, in this dissertation, we have extended the proposed coding structure to more than two transmit antennas by considering orthogonal and quasi-orthogonal structures. We are interested in exploiting other coding structures for two or more transmit antennas.

Bibliography

[1] D. Aktas, H. El Gamal, M. P. Fitz, "Towards optimal space-time coding," in *Proc. Asilomar Conf.,* pp. 1137-1141, 2002.

[2] S. M. Alamouti, "A simple transmitter diversity scheme for wireless communications," *IEEE J. on Sel. Areas in Comm.*, vol. 16, no. 8, pp. 1451-1458, 1998.

[3] S. Baro, G. Bauch, and A. Hansmann, "Improved codes for space-time trellis-coded modulation," *IEEE Commun. Letters,* vol. 4, pp. 20-22, Jan. 2000.

[4] E. Biglieri, G. Taricco, A. Tulino, "Performance of space-time codes for a large number of antennas," *IEEE Trans. Inform. Theory,* vol. 48, no. 2, pp. 1794-1803, Feb. 2002.

[5] H. Boleskei, D. Gesbert, and A. J. Paulraj, "On the capacity of OFDM-based multiantenna systems," *In Proc. of 2000 IEEE ICASSP'00,* vol. 5, pp. 2569-2572, Jun. 2000.

[6] Z. Chen, J. Yuan, and B. Vucetic, "Improved space-time trellis coded modulation scheme on slow fading channels," *Electron. Lett.,* vol. 37, pp. 440-441, Mar. 2001.

[7] K. L. Clarkson, W. Sweldens, and A. Zheng, "Fast multiple antenna differential decoding," *IEEE Trans. on Commun.,* vol. 49, no. 2, pp. 253-261, Feb. 2001.

[8] S. N. Diggavi, N. Al-Dhahir, A. Stamoulis and A. R. Calderbank, " Differential space-time coding for frequency-selective channels," *IEEE Commun. Letters,* vol. 6, pp. 253-255, 2002.

[9] S. N. Diggavi, N. Al-Dhahir, A. Stamoulis and A. R. Calderbank, "Great expectations: the value of spatial diversity in wireless networks," *Proceeding of IEEE*, VOL. 92, pp. 219-270, Feb. 2004.

[10] D. Divsalar and M. K. Simon, "Multiple-symbol differential detection ofMPSK," *IEEE Trans. Commun.,* vol. 38, no. 3, pp. 300308, 1990.

[11] D. Divsalar and M. K. Simon, "Maximum-likelihood differential detection of uncoded and trellis coded amplitude phase modulation over AWGN and fading channels: metrics and performance," *IEEE Trans. Commun.,* vol. 42, no. 1, pp. 7689, 1994.

[12] A. Edelman, "Eigenvalues and condition numbers of random matrices ," *PhD Thesis, MIT, Dept. of Math.,* 1989.

[13] G. J. Foschini, "Layered space-time architecture for wireless communication in a fading environment when using multi-element antennas," *Bell Labs Tech. Journal,* vol. 1, pp. 41-59, 1996.

[14] G. J. Foschini and M. Gans, " On limits of wireless communications in a fading environment when using multiple antennas,", *Wireless Personal Communications,* vol. 6, pp. 311-335, 1998.

[15] H. E. Gamal and M. O. Damen, "Universal space-time coding," *IEEE Trans. on Inform. Theory,* vol. 49, pp. 1097-1119, May. 2003.

[16] D. Gesbert, M. Shafi, D. Shiu, P. J. Smith, A. Naguib, "From theory to practice: an overview of MIMO spacetime coded wireless systems", *IEEE J. on Sel. Areas in Comm.*, vol. 21, pp. 281-302, Apr. 2003.

[17] S. G. Glisic, *Advanced wireless communications* $4G$ *technologies,*, Wiley, 2004.

[18] G. D. Golden, G. J. Foschini, R. A. Valenzuela, and P. W. Wolniansky, "Detection algorithm and initial laboratory results using the V-BLAST spacetime communication architecture," *Electron. Lett.,* vol. 35, pp. 14-15, Jan. 1999.

[19] I. S. Gradshteyn, and I. M. Ryzhik, *Tables of integrals, series, and products,* San Diego: Academic Press, 1994.

[20] J. Guey, M. P. Fitz, M. R. Bell, and W. Kuo, "Signal design for transmitter diversity wireless communication systems over Rayleigh fading channels," *In Proc. IEEE VTC,* vol. 1, pp. 136-140, 1996.

[21] B. Hassibi, B. M. Hochwald, "Cayley differential space-time modulation," *IEEE Trans. Inform. Theory,* vol. 48, no. 6, pp. 1485-1503, June 2002.

[22] B. Hassibi and T. L. Marzetta, "Multiple-antennas and isotropically random unitary inputs: the received signal density in closed form," *IEEE Trans. on Inform. Theory,* vol. 48, pp. 1473-1484, Jun. 2002.

[23] B. M. Hochwald and T. L. Marzetta, "Unitary space-time modulation for multiple-antenna communications in Rayleigh flat fading," *IEEE Trans. Inform. Theory,* vol. 46, no. 2, pp. 543-564, Mar. 2000.

[24] B. Hochwald and W. Sweldens, "Differential unitary space-time modulation," *IEEE Trans. Commun.,* vol. 48, pp. 2041-2052, Dec. 2000.

[25] Z. Hong "Robust coding methods for space-time wireless communications ", *Ph.D dissertation, NCSU*, 2002.

[26] B. L. Hughes, "Differential space-time modulation," *IEEE Trans. Inform. Theory,* vol. 46, no. 7, pp. 2567-2578, Nov. 2000.

[27] B. L. Hughes, "Optimal space-time constellations from groups," *IEEE Trans. Inform. Theory*, Vol. 49, pp. 401-410, Feb. 2003.

[28] H. Jafarkhani, " A quasi-orthogonal space-time code," *IEEE Trans. on Commun.,* vol. 49, pp. 1-4, Jan. 2001.

[29] H. Jafarkhani, V. Tarokh, "Multiple transmit antenna differential detection from generalized orthogonal designs," *IEEE Trans. on Inform. Theory,* vol. 47, pp. 2626-2631, Sept. 2001.

[30] H. Jafarkhani and N. Seshadri, "Super-orthogonal space-time trellis codes," *IEEE Trans. Inform. Theory,* vol. 49, pp. 937-950, Apr. 2003.

[31] W. C. Jakes, *Microwace Mobile Communications,* IEEE Press, 1993.

[32] M. Jankiraman, *Space-Time Codes and MIMO Systems,* Artech House, 2004.

[33] Y. Jing and B. Hassibi, "Design of fully-diverse multiple-antenna codes based on Sp(2)", *IEEE Trans. on Inform. Theory*, vol. 50, pp. 2639-2656, Nov. 2004.

[34] X. Liang, X. Xia, "Unitary signal constellations for differential space-time modulation with two transmit antennas: parametric codes, optimal designs and bounds," *IEEE Trans. Inform. Theory,* vol. 48, pp. 2291-2321, Aug. 2002.

[35] C. Ling, K. H. Li and A. C. Kot, "Decision-feedback multiple-symbol differential detection of differential space-time modulation in continuously fading channels", *In Proc. IEEE ICASSP,* page: IV. 45-48, 2003.

[36] Y. Liu, X. Wang, "Multiple-symbol decision-feedback space-time differential decoding in fading channels," *EURASIP J Appl. Sig. Proc.,* vol. 2002, pp. 297-304, Mar. 2002.

[37] Z. Liu, G. B. Giannakis and B. L. Hughes, "Double differential space-time block coding for time-selective fading channels," *IEEE Trans. Commun.,* vol. 49, pp. 1529-1539, Sept. 2001.

[38] T. L. Marzetta and B. M. Hochwald, "Capacity of a mobile multiple-antenna communication link in Rayleigh flat-fading," *IEEE Trans. on Inform. Theory,* vol. 45, pp: 139- 157, Jan. 1999.

[39] A. J. Paulraj, D. A. Gore, R. U. Nabar, *Introduction to Space-Time Wireless Communications,* Cambridge University Press, May 2003.

[40] C. B. Peel and A. L. Swindlehurst, "Performance of unitary space-time modulation in continous changing channel," In *Proc. IEEE ICC,* Jun. 2001.

[41] J. G. Proakis, *Digital Communications,* 3rd ed. New York: McGraw-Hill, 1995.

[42] M. Qin and R. S. Blum, " Properties of space-time codes for frequency selective channels and trellis code designs," In *Proc IEEE ICC'03,* pp. 2286-2290, 2003.

[43] T. S. Rappaport, *Wireless Communications: Principles and Practice,* Prentice-Hall, 1996.

[44] K. W. Richardson, "UMTS overview," *Electronics and Commun. Engineering Journal,* pp. 93-100, June 2000.

[45] R. Schober, W. H. Gerstacker, and J. B. Huber, "Decision feedback differential detection of MDPSK for flat Rayleigh fading channels," *IEEE Trans. Commun.,* vol. 47, no. 7, pp. 1025-1035, 1999.

[46] R. Schober, L. H.-J. Lampe, "Noncoherent receivers for differential space-time modulation," *IEEE Trans. Commun.,* vol. 50, pp. 768-777, May 2002.

[47] N. Seshadri, and J. H. Winters, "Two signaling schemes for improving the error performance of frequency-division-duplex (FDD) transmission systems using transmitter antenna diversity," In *Proc. IEEE VTC,* pp. 508-511, May 1993.

[48] C. E. Shannon, "mathematical theory of communication",*Bell System Technical Journal,* vol. 27, pp. 379-423, Jul. 1948.

[49] A. N. Shiryayev, *Probability*, New York: Springer, 1984.

[50] A. Shokrollahi, B. Hochwald and W. Sweldens, "Representation theory for high-rate multiple-antenna code design ," *IEEE Trans. Inform. Theory,*" vol. 47, pp. 2335-2367, Sept. 2001.

[51] A. Steiner, M. Peleg, and S. Shamai (Shitz), "Turbo-coded space-time unitary matrix differential modulation," *In Proc. IEEE VTC, Spring,* pp. 1352-1356, May 2001.

[52] A. Steiner, M. Peleg and S. Shamai, "SVD iterative detection of turbo-coded multiantenna unitary differential modulation," *IEEE Trans. Commun.,* vol. 51, pp. 441-452, Mar. 2003.

[53] A. Steiner, M. Peleg and S. Shamai, "SVD Iterative Decision Feedback Demodulation and Detection of Coded Space-Time Unitary Differential Modulation," *IEEE Trans. Inform. Theory,* vol. 49, pp. 2648-2657, Oct. 2003.

[54] M. Taherzadeh and A. K. Khandani, "Spectrally-efficient differential space-time coding using non-full-diverse constellations," *IEEE Globecom,* Nov. 2004.

[55] V. Tarokh, N. Seshadri and A. R. Calderbank, "Space-time codes for high data rate wireless communication: performance criterion and code construction," *IEEE Trans. Inform. Theory,* vol. 44, no. 2, pp. 744-765, Mar. 1998.

[56] V. Tarokh, H. Jafarkhani, A. R. Calderbank, "Space-time block codes from orthogonal designs," *IEEE Trans. on Inform. Theory,* vol. 45 pp. 1456-1467, Jul. 1999.

[57] V. Tarokh and H. Jafarkhani, "A differential detection scheme for transmit diversity," *IEEE J.Selected Areas Commun.,* vol. 18, no. 7, pp. 1169-1174, Oct. 2000.

[58] E. Telatar, "Capacity of multi-antenna Gaussian channels," *European Trans. Telecom.(ETT),* vol. 10, Nov./Dec. 1999.

[59] TIA 45.5 Subcommittee, "*The CDMA 2000 Candidate Submission,"* draft, Jun. 1998.

[60] O. Tirkkonen and A. Hottinen, "Square-matrix embeddable space-time block codes for complex signal constellations," *IEEE Trans. on Inform. Theory,* vol. 48, pp. 384-395, 2002.

[61] B. Vucetic, J. Yuan *Space-time coding,* Wiley, 2003.

[62] J. Wang, M. Fitz and K. Yao, "Differential unitary space-time modulation for a large number of receive antennas," *Proc. Asilomar Conf.,* pp. 565-569, 2002.

[63] R. Wichman and A. Hottinen, "Transmit diversity WCDMA system," Tech. Rep., Nokia Research Center, 1998.

[64] X. Yu and B. L. Hughes, "Differential space-time modulation for large arrays," In *Proceeding of the 40th Annual Allerton Conference*, Oct. 2002.

[65] X. Yu and B. L. Hughes, "Codes for differential signals in the presence of large numbers of antennas," In *Proc. IEEE Asilomar Conf. on Signals, Systems and Computers,* pp. 510-514, 2002.

[66] X. Yu and B. L. Hughes, "Improved space-time coding with low-complexity decoders," In *Proc. IEEE Asilomar Conf. on Signals, Systems and Computers,* Oct. 2005.

[67] X. Yu and B. L. Hughes, "A low-complexity differential space-time transmission scheme for large numbers of receive antennas," In *Proc. IEEE Globecom,* Nov. 2005.

[68] X. Yu and B. L. Hughes, "Efficient space-time transmission scheme for large receive arrays," *to be submitted to IEEE Trans. on Communications,* 2005.

[69] J. Yuan, B. Vucetic, Z. Chen and W. Firmanto, "Performance of space-time coding on fading channels," In *Proc. IEEE Int. Symp. Inform. Theory,* pp. 153, 2001.

[70] J. Yuan, Z. Chen, B. Vucetic and W. Firmanto, "Performance and design of space-time coding in fading channels," *IEEE Trans.*

[71] L. Zheng and D. Tse, "Communication on the Grassman manifold: A geometric approach to the noncoherent multiple-antenna channel," *IEEE Trans. Inform. Theory,* vol. 48, pp. 359-383, Feb. 2002.